Mechanisms of the Anti-Apoptotic Effect of High-Density Lipoproteins and Its Components on Pancreatic β-Cells

---

Dissertation zur

Erlangung der naturwissenschaftlichen Doktorwürde

(Dr. sc. nat.)

vorgelegt der

Mathematisch-naturwissenschaftlichen Fakultät der

Universität Zürich von

Rahel Sibler

von

Zürich ZH

Promotionskommission

Prof. Dr. Arnold von Eckardstein (Vorsitz, Leitung der Dissertation)

Dr. Lucia Rohrer

Prof. Dr. Thierry Hennet

Prof. Dr. Christian Widmann

Prof. Dr. Marc Donath

Zürich, 2020

Table of Contents

1. Abstract

The transition from normal glucose tolerance to impaired glucose tolerance and finally type 2 diabetes mellitus (DM) is driven by the cumulative loss of pancreatic β-cell function and mass in the background of peripheral insulin resistance. Inflammatory cytokines, e.g. interleukin (IL)-1β, which are elevated in inflammatory conditions of patients with metabolic diseases, induce β-cell apoptosis. A protective effect of high density lipoprotein (HDL) on pancreatic β-cells against high glucose- and IL-1β-induced apoptosis was described previously. Thus, the goal of this project was to elucidate the mechanism underlying the protective effects of HDL and its components in β-cells.

We investigated IL-1β-induced apoptosis in INS-1E cells, a rat β-cell line, in the presence or absence of HDL and several of its components. The anti-apoptotic effect of HDL and the HDL protein moiety was specific and dose-dependent. However, an anti-apoptotic effect was not found for neither purified apolipoprotein (apo) A1, nor the HDL lipid moiety, nor spingosine-1-phosphate. ApoC1 was identified as anti-apoptotic protein in HDL by mass spectrometry. Our experiments with HDL from apoC1-deficient and apoC1-transgene mice were ambiguous. Obviously, the protective effects of human and murine HDL on INS-1E cells were not easily comparable. A first study with human HDL from patients with metabolic diseases – who have decreased apoC1 levels in general – revealed a correlation between the apoC1 content of HDL and its anti-apoptotic potential irrespective of the glycemic state of the patient. However, there was no correlation between the apoC1 content of HDL and incident type 2 DM in a longitudinal study.

A gene array analysis revealed a massive effect of IL-1β on gene transcription in INS-1E cells. The relatively small attenuation by HDL on IL-1β-induced changes in gene expression was located in genes related to the unfolded protein response among others. Our results and results from other laboratories confirmed a protective role for HDL against endoplasmic reticulum (ER) stress. These protective effects were not mediated by apoC1, however.

Unfortunately, additional experiments on the anti-apoptotic effect of apoC1 were impeded by major problems with our apoptosis model.

Concluding experiments on the protective effects of HDL from type 1 and type 2 diabetic patients against ER-stress-induced apoptosis were performed with thapsigargin (ThG)-stimulated apoptosis in INS-1E cells. Several adverse effects of metabolic diseases on the

protective properties of HDL were reported previously. Therefore, comprehensive experiments were done in endothelial cells and macrophages to check whether HDL from type 1 and type 2 DM patients share dysfunctions, and whether the different functionalities of HDL correlate with each other. Unfortunately, the HDL samples from the different patient groups did not differ by their abilities to protect pancreatic β-cells from ThG-induced apoptosis. In the comprehensive experiments no significant differences were detected neither with endothelial cells (i.e. measurements of the stimulated nitride oxide production, adhesion molecule expression, and inhibition of starvation-induced apoptosis), nor macrophages (i.e. cholesterol efflux measurements). With regard to the relatively high analytical variation of the bioassays and the rather small sample number, our study may have not been powered enough to find any significant differences between the control subjects and the patient groups.

In conclusion, the ability of HDL to protect INS-1E cells from IL-1β- and ThG-/ER-stress-induced apoptosis seems to rely on different structural determinants and mechanisms. However, our in vitro findings on the anti-apoptotic activities of apoC1 in HDL and could not be translated into biomarkers that help to identify patients with increased risk of diabetes.

2. Zusammenfassung

Der zunehmende Verlust von Funktion und Anzahl der pankreatischen β-Zellen im Kontext der peripheren Insulinresistenz führt zum Übergang von normaler zu gestörter Glukosetoleranz und schliesslich zu manifestem Typ 2 Diabetes Mellitus (DM). Entzündungszustände, die bei Patienten mit metabolischen Erkrankungen häufig auftreten, führen zu zytokinvermittelter Apoptose der β-Zellen. Vorgängig wurde bereits eine schützende Wirkung von High density Lipoprotein (HDL) auf pankreatische β-Zellen gegen durch Glukose- und Interleukin (IL)-1β-induzierte Apoptose beschrieben. Das Ziel der hier vorgelegten Arbeit war nun die Entschlüsselung der Mechanismen des schützenden Effektes von HDL und seinen Bestandteilen auf β-Zellen.

Wir untersuchten die IL-1β-induzierte Apoptose in INS-1E Zellen, einer β-Zelllinie aus Ratten, mit und ohne HDL und verschiedenen HDL-Bestandteilen. Die anti-apoptotische Wirkung von HDL und seines Proteinanteils war spezifisch und dosisabhängig. Weder für das aufgereinigte Apolipoprotein (Apo) A1, noch für den Lipidanteil von HDL, noch für Sphingosin-1-Phosphat konnte jedoch ein solcher Effekt gezeigt werden. Mittels Massenspektrometrie wurde ApoC1 als ein anti-apoptotisches Protein in HDL gefunden. Unsere Experimente mit HDL von ApoC1-defizienten oder ApoC1-transgenen Mäusen waren leider uneindeutig. Die Wirkungen von menschlichem und murinem HDL liessen sich nicht direkt vergleichen.

Eine erste Studie mit humanem HDL von Patienten mit metabolischen Erkrankungen, welche üblicherweise tiefere ApoC1-Spiegel haben, zeigte eine Korrelation zwischen dem ApoC1-Spiegel und der anti-apoptotischen Wirkung des zugehörigen HDLs – ungeachtet des Nüchternen-Blutzuckers. Es fand sich jedoch keine Beziehung zwischen dem ApoC1-Spiegel des HDLs und Neuerkrankungen an Typ 2 DM in unserer prospektiven Studie.

Eine Genexpressionsanalyse zeigte deutliche Veränderungen im Transkriptom von INS-1E Zellen nach IL-1β-Exposition. Die Abschwächungen dieser Veränderungen durch HDL waren relativ klein und wurden unter anderem in der Unfolded Protein Response angezeigt. Unsere weiteren Resultate wie auch Resultate von anderen bestätigten eine schützende Wirkung von HDL gegen Stress im Endoplasmatischen Retikulum (ER) in β-Zellen. Diese Wirkung wurde jedoch nicht von ApoC1 ausgeübt. Weiterführende Experimente zur anti-apoptotischen Wirkung von ApoC1 wurden unglücklicherweise durch schwerwiegende Probleme mit dem bisherigen Apoptosemodell verhindert.

Abschliessende Experimente zur schützenden Wirkung von HDL von Patienten mit Typ 1 und Typ 2 DM wurden in INS-1E-Zellen mit durch den ER-Stressor Thapsigargin (ThG)-induzierter Apoptose durchgeführt. Verschiedene Verschlechterungen der schützenden HDL-Wirkungen auf Endothelzellen waren bereits beschrieben worden. Daher führten wir weitergehende Experimente in Endothelzellen und Makrophagen mit diesen HDL-Proben durch, um zu testen, ob HDL von Patienten mit Typ 1 und Typ 2 DM ähnliche Funktionsstörungen tragen und ob diese miteinander korrelieren. Leider fanden wir keine signifikanten Unterschiede zwischen diesen HDL-Proben und den Kontroll-HDLs in der schützenden Wirkung gegen ThG-induzierte Apoptose in β-Zellen. Auch in den Experimenten mit Endothelzellen (Messungen der stimulierten Stickstoffmonoxidproduktion, der Expression von Adhäsionsmolekülen und Verhinderung von durch Aushungern induzierter Apoptose) und Makrophagen (Messungen des Cholesterineffluxes) zeigten sich keine Unterschiede. Angesichts der relativ grossen Variation der Daten aus den Bioassays und der eher kleinen Probandenzahl, war unsere Studie vermutlich unterpowert, um signifikante Unterschiede zwischen den Patienten- und Kontrollgruppen festzustellen.

Zusammenfassend kann man sagen, dass die Fähigkeit von HDL, INS-1E-Zellen vor der durch IL-1β- und ThG-/ER-Stress-induzierte Apoptose offenbar auf verschiedenen strukturellen Faktoren und Mechanismen beruht. Leider konnten wir unsere Resultate zu den anti-apoptotischen Wirkungen von HDL und ApoC1 nicht in Biomarker umsetzen, welche uns helfen würden, Patienten mit einem erhöhten Diabetesrisiko zu identifizieren.

3. Abbreviations

ABC	ATP-binding Cassette Transporter
ACS	Acute Coronary Syndrome
AIF	Apoptosis-Inducing Factor
AMPK	AMP-Activated Protein Kinase
APAF-1	Apoptotic Protease Activating Factor 1
apo	Apolipoprotein
ATF6	Activating Transcription Factor 6
ATP	Adenosin Triphosphate
ATPIII	Adult Treatment Panel III
Bad	Bcl-2-associated Death Promotor
BAEC	Boviane Aortic Endothelial Cells
Bak	Bcl-2 Homologous Antagonist/Killer
Bax	Bcl-2-associated X Protein
Bcl-2	B-cell lymphoma 2
Bcl-xL	Bcl-extra Large
Bid	BH3 Interacting-domain Death Agonist
Bim	Bcl-2-like Protein 11
BMI	Bodymass Index
CAD	Stable Coronary Artery Disease
cAMP	cyclic Adenosine Monophosphate
CE	Cholesterol Esters
CETP	Cholesterol Ester Transfer Protein
CFLAR/FLIP	CASP8 and FADD-like apoptosis regulator / FLICE-like inhibitory protein
CHOP	C/EBP Homologous Protein
CKD	Chronic Kidney Disease
Ctrl	Control
DAPI	4’,6-Diamidino-2-Phenylindole
dATP	Deoxyadenosine Triphosphate
db/db	Deficient Leptin Receptor
DIABLO/SMAC	Direct IAP (Inhibitor of Apoptosis Protein)-Binding Protein with low PI / Second Mitochondria-derived Activator of Caspases
(T1/T2)DM	Diabetes Mellitus (type 1 / type 2)
DP5	Death Protein 5
EDTA	Ethylendiaminetetraacetic Acid
eGFR	estimated Glomerular Filtration Rate
EL	Endothelial Lipase
EndoG	Endonuclease G
ER	Endoplasmic Reticulum
ERAD	ER-Associated Protein Degradation
FACS	Fluorescence Activated Cell Sorter
FBS	Fetal Bovine Serum
FC	Free Cholesterol
GLP-1	Glucagon-Like Peptide-1
GLUT	Glucose Transporter

GTT	Glucose Tolerance Test
HAEC	Human Aortic Endothelial Cells
HbA1c	Glycated Hemoglobin A1c
HDL (-C)	High-Density Lipoprotein (-Cholesterol)
hIAPP	Human Islet Amyloid Peptide
HMG-CoAR	Hydroxymethylglutaryl Coenzmy A Reductase
HL	Hepatic Lipase
HOMA-IR	homeostatic model assessment-insulin resistance
hs-CRP	high-sensitivity C-reactive Protein
HTRA2	High-Temperature Requirement Serine Peptidase 2
IFG	Impaired Fasting Glucose
IFN	Interferon
IL-1β	Interleukin-1β
IL-1R	IL-1 Receptor
IL-1RA	IL-1 Receptor Antagonist
IMS	Mitochondrial Intermembrane Space
iNOS	inducible NO Synthase
INS-1E	Rat β-cells from Insulinoma Tumor, Clone 1E
IRE	Inositol-Requiring Enzyme
iT2DM	incident Type 2 Diabetes Mellitus
JNK	c-Jun N-terminal Kinase
LCAT	Lecitin-Cholesterol Acyltransferase
LC-ESI-MS/MS	Liquid Chromatography Electrospray Ionization Tandem Mass Spectrometry
LDL	Low-Density Lipoprotein
MAPK	Mitogen-Activated Protein Kinase
Mcl-1	Myeloid Cell Leukemia 1
MCP-1	Monocyte Chemoattractant Protein 1
MetS	Metabolic Syndrome
Min6	Min6B1 cells, Murine β-cells from Insulinoma Tumor
MOMP	Mitochondrial Outer Membrane Permeabilization
NFG	Normal Fasting Glucose
NF-κB	Nuclear Factor kappa B
NO	Nitric Oxide
PC	Phosphatidyl Choline
PCR	Polymerase Chain Reaction
PCSK9	Proprotein Convertase Subtilisin/Kexin Type 9
PDX-1	Pancreatic and Duodenal Homeobox 1
PERK	Protein Kinase R-like Endoplasmic Reticulum Kinase
PFA	Paraformaldehyde
PI3K	Phosphatidylinositol 3-Kinases
PL	Phospholipids
PLTP	Phospholipid Transfer Protein
PON	Paraoxonase
POPC	1-palmitoyl-2-oleoylphosphatidylcholine
PS	Phosphatidylserine
Puma	p53 Upregulated Modulator of Apoptosis
qPCR	quantitative PCR

RCT	Reverse Cholesterol Transport
ROS	Reactive Oxigen Species
S1P	Sphingosine-1-Phosphate
SAA	Serum Amyloid A
SDMA	Symmetric Dimethylarginine
SDS-PAGE	Sodium Dodecyl Sulfate Polyacrylamide Gel Electrophoresis
SERCA	Sarco/endoplasmic Reticulum Calcium ATPase
SR-BI	Scavenger Receptor Class B Type I
SREBP	Sterol Regulatory Element Binding Protein
STAT1	Signal Transducer and Activator of Transcription 1
TG	Triglycerids
ThG	Thapsigargin
TNF	Tumor Necrosis Factor
UPR	Unfolded Protein Response
VCAM-1	Vascular Cell Adhesion Molecule 1
VIVIT	Vorarlberg Institute for Vascular Investigation and Treatment
VLDL	Very-Low-Density Lipoprotein
WT	Wild-Type
XBP1	X-box Binding Protein 1

4. Introduction

4.1. Diabetes Mellitus

The term “diabetes mellitus” (DM) describes several diseases that all are characterized by chronically elevated blood glucose levels, i.e. hyperglycemia [1]. Hyperglycemia can be caused by the lack of insulin, the absence of insulin action, or both. Acute symptoms of DM are frequent urination, increased thirst and hunger, and weight loss. However, macrovascular and microvascular complications, the clinical sequelae of chronical hyperglycemia, are severe.

4.1.1. History of Diabetes Mellitus

Before 1500 A.C., the ancient Egyptian physician Hesy-Ra was the first known in history to describe polyuria in disease [2]. About 1000 A.C., the Indian physician Shushruta Samhita described the sweet taste of the urine along with polyuria. The ancient Greek physicians associated the disease with the kidneys. In the end of the second century A.D., the Greek physician Aretaeus applied the term “diabetes” (which means “siphon”) in his very detailed description of the symptoms and stages of the disease [3]. Around 1000 A.D., the Persian physician Avicenna differentiated between “primary” and “secondary” diabetes, the former being found in children, the latter associated with obesity. In the 17th century, the English physician Th. Willis differentiated between diabetes insipidus and diabetes mellitus, and thereby coined the terms. In 1889, J. von Mering and O. Minkowski performed pancreatectomy experiments with dogs, and linked the pancreas to diabetes mellitus [4,5]. Later, Minkonwski and colleagues used pancreatic extracts to cure diabetes mellitus after pancratectomy in dogs. In 1921, insulin was isolated as a pure substance by F.G. Banting, Ch.H. Best, J. MacLeod, and J. Collip [6]. One year later, purified bovine insulin was successfully used to treat a diabetic boy. In 1923, Banting and MacLeod were awarded the Nobel Prize in Physiology or Medicine for this discovery. Best and Banting made the purification procedure publicly disposable free of charge. Thus, insulin was rapidly available for treatment of diabetes around the world. In 1936, H.P. Himsworth established the clear differentiation between an insulin-sensitive and insulin-insensitive form of diabetes mellitus [7]. However, researchers did not realize that most mature diabetic patients suffered from insulin-resistant tissue rather than secretory defects in β-cells before the technology to quantify human insulin in plasma

with a radioimmunoassay was established in 1960 [8,9]. Furthermore, the fact that obese, non-diabetic individuals showed higher insulin levels in response to a glucose load than healthy men at comparable glucose levels during the test led to the concept of a prediabetic state [10]. Additionally, young diabetic patients were found to have low to undetectable levels of insulin. Thus, the different pathogenesis of type 1 and type 2 diabetes mellitus was established.

4.1.2. Blood Glucose Homeostasis

In healthy individuals, blood glucose levels are tightly regulated by the hormones insulin and glucagon. Both are produced by endocrine cells of the islets of Langerhans within the pancreas: Insulin by the β-cells, glucagon by the α-cells. Blood glucose regulation is important because a minimal glucose level is required for proper brain function. On the other hand, permanently high glucose levels induce macro- and microvascular diseases, and damage nerves. Diseases associated with chronically elevated blood glucose levels include atherosclerosis, neuropathy, retinopathy, and nephropathy [1].

Blood glucose rises physiologically in the postprandial state. Thus, glucose diffuses from the bloodstream into the β-cells via facilitated diffusion (mediated by glucose transporter GLUT-2) where it stimulates insulin release. Insulin lowers the blood glucose levels via signaling to target cells: Adipocytes and muscle cells incorporate glucose via the insulin-sensitive glucose transporter GLUT-4 [11,12]. Glucose is stored in the form of glycogen (glycogenesis) in hepatocytes and muscle cells. In adipocytes, glucose is converted to fatty acids, and stored as triglycerides. These processes are stimulated by insulin. Moreover, the catabolism of fatty acids and amino acids into glucose (gluconeogenesis), and the catabolism of glycogen stocks in the liver (glycogenolysis) are inhibited by insulin.

Glucagon, the antagonist of insulin, raises blood glucose levels by the induction of glycogenolysis in hepatocytes.

4.1.3. β-Cell Mass and Function

A healthy human adult has approximately 1 million islets of Langerhans scattered in his pancreas that contain 2000 to 3000 β-cells each [13]. β-cell mass is determined by the individual genome, intrauterine and early-life environmental factors, and lifestyle. It can expand in

adults upon demand, such as pregnancy, overweight, and insulin resistance in metabolic syndrome [14–16]. β-cell mass was found to be increased by 50 to 90% in overweight and obese individuals [17]. The proliferative capacity of rodent β-cells seems to be much higher compared to human β-cells [13]. However, neogenesis could possibly provide additional β-cells for β-cell mass expansion [18].

The main functions of β-cells are insulin production and insulin secretion upon demand. Insulin is expressed as preproinsulin which undergoes massive procession to form active insulin. In the endoplasmic reticulum (ER), the signal peptide is cleaved off, and the three disulfide bridges are formed to stabilize the protein. The folded proinsulin is then transported to the trans Golgi network where it is packed into immature vesicles. During the maturation of the insulin vesicles, the C-peptide is cleaved from proinsulin. Thus, mature vesicles filled with fully processed insulin are in stand-by for release [19]. For the elucidation of the primary structure of bovine insulin, F. Sanger received the Nobel Prize in Chemistry in 1958.

In non-diabetic individuals, a pulsatile insulin secretion is present in the fasted state, though at low levels [20]. Cytosolic Ca^{2+} levels, which have a pulsatile pattern itself, regulate this oscillation. At elevated blood glucose levels, glucose enters β-cells via GLUT-2 [21]. In the cytosol, glucose is metabolized to glucose-6-phosphate which enters glycolysis in the mitochondria. The generated adenosine triphosphate (ATP) induces the closure of ATP-sensitive K^+-channels, which in turn depolarizes the plasma membrane of the cell. Consequently, voltage-gated Ca^{2+}-channels open, and calcium ions enter the cell. The elevated Ca^{2+} concentration in the cytosol leads to the fusion of primed (“readily releasable”) insulin-filled vesicles to the plasma membrane, i.e. the first-phase insulin secretion. This first-phase insulin secretion happens three to five minutes after the rise in blood glucose, and lasts about ten minutes. The first-phase insulin secretion mediates the switch from the fasted to the fed state, including the suppression of hepatic glycogenolysis and lipolysis in adipocytes [20]. The second-phase insulin secretion is slower but more enduring. It requires insulin-filled vesicles to be transported to the cell membrane and priming. This process is promoted by incretins, i.e. gastro-intestinal hormones that are secreted in the postprandial state.

To maintain insulin secretion, more insulin has to be produced, and new granules have to be prepared. Several transcription factors regulate the expression of the insulin gene. Among others, glucose and the resulting cyclic adenosine monophosphate (cAMP, which binds to the

transcription factor cAMP response element binding protein (CREB)) induce the expression of insulin [22].

In addition to the above described expansion of β-cell mass in response to an increased metabolic demand, β-cells are able to upregulate insulin production by several fold [17]. Nevertheless, insulin hypersecretion of β-cells of non-diabetic, obese individuals still follows a physiologically pulsatile pattern with about 11 pulses per day [23].

4.1.4. Type 1 and Type 2 Diabetes Mellitus

The global report on diabetes [24] estimated that 422 million adults suffered from diabetes in 2014, a pronounced rise compared to 108 million in 1980. Since then, the global prevalence (age-standardized) of diabetes augmented from 4.7% to 8.5% in the adult population. In Switzerland, the prevalence of diabetes in adults was estimated to be 5.6% for 2014 [24]. Since Western life-style with an abundance of high caloric food and a lack of physical exercise is spreading, it is expected that worldwide the cases of type 2 DM will increase to 693 million by 2045 [25].

Both, type 1 and type 2 diabetes mellitus (DM) are characterized by chronically elevated blood glucose levels [1]. In type 1 DM the cause for the hyperglycemia is the absence of sufficient β-cells: In an autoimmune reaction, the immune system attacks the β-cells and destroys most of them. The remaining β-cells cannot produce an adequate amount of insulin to maintain normoglycemia: We observe an absolute insulin deficiency with decreased insulin production but normal insulin demand.

In type 2 DM, which accounts for the majority of all DM cases, subjects have a pronounced insulin resistance in peripheral tissues [15]. As long as the body compensates the increased insulin demand with increased insulin production and secretion, subjects maintain normoglycemia. Type 2 DM manifests when the insulin production fails to control blood glucose levels: We observe a relative insulin deficiency with a normal or decreased insulin production, and increased insulin demand.

4.1.5. Pathogenesis of Type 2 Diabetes Mellitus

Long before the possible manifestation of type 2 diabetes, insulin resistance in hepatocytes, myocytes, adipocytes, and other cells is found as part of the metabolic syndrome [26]. Furthermore, the metabolic syndrome is associated with obesity, ageing, and physical inactivity. In insulin resistance, glucose uptake into myocytes and adipocytes is reduced, and glycogen synthesis is decreased in hepatocytes [11]. Thus, less glycogen is stored in muscle and liver cells, and lipogenesis is decreased in the adipose tissue. Moreover, gluconeogenesis and glycogenolysis in hepatocytes, as well as hydrolysis of triglycerides in adipocytes are not suppressed sufficiently in the insulin resistant state. This results in increased glucose and free fatty acid levels in the circulation. The latter further attenuates insulin sensitivity in peripheral tissues. In response to insulin resistance, insulin production is increased by upregulation of insulin synthesis and secretion, and/or expansion of β-cell mass [15]. Thus, most of insulin resistant individuals maintain normoglycemia for years or even the rest of their life. Hyperglycemia and type 2 DM develop once the β-cells fail to produce and secrete sufficient insulin to meet the metabolic demand.

Butler and colleagues analyzed the pancreatic tissue of 124 autopsies [27]. Whereas the β-cell mass of diabetic patients was in the range of healthy, lean individuals, β-cell mass was up to 50% higher in obese non-diabetic subjects. Subjects with type 2 DM thus had less β-cell mass than their non-diabetic weight- and age-matched controls. The abundance of a marker for proliferation was low but did not differ between obese subjects with and obese subjects without type 2 DM. Conversely, apoptosis was tenfold elevated in the islets of obese subjects with type 2 DM compared to non-diabetic, obese subjects. This indicates that during the pathogenesis of type 2 DM there is a concomitant loss of (previously expanded) β-cell mass. In accordance with this, a reduction in β-cell mass of 24 to 65%, possibly depending on disease duration, has been reported by different studies [17]. Mechanisms leading to β-cell apoptosis are described in section 4.2.4 below.

The remaining β-cells exhibit impaired function. Compared to healthy individuals, the insulin secretion capacity was found to be decreased by 50 to 97% in type 2 DM patients [17]. Insulin synthesis is decreased in β-cells of diabetic patients. The transcription of the insulin gene is regulated by the interaction of ubiquitous and islet specific transcription factors which activate the insulin promoter [28]. High glucose levels as well as the incretin GLP-1 (glucagon-

like peptide-1) increase intracellular cyclic adenosine monophosphate (cAMP) concentration. cAMP induces PDX-1 (pancreatic and duodenal homeobox 1), an important transcription factor for insulin via PI3 (phosphatidylinositide 3) and MAPK (mitogen-activated protein kinase) pathways. These can be induced by external (acute) stimuli such as glucose, GLP-1, insulin, or palmitate. However, prolonged exposure to high glucose or palmitate concentration was found to reduce PDX-1 levels in β-cells. Moreover, preproinsulin needs to undergo posttranslational modification before it is active: Cleavage of the signal peptide, formation of disulfide bridges, and protein folding happen in the ER [19]. ER stress, which occurs as a consequence of chronic exposure to high glucose concentration or high free fatty acid levels, stalls the procession of the protein [29]. Increased levels of free fatty acids, such as palmitate, are found in obese subjects before hyperglycemia occurs. Since palmitate alone elicits ER stress by hampering the transfer of proteins to the trans-Golgi network, it is possible that this fatty acid impedes the procession of preproinsulin. When ER stress persists, chronic ER stress can lead to apoptosis. Studies in transgenic mice and with mutated cholesterol efflux-related proteins in humans indicate that cholesterol homeostasis is crucial for proper β-cell function. These studies are discussed below in section 4.3.5.

Besides decreased insulin synthesis, the remaining β-cells display a disturbed secretion pattern in type 2 DM. As mentioned above, insulin is secreted in a first and second peak when blood glucose rises in normoglycemic subjects. The first-phase insulin secretion is lost in type 2 DM patients at the time of diagnosis [20]. The second-phase insulin secretion is usually delayed and reduced. Reduction in the first-phase insulin secretion is often found before the manifestation of the disease, i.e. in individuals with impaired glucose tolerance, as well as in first-degree relatives of type 2 DM patients. Subjects without first-phase insulin secretion are therefore considered at high risk for developing type 2 DM.

The exact causes – as well as their interactions – that lead to β-cell dysfunction and apoptosis are still to be determined. Possible pathogenic mechanisms include mitochondrial dysfunction, oxidative stress, ER stress, glucolipotoxicity, and amyloid deposition [15,30]. Moreover, most of these mechanisms are related to tissue inflammation and influence both, insulin resistance and β-cell failure. Clinical studies in which different inflammatory pathways were modulated are discussed in section 4.2.5. below.

4.2. Apoptosis

4.2.1. Different Cell Death Routines

Several modalities of cell death are differentiated into apoptosis, necrosis, autophagy, and other, more specialized forms. Historically, the cell death categories were defined by morphological changes occurring in the dying cell. Apoptosis was defined by cell shrinkage, chromatin condensation, nuclear fragmentation, extracellular exposure of phosphatidylserine, membrane blebbing, and engulfment of cell components into "apoptotic bodies" [31]. The remainders of the apoptotic cell are phagocytosed by macrophages or taken up by neighboring cells. In contrast to this regulated cell death, necrosis was defined as uncontrolled cell death in response to harsh cell or tissue damage. Here, the cells swell, cell membranes rupture, and cell components are released that cause a local inflammatory response.

Nowadays, several biochemical parameters are measured to determine and quantify apoptosis as well as other forms of cell death [32]. Since there is an overlap of features of different cell death pathways, several biochemical parameters should be measured in order to define the cell death mechanism. Moreover, biochemical actions related to cell death can occur at a sublethal level (i.e. at a reversible state) or be caused by a process other than cell death (e.g. proliferation).

4.2.2. Extrinsic Apoptosis

Extrinsic apoptosis is a cell death pathway in which an extracellular stress signal (e.g. FAS-ligand, tumor necrosis factor (TNF)) induces caspase-dependent apoptosis via specific transmembrane receptors (e.g. FAS receptor, TNF receptor) [32]. Specific cytosolic proteins and procaspases (e.g. procaspase 8, procaspase 10) are recruited to the intracellular death domain, where these (initiator) caspases are cleaved and thereby activated. Activated caspase 8 (or 10) cleaves and activates effector caspases (e.g. caspase 3, 6, and 7) directly in some cell types. In other cells, such as pancreatic β-cells, active caspase 8 cleaves *BID* (Bcl-2 homology 3 interacting-domain death agonist), a pro-apoptotic member of the *Bcl-2* (B-cell lymphoma 2) family proteins which initiates mitochondrial outer membrane permeabilization (MOMP).

MOMP induces the formation of the apoptosome (described below) which activates procaspase 9 by cleavage. Thus, caspase 9 activates the effector caspases.

4.2.3. Intrinsic Apoptosis

Intrinsic apoptosis occurs via a caspase-dependent or -independent pathway [32]. The elicitor of intrinsic apoptosis is pronounced intracellular stress which possibly originates from DNA damage, oxidative stress, cytosolic Ca^{2+} overload, and/or accumulation of unfolded proteins in the endoplasmic reticulum (ER). Such stress signals unbalance the homeostasis of pro- and anti-apoptotic signals at the mitochondrial membrane. In healthy cells, anti-apoptotic Bcl-2 family proteins such as *Bcl-2* (B-cell lymphoma-2), *Bcl-xL* (Bcl-extra large), and *Mcl-1* (myeloid cell leukemia 1) maintain the mitochondrial transmembrane potential as they prevent pro-apoptotic *BCL-2* family proteins such as *Bak* (*Bcl-2* homologous antagonist/killer), *Bax* (*Bcl-2*-associated X protein), *Bad* (*Bcl-2*-associated death promoter), *Bid* (*BH3* interacting-domain death agonist), *Bim* (*Bcl-2*-like protein 11), and *Puma* (p53 upregulated modulator of apoptosis) from the induction of pore formation in the outer mitochondrial membrane by physical interaction [33]. Once the mitochondrial outer membrane is permeable (MOMP), proteins residing in the mitochondrial intermembrane space (IMS) are released into the cytosol. These IMS-proteins have different functions in the intrinsic apoptotic pathway: cytochrome C becomes part of the apoptosome, apoptosis-inducing factor (*AIF*) and endonuclease G (*endoG*) digest DNA in the nucleus, *HTRA2* (high-temperature requirement serine peptidase 2) cleaves actin filaments, *DIABLO/SMAC* (direct *IAP* (inhibitor of apoptosis protein)-binding protein with low PI / second mitochondria-derived activator of caspases) and *HTRA2* inhibit anti-apoptotic factors. Besides the release of IMS-proteins, lethal consequences of MOMP are the dissipation of the mitochondrial membrane potential with the resulting cessation of mitochondrial ATP synthesis, and the inhibition of the respiratory chain, which is accompanied by overproduction of reactive oxygen species (ROS). The apoptosome, consisting of cytochrome C, *APAF-1* (apoptotic protease activating factor 1), and dATP (deoxyadenosine triphosphate), activates caspase 9 which in turn cleaves procaspase 3 into active caspase 3 that commonly operates apoptosis.

The caspase-independent intrinsic apoptosis is executed directly by enzymes from the IMS (i.e. *HTRA2, endoG* and *AIF*), which digest cell components such as DNA and the cytoskeleton,

or is induced by the cessation of ATP, excess ROS production, or the inhibition of the respiratory chain.

4.2.4. β-Cell Apoptosis

In both, type 1 and type 2 DM, β-cell apoptosis is a major pathogenic event [33,34]. In type 2 DM, death receptor-mediated (extrinsic) as well as intrinsic apoptosis are potentially relevant for apoptosis [35].

Intrinsic apoptosis in pancreatic β-cells has been described as a reaction to ER stress [36] (Fig 4.1). High glucose and/or elevated free fatty acid levels stimulate insulin secretion if they are present for a short time – if theses stimuli persist, they induce ER stress. Constantly high glucose levels were found to cause a maladjustment of the pro- and anti-apoptotic *BCL-2* family proteins, which induces MOMP and subsequent apoptosis [37]. Whereas short term glucose exposure induces the expression of chaperones which sustain the elevated demand for insulin, long term exposure to high glucose was found to cause ER stress-induced apoptosis [38]. *CHOP* (C/EBP homologous protein) is an ER stress induced transcription factor downstream of *PERK* (protein kinase R-like endoplasmic reticulum kinase) and *ATF6* (Activating transcription factor 6). CHOP downregulates *BCL-2* and upregulates *DP5* (death protein 5) as well as *Bim* (*Bcl-2* interacting mediator of cell death). The consequences of ER stress-induced *CHOP* expression are therefore likely to induce apoptosis via MOMP. The fatty acid palmitate was shown to induce factors of the unfolded protein response (UPR; i.e. *PERK, ATF6,* and *IRE* (inositol-requiring enzyme) 1α signaling) and apoptosis in INS-1E cells, rat β-cells, and human islets [39]. Potentiation of this effect with high glucose was minor, however. Subsequently, palmitate-induced factors of the UPR were found to be associated with the up- and downregulation of pro- and anti-apoptotic *BCL-2* family proteins in a manner that favors apoptosis [40].

As mentioned above, metabolic syndrome and obesity often precede type 2 DM. Adipose tissue secretes inflammatory factors such as interleukin (IL)-1β and tumor necrosis factor (TNF) [30]. Since the IL-1 receptor is highly expressed in β-cells, these cells are potentially very susceptible to IL-1β. At elevated glucose levels, β-cells produce and release IL-1β [41]. Furthermore, free fatty acids and their metabolites stimulate IL-1β release from β-cells [30]. Macrophages are attracted to pancreatic islets in the diabetic milieu [42]. *NLRP3* (NLR family

pyrin domain containing 3) which is highly expressed in macrophages could further contribute to the IL-1β production in pancreatic islets [35]. The fact that β-cells seem to possess an internal protection system against IL-1β, i.e. the local expression of the IL-1 receptor antagonist, emphasizes the vulnerability of β-cells to inflammation [43].

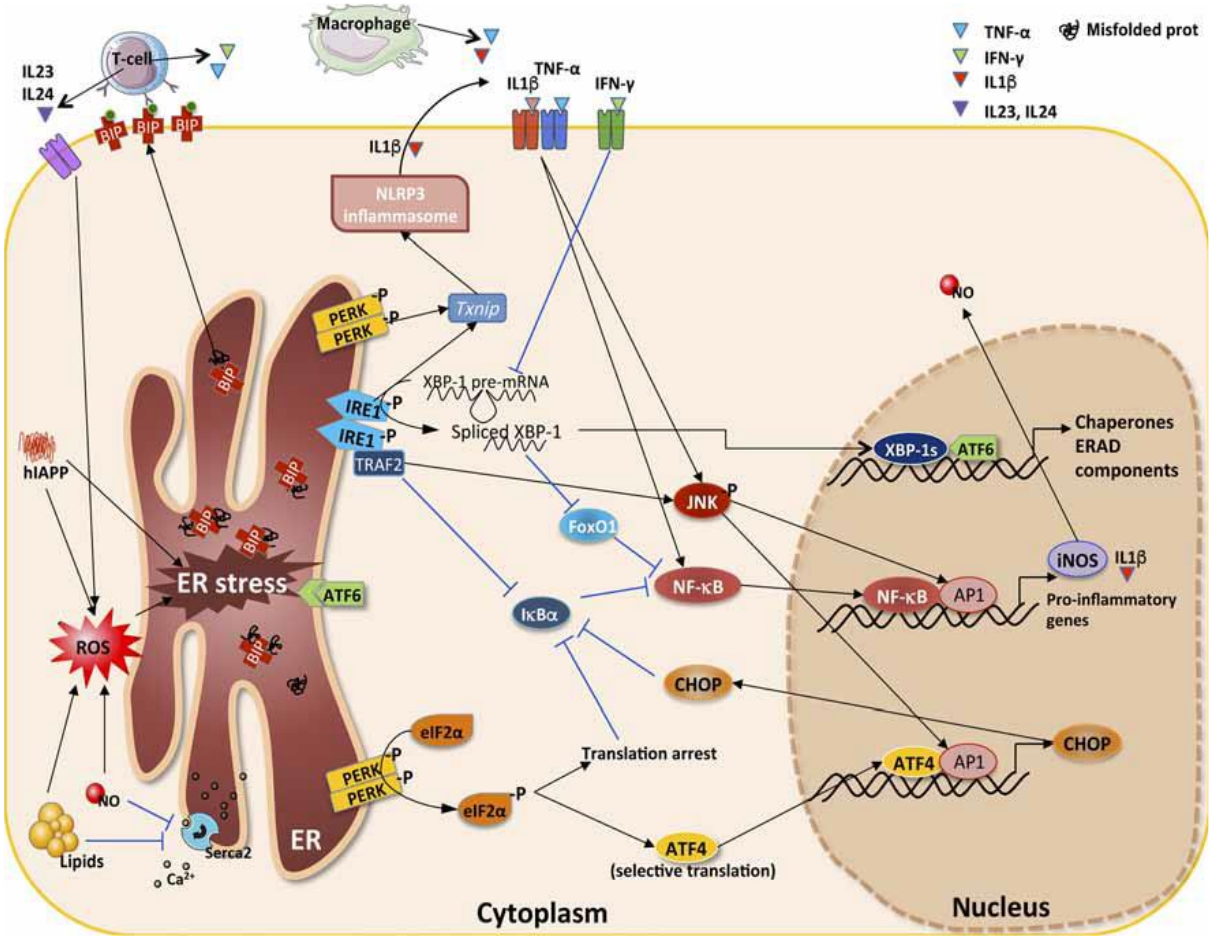

Figure 4.1: Schematic representation of the possible cross talks between UPR and pro-inflammatory pathways in pancreatic β-cells under ER stress [36].
Pro-inflammatory cytokines (IL1β, TNF, and IFN among others), lipids (free fatty acids), human islet amyloid polypeptides (hIAPP) aggregates, and SERCA2 Ca^{2+} pump blockers induce ER stress by diverse mechanisms such as NO formation, ROS production, and ER calcium depletion leading to UPR activation in pancreatic β-cells. ER stress induced phosphorylation of PERK, and the activation of ATF6 and IRE1α induce signaling cascades, partially via JNK and NF-κB, which increase the expression of chaperones, endoplasmic-reticulum-associated protein degradation (ERAD) components, CHOP, and several pro-inflammatory genes. This ER stress-mediated inflammatory state contributes to the maintenance of ER stress and probably leads to β-cell demise.

In β-cells, IL-1β and TNFα (a ligand which induces extrinsic apoptosis via TNF receptor) both activate nuclear factor kappa B (NF-κB) which can promote cell survival or mediate cell death via increased nitric oxide (NO) production [44,45]. The cytokines IL-1β and interferon (IFN)-γ were

found to induce NO production via NF-κB/iNOS (inducible NO synthase) in β-cells [46]. The elevated NO levels disturb the Ca^{2+} homeostasis of the ER by down regulation of SERCA (sarco/endoplasmic reticulum Ca^{2+}-ATPase), a Ca^{2+} pump, and thus induce ER stress and apoptosis. Chan and colleges suggested the c-Jun N-terminal kinase (JNK) as a key regulator in the transition from the adaptive UPR which resolves ER stress to the destructive UPR which initiates apoptosis [47]. They described that the imbalance of *CHOP* and *XBP1* (X-box binding protein 1), which occurs in ER stress conditions as a response to cytokine or palmitate exposure, favors the apoptotic over the adaptive UPR. Moreover, they postulated that ER stress as an early event in the pathogenesis of diabetes precedes oxidative stress and inflammation. The important role of JNK and cytokine-induced ER stress in β-cell apoptosis of mice, rats, and humans was also described by Brozzi and colleges [48]. Additionally, they found differences between species: Whereas NO inhibition prevented cytokine-induced apoptosis in rat β-cells, murine and human β-cells were not protected from ER stress and apoptosis induced by cytokines.

Besides a plausible role for cytokine-induced ER stress in β-cell apoptosis, direct effects of the inflammatory cytokines IL-1β, IFN-γ, and/or TNF-α on the mitochondrial apoptotic pathways have been described [33]. Inflammatory cytokines may shift the balance of pro- and anti-inflammatory members of the *Bcl-2* family of proteins by modulating the activity and expression of these proteins. This triggers the mitochondrial outer membrane permeability (MOMP, described in section 4.2.3.).

Another factor described to induce apoptosis is the deposition of human islet amyloid poly-peptide (hIAPP) in β-cells. The amount of these depositions was found to correlate with β-cell apoptosis and decreased β-cell area in human pancreatic samples [49]. The treatment of islets isolated from transgenic mice overexpressing human IAPP with elevated glucose conditions resulted in the upregulation of genes belonging to the extrinsic pathway (Fas ligand and Fas-associated protein with death domain (FADD)) and the intrinsic pathway (*Bim*) [50]. In both apoptotic pathways, hIAPP activated JNK signaling and caspase 3 cleavage. Moreover, islet macrophages may produce IL-1β in response to hIAPP-deposits which is harmful for the islet β-cells [51]. A more recent study found that besides the upregulation of IL-1β in human islets concomitant with β-cell dysfunction and apoptosis, the natural IL-1β antagonist, IL-1 receptor antagonist (IL-1RA) was downregulated by amyloid formation [52].

Whereas FAS ligand is not expressed in β-cells at normal circumstances, high glucose concentrations were found to induce FAS ligand expression in pancreatic β-cells [53]. Thus, the constitutional expression of FAS ligand could induce extrinsic apoptosis.

Several compounds that influence inflammatory cytokines and possibly β-cell apoptosis have been tested in clinical trials which are described in the following section.

4.2.5. Clinical Studies on Inflammation in Type 2 Diabetes Mellitus

Methods to monitor β-cell apoptosis in living humans are not available to date. Therefore, clinical studies cannot provide detailed information about anti-apoptotic effects of the tested compounds [33]. Nevertheless, indirect evidence points to an interference of inflammatory pathway modulators with β-cell apoptosis. Blocking systemic inflammation by the use of salicylates was demonstrated to be an effective strategy to improve hyperglycemia in type 2 diabetes patients [30,54,55]. The relevance of TNFα, macrophages, and IL-1β in the development of type 2 DM and possibly in β-cell apoptosis was demonstrated in several studies in which the respective targets were inhibited or antagonized [56].

Treatment with a TNFα inhibitor reduced HbA1c levels in patients with newly diagnosed type 1 DM as well as their daily insulin dose compared to the placebo-treated patients in a pilot study [57]. In obese individuals, albeit without type 2 DM, 6 months TNFα inhibition treatment reduced fasting glucose levels [58].

A small study found modest glycemic improvements, possibly due to improved β-cell function, in type 2 DM patients treated with C-C chemokine receptor-2 (CCR2) antagonist, which impedes macrophage recruitment [59].

Administration of an IL-1 receptor antagonist improved glycemia durably in type 2 DM patients [60,61]. This effect was confirmed in several smaller studies [33,62]. In a crossover study, treatment with an IL-1β receptor antagonist improved first-phase insulin secretion and the insulinogenic index in subjects with impaired glucose tolerance [63]. The subsequent hypothesis that IL-1β antagonism could prevent incident type 2 DM was addressed within the CANTOS (Canakinumab Anti-inflammatory Thrombosis Outcomes Study) trial which included more than 10’000 individuals with prior myocardial infarction and elevated high-sensitivity C-reactive protein (hs-CRP) [64]. Treatment with three different doses of the monoclonal IL-1β antibody resulted in significant reductions of cardiovascular events compared to placebo.

Despite remarkable reductions in markers of subclinical inflammation (i.e. hs-CRP and interleukin 6) however, the rates of incident diabetes were not significantly different between the treatment groups among the almost 5000 persons with pre-diabetes (i.e. HbA1c of 5.7 to <6.5% and/or fasting plasma glucose of 5.6-6.9 mmol/L). There was but a trend towards lesser cases of incident type 2 DM with anti-IL-1β treatment in the first three years of the study which was inverted in participants after four years of treatment. Study participants with pre-diabetes profited from IL-1β neutralization in terms of reduced HbA1c levels in the first six to nine months of the study. Moreover, a reduction in HbA1c was observed in normoglycemic and diabetic participants at trial entry. Then, the effect on HbA1c was attenuated in all participants and after 48 months, no statistically significant differences in HbA1c levels were recorded between the treatment groups irrespective of their glycemic status. Possibly, the attenuation of the differences in HbA1c originated from lifestyle interventions or changes in other anti-diabetic therapies which were allowed by the study protocol. The absence of an effect of the IL-1β inhibitor on incident type 2 DM might arise from the inclusion criteria (prior myocardial infarction and elevated hs-CRP) of the study which in turn limit the informative value of the results on the general population.

Thus, further studies on inflammatory mediators are required to clarify the role of inflammation in the development and progression of type 2 DM.

4.3. Lipoproteins

4.3.1. Cholesterol

Cholesterol is a vital component of the cell membranes of vertebrate cells [65]. As such, it regulates membrane fluidity and permeability. Regions with high cholesterol content, termed lipid rafts, are characterized by low fluidity. Lipid rafts are often involved in signaling processes, as many receptors reside within these parts of the membrane. Moreover, cholesterol is the precursor for bile acids, steroid hormones, and vitamin D.

In humans, about 30% of the required cholesterol is food-derived, the remainder is synthesized de novo by the cells of the body. Cholesterol synthesis is tightly regulated. Changes in dietary cholesterol are physiologically compensated by up- or downregulated de novo cholesterol synthesis. All nucleated cells are capable of cholesterol synthesis by the mevalonate pathway, in which the rate-limiting step is catalyzed by hydroxymethylglutaryl CoA reductase (HMG-CoAR). The sterol regulatory element binding protein (SREBP) upregulates cholesterol synthesis by the upregulation of HMG-CoAR.

Cholesterol is a lipid and thus not soluble in the aqueous lymph and blood stream. Nevertheless, it needs to be transported from the sites of uptake or de novo synthesis to target cells, including steroidogenic cells. This is termed forward lipid transport. In the reverse lipid transport, excess cholesterol from peripheral tissue is transported to the liver for excretion. For both directions of transport, cholesterol is packed into lipoproteins.

4.3.2. Lipoprotein Structure and Metabolism

The main function of lipoproteins is the transport of lipids in the blood stream and lymph [66]. Amphipathic apolipoproteins, phospholipids (PL), and free cholesterol (FC) emulsify different hydrophobic lipids (mainly triglycerides (TG) and cholesterol esters (CE)) in the hydrophobic core. Lipoproteins have a similar general structure. However, coinciding with their composition, they have specific transport tasks.

Lipoproteins are categorized according to their density (Tab. 4.1) with high-density lipoprotein (HDL) having the highest density and smallest diameter, and chylomicrons at the other edge of the scale.

	Density [g/ml]	*Size*	*Lipids*	*Apolipoproteins*
Chylomicron	<0.940	100-600 nm	TG, PL, CE, FC	B_{48}, A1, A4, C1, C2, C3, E
VLDL	0.940-1.006	60 nm approx.	TG, PL, CE, FC	B_{100}, C1, C2, C3, E
LDL	1.006-1.063	25 nm approx.	CE, PL, FC, TG	B_{100}
HDL	1.063-1.210	7-12 nm	PL, CE, FC, TG	A1, A2, A4, A5, C1, C2, C3, C4, D, E, F, H, J, L1, M

Tab. 4.1: Lipoprotein characteristics and composition [67,68]

Chylomicrons originate from the enterocytes after a meal [66,69]. Their main apolipoprotein (apo) is apoB_{48}, a truncated form of apoB_{100} which is produced by the intestine. Chylomicrons transport dietary lipids initially in the lymph, and enter the systemic bloodstream via the thoracic duct. There, they deliver their lipids either to adipose tissue for energy storage, or to striated muscle for combustion. The lipoprotein lipase hydrolyses the TG in the chylomicrons on thin capillaries of adipose tissue and striated muscle cells. Alternatively, chylomicrons can transfer lipids to HDL in circulation. The lipid-depleted chylomicron remnants are internalized by hepatocytes, where the remaining cholesterol is used for bile acid synthesis, integrated in other lipoproteins, or excreted via feces [66,69].

Very low density lipoproteins (VLDL) have a similar role in forward lipid transport as chylomicrons. However, they are synthesized in hepatocytes, and export endogenously synthesized or recycled TG and CE from the liver to peripheral tissue. VLDL contain the full-length apolipoprotein apoB_{100} as its main apolipoprotein. After the transfer of TG and several apolipoproteins other than apolipoprotein B_{100} to HDL, VLDL remnants are taken up by the liver, or further remodeled into low density lipoprotein (LDL) in circulation [66].

LDL is the product of VLDL remodeling in circulation. It contains apoB_{100} as the only apolipoprotein. The main function of LDL in the human body is to deliver CE to peripheral tissue and the liver [68]. CE is imported by LDL receptor-mediated endocytosis of LDL into target cells [70]. An increase in cellular cholesterol causes the downregulation of the LDL receptor via the transcription factor SREBP.

Depending on its composition, HDL occurs as spherical or discoidal particle [68,71]. HDL is synthesized in the liver and intestine, where apoA1 (HDL's main apolipoprotein) is produced and subsequently lipidated with phosphatidyl choline (PC) and cholesterol by ABC (ATP-binding cassette transporter) A1 (Fig. 4.2) [72]. Although ABCA1 is expressed ubiquitously in the body, lipidation of apoA1 by hepatocytes and enterocytes directly after secretion accounts for

the majority of HDL formation. PL, mostly PC, and other proteins are added to HDL in circulation. The enzyme lecithin-cholesterol acyltransferase (LCAT) mediates the conversion of free cholesterol (FC) into cholesterol ester (CE), and thereby rapidly induces the conversion of discoidal HDL precursors into spherical particles [73]. Cholesterol ester transfer protein (CETP) activity introduces TG from VLDL, LDL, and chylomicrons to HDL in exchange for CE. HDL receives small exchangeable apolipoproteins from other lipoproteins; cholesterol and PC from cells mediated by the ABCA1, the ABC transporter G1 (ABCG1) or scavenger receptor class B type I (SR-BI). The assembly of PL from TG-rich lipoproteins is mediated by phospholipid transfer protein (PLTP). HDL is an important acceptor for excess cholesterol from extrahepatic tissues which are not able to catabolize cholesterol. HDL transports the cholesterol to the liver for excretion with the bile (i.e. reverse cholesterol transport) [66,74].

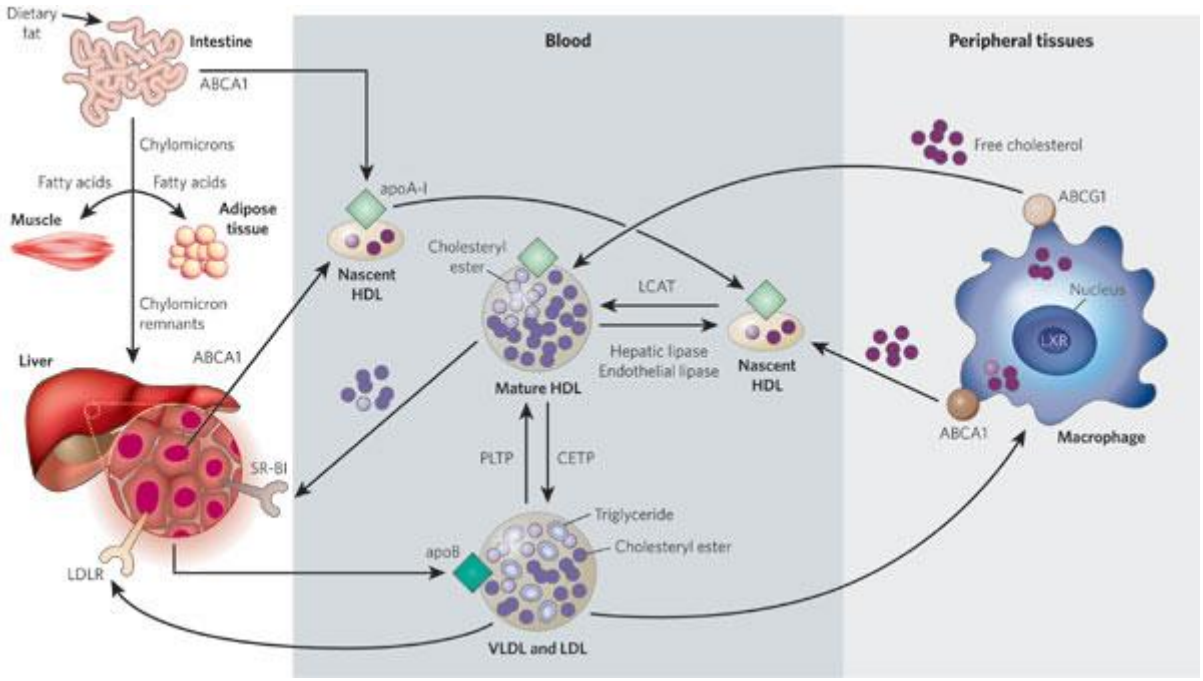

Figure 4.2: Lipoprotein metabolism and generation of HDL[75].
Abbreviations are described in the text, apoA-I corresponds to apoA1

4.3.3. HDL Composition

Lipids

Similarly to other lipoproteins, HDL carries phospholipids (PL, 37-49 mol % of total lipids of HDL) and unesterified/free cholesterol (FC, 9-14% mol % of total lipids of HDL) on the surface [71,76]. The amount of PL per particle is related to the surface of the particle. The hydrophobic

core of HDL consists of cholesterol ester (CE, 35-37 mol % of total lipids of HDL) and triglycerides (TG, approximately 3 mol % of total lipids of HDL). The amount of FC is rather low because the enzyme lecithin-cholesteryl-acyl transferase (LCAT), which converts FC to CE, resides on HDL. HDL also contains several sphingolipids at lower abundance, including sphingosine-1-phosphate, a bioactive lipid. Moreover, oxysterols, steroid hormones, and lipid-soluble vitamins (A and E) are transported by HDL. In total, more than 200 lipid species have been identified in HDL [67].

Proteins

Around 100 different proteins are regularly identified in HDL [67,71,77,78]. By weight, 70% of HDL proteins consist of apoA1, 20% of apoA2, and the remaining 10% are other apolipoproteins as well as enzymes and other proteins. Interestingly, not every HDL particle contains all proteins found in the whole HDL fraction [79]. All of the apolipoproteins found on HDL (Tab. 4.1) are relatively small and exchangeable between lipoproteins [74,78].

Two to five molecules of apoA1 molecules are usually found per HDL particle [67]. Lipid-poor or lipid-free apoA1 is rapidly cleared from the circulation by the kidneys [74]. The second most abundant apolipoprotein on HDL, apoA2, is predominantly produced in hepatocytes [71]. It has a high affinity for lipids [72]. About half of all HDL particles contain apoA2 [71]. ApoA4 is mainly synthesized in the intestine from where it is released as chylomicron component. In the blood circuit it is transferred to HDL [72]. ApoE is predominately synthesized in the liver and integrated into VLDL particles. Upon hydrolysis of VLDL, apoE is incorporated by HDL. The apolipoproteins apoC1, apoC2, apoC3, apoC4, apoD, apoF, apoH, apoJ, apoL1, and apoM, are found on HDL less abundantly. Nevertheless, these apolipoproteins do have specific functions. They activate or inhibit enzymes involved in HDL metabolism [68,71]: LCAT is activated by apoA1, apoA4, apoE, apoC1; LPL is activated by apoA5 and apoC2, and inhibited by apoC1 and apoC3 [80]; hepatic lipase is activated by apoA1 and apoE [72], but inhibited by apoC1, apoC3 and apoA2; CETP is inhibited by apoC1 [81] and apoF. In addition to its functions as activator or inhibitor of specific enzymes, apoC1 was found to inhibit the SR-BI-mediated CE uptake in hepatocytes [82]. Thus, apoC1 increases HDL cholesterol (HDL-C) levels. Since VLDL levels are increased by apoC1 as well, a therapeutic application of apoC1 seems limited [82]. Moreover, apolipoproteins mediate the interaction of lipoproteins with specific receptors, e.g. ABCA1 interacts with apoA1.

Besides apolipoproteins, lipoprotein remodeling proteins are carried by HDL, e.g. LCAT, PLTP, and CETP [67,71,78]. Furthermore, antioxidant enzymes like paraoxonases (PON1 and PON3) or myeloperoxidase, and proteins of the acute phase response, complement regulation, proteinase inhibitors, and proteins involved in the immune response and homeostasis have been identified in HDL [71].

4.3.4. Cellular HDL-Interacting Proteins

After the secretion of apoA1 from the liver and intestine, apoA1 interacts with the ABC transporter A1 (ABCA1) on hepatocytes and enterocytes. At this rate-limiting step in HDL biogenesis, apoA1 acquires cholesterol and phospholipids [73,83]. Whereas mature HDL is not able to bind to ABCA1, poorly lipidated apoA1, newly synthesized or as a result of HDL recycling, induces lipid efflux via ABCA1. For this efflux, lipids are sequestered in the extracellular domains of ABCA1 in an ATP-dependent manner [84]. Lipid-laden ABCA1 monomers dimerize and transfer phospholipids and cholesterol to apoA1. Moreover, the interaction of apoA1 with ABCA1 protects ABCA1 from degradation and induces intracellular signaling pathways, such as protein kinases A and C, and Janus kinase 2 [85]. ABC transporter G1 (ABCG1) plays a role in lipid homeostasis of cell and organelle membranes. It mediates cholesterol efflux to HDL. However, this process is not rate-limiting in the formation of HDL [73,83]. Both, ABCA1 and ABCG1, are regulated on transcriptional and posttranscriptional levels. Excess cholesterol, notably after oxidation to oxysterols, activates the liver X receptor which upregulates the expression of ABCA1 and ABCG1, thus promoting cholesterol efflux [74]. ABCG1 and ABCA1 were shown to balance the cholesterol content of lipid rafts which is crucial for signaling processes including proliferation and inflammation [85].

Savenger receptor class B type I (SR-BI), another cholesterol transporter, mediates passive cellular cholesterol export as well as import, depending on the cholesterol gradient [73,85]. The main function of SR-BI is cholesterol uptake into hepatocytes and steroidogenic tissues [83]. SR-BI is also expressed by macrophages and endothelial cells, where it mediates cholesterol efflux to HDL. Besides cholesterol trafficking, HDL binding to SR-BI induces several protein kinases such as Akt or mitogen activated protein kinase (MAPK). These pathways increase insulin sensitivity, reendothelialization, and NO-mediated vasorelaxation in the endothelium [85]. The latter is also induced by the interaction of HDL with ABCG1 [67].

Hepatic lipase hydrolyzes preferentially TG and to some extent PL in HDL [72,73]. TG-enriched HDL (a result of CETP action) are excellent substrates for HL, generating small, core-lipid depleted HDL with unstable apoA1 binding. Endothelial lipase (EL) preferentially hydrolyzes HDL PL. EL reduces the size of HDL moderately, whereby the association of apoA1 is not attenuated. EL captures HDL on the endothelium and thereby facilitates the transport of HDL through the endothelium [86]. This is necessary for reverse cholesterol transport.

Sphingosine-1-phosphate (S1P), an active lipid mediator transported by HDL, interacts with S1P receptors. The S1P receptor isoforms are G protein-coupled receptors that induce diverse signaling pathways in different cell types [85]. Among other functions, S1P supports proliferation and survival, and interferes with inflammatory signaling cascades. In β-cells, extracellular S1P was described as protective agent against cytokine-induced apoptosis [87,88].

4.3.5. Alterations of Lipoprotein Metabolism, HDL Structure and Function in Metabolic Diseases

Diabetic dyslipidemia is characterized by increased levels of VLDL triglycerides, reduced levels of HDL cholesterol, and increased levels of small dense LDL [89]. In insulin resistance, lipoprotein lipase activity in muscle cells was described to be reduced. Therefore chylomicron remnants deliver more TG to the liver which in turn secrets more VLDL. The elevated VLDL TG levels promote the exchange for CE with HDL and LDL mediated by CETP. Thus, TG are hydrolyzed from HDL and LDL by HL leaving smaller and denser lipoproteins [90]. Small dense LDL are more atherogenic compared to normal LDL, whereas small dense HDL are unstable and rapidly degraded. Besides the loss in particle stability, TG-enrichment of HDL in type 2 DM often implies decreased anti-inflammatory, antioxidative, and vasodilatory effects [67].

In the insulin resistant state, insulin loses its effect in the suppression of lipolysis. This leads to increased levels of free fatty acids in circulation. Elevated free fatty acids decrease the expression of ABCA1 and ABCG1 in various cells [91]. This decreases HDL levels in circulation. Additionally, non-enzymatic glycation of HDL apolipoproteins was found in people with chronically elevated blood glucose levels [72]. The glycated apolipoproteins had lost their ability to interact with enzymes such LCAT which reduced the stability of HDL. Moreover, the inflammatory cytokine TNF-α inhibited SR-BI- and ABCA1-mediated cholesterol efflux from adipocytes to HDL and apoA1, respectively [92]. This further decreased HDL levels.

Alongside with the decrease in total HDL levels observed in subjects with metabolic syndrome, changes in apolipoprotein composition were found in patients with type 2 DM [93], acute coronary syndrome (ACS), and stable coronary artery disease (CAD) [77]. HDL of both, ACS and CAD patients, was enriched with the pro-apoptotic apoC3, whereas the anti-apoptotic apoJ was decreased. Furthermore, a causal link was established between endothelial cell apoptosis and apoC3 as well as apoJ in that study.

Myeloperoxidase, which is elevated in the plasma and HDL of CAD patients, oxidizes HDL and apoA1 [67]. Oxidation compromises the cholesterol efflux potential of HDL and apoA1. Moreover, oxidized HDL and apoA1 become pro-atherogenic, as they induce NF-κB activation and VCAM-1 (vascular cell adhesion molecule 1) expression in endothelial cells.

Low grade systemic inflammation, which is present in patients with perdidontitis, was found to change the endothelial protective properties of HDL as well [94]. Compared to HDL from healthy donors, HDL from peridontitis patients provoked less PON1 activity in serum, less NO release, and more superoxide production in endothelial cells. Upon an acute inflammatory stimulus in the peridontitis patients, HDL temporarily contained higher levels of prothrombin as well as the acute phase proteins serum amyloid A (SAA) and complement factor C3. These changes in HDL composition were accompanied by an acute deterioration of the endothelial protective HDL functions (i.e. decreased NO production and PON1 activity, increased superoxide production). Whilst no change in cholesterol efflux from macrophages was found between the HDL samples of this study, the changed HDL properties in an inflammatory condition could impair the protective effects of HDL on β-cells.

Type 2 DM patients often suffer from chronic kidney disease (CKD). Mild CKD in children already induced changes in HDL composition which impaired the protective actions of HDL on endothelial repair and relaxation [95]. In this study, symmetric dimethylarginine (SDMA) was found in HDL isolated from CKD patients. Moreover, SDMA was sufficient to obliterate the protective HDL functions on the endothelium. Another study with adult type 2 DM patients reported that HDL lost its anti-inflammatory activity gradually with the progression of CKD [96]. Blood monocytes pretreated with HDL from healthy donors secreted significantly less TNF-α in response to lipopolysaccharides than monocytes pretreated with HDL from type 2 DM patients among which the stimulation of TNF-α was most pronounced with end stage CKD. Moreover, HDL of the latter patient group was found to have the highest concentration of SAA. In response to chronic inflammation, SAA can replace apoA1 and PON1 in HDL [67]. The

consequences of this substitution for cholesterol efflux are controversial. However, the antioxidative effect of SAA enriched HDL was found to be decreased. Furthermore, SAA enriched HDL stimulated the release of inflammatory cytokines from vascular smooth muscle cells.

4.3.6. HDL Functions in Health and Disease

Reverse cholesterol transport (RCT) is the best studied function of HDL. About 50 years ago, the negative association between HDL cholesterol plasma levels and the risk of developing coronary artery disease (CAD) was discovered and reviewed [97,98]. HDL-mediated RCT was presumed to be the protective mechanism for the removal of excess cholesterol from macrophage foam cells in the atherosclerotic plaque. Cholesterol is loaded on HDL by the interaction with ABCG1 and SR-BI on the cell surface. To access the foam cells, HDL has to cross the endothelium. ABCG1 and SR-BI were shown to be involved in the HDL uptake by as well as the transport of HDL through the endothelium [99]. However, the detailed itinerary of HDL through endothelial cells, which involves dynamin and the cytoskeleton, remains to be clarified [100]. Especially the fact that HDL did not traffic the cells by the classical endocytic pathways (i.e. clathrin coated pits, caveolae, or fluid phase), and HDL's intracellular allocation to unknown vesicular organelles need further investigation.

It was found by in vitro and in vivo studies that HDL reduces the expression of adhesion molecules for monocytes (e.g. VCAM-1) in endothelial cells [67]. These are upregulated by inflammatory cytokines on the endothelium and facilitate monocyte infiltration, an early event in atherosclerosis. Moreover, HDL can scavenge molecules which are harmful to cells such as lipopolysaccharides or oxidized lipids [79]. Whereas oxidized LDL and their uptake by macrophages are pro-atherogenic, the oxidation of LDL is prevented by PON1 and other antioxidative enzymes carried by HDL [67].

Other beneficial effects of HDL on the endothelium include the promotion of the endothelial barrier function and re-endothelialization after injury [95]. Moreover, HDL promotes the proliferation of vascular smooth muscle cells. These cells stabilize atherosclerotic plaques and have anti-thrombotic properties. HDL protects endothelial cells from oxidized LDL, TNF-α, and serum deprivation induced apoptosis [67,77].

The above mentioned protective functions were collected from experiments with HDL from healthy donors. As discussed in section 4.3.5., numerous studies have shown that HDL is subjected to structural and compositional changes in subjects with chronic diseases such as metabolic syndrome, diabetes, atherosclerosis, and chronic kidney disease [79]. It is plausible, that the decreases in HDL levels and functionality as consequences of the above mentioned conditions hamper the protective effects of HDL. Moreover, the resulting dysfunctional HDL may even gain noxious properties.

4.4. Antidiabetogenic Functions of HDL

A low HDL-C level is a well-established risk factor for the development of type 2 DM [101,102]. The issue whether this association reflects causality has been addressed by several Mendelian randomization studies that yielded contradicting results. Haase and colleges found no causal association between the development of type 2 DM and genetic mutations which reduce the levels of HDL in a prospective study [103]. They concluded that the observed low HDL-C levels in patients with type 2 DM would be a consequence of alterations in lipid metabolism secondary to type 2 DM. Otherwise, Fall et al. and White and colleges both described an inverse relationship between HDL-C levels and type 2 DM, as well as LDL-C and type 2 DM [104,105]. A recent study that combined metabolomics with Mendelian randomization found presumably causal associations between the CE and FC levels of very large and large HDL particles, and HDL-C with low glucose levels [106]. Moreover, the TG content of small HDL particles as well as total TG levels were positively correlated with blood glucose levels, the latter even correlated with type 2 DM. In addition, the protective functions of HDL on β-cell survival and secretory function as well as on peripheral insulin resistance are under investigation.

4.4.1. β-Cell Survival

Apoptosis pathways relevant for β-cells in type 2 DM are described in section 4.2.4 above. Diverse β-cell protective effects of HDL and its components have been identified to date [91]. HDL prevented primary murine islet-cells as well as βTC3 cells (a mouse β-cell line) from apoptosis induced by supraphysiological LDL concentrations [107]. In Min6 cells (another mouse β-cell line) oxidized LDL-induced apoptosis was prevented by simultaneous incubation with HDL [108]. In the same cell line, protective effects of HDL were described against starvation-, IL-1β-, thapsigargin-, and tunicamycin-induced apoptosis [109]. Whereas HDL-mediated protection against starvation- and IL-1β-induced apoptosis involved the modulation of the expression of the translation regulator 4E-BP1, the ER stress inducers thapsigargin and tunicamycin did not.

Our research group previously demonstrated a protective effect of HDL against apoptosis induced by high glucose concentrations in primary human and murine β-cells [88]. Moreover, we found an anti-apoptotic effect for HDL as well as for its components apoA1 and S1P against

IL-1β-induced apoptosis. That apoA1 was found to increase the expression of the survival gene Pdx-1 in INS-1E cells could provide a possible explanation for this finding [110].

Surprisingly, differences in the protective effect of HDL against different ER stressors have been described. HDL resolved both, ER stress and apoptosis, if induced by thapsigargin (an inhibitor of the SERCA Ca^{2+} pump), palmitate or insulin overexpression [111]. In contrast, ER stress-induced apoptosis by tunicamycin (a protein glycosylation inhibitor) was prevented by HDL without resolving the ER stress [112].

4.4.2. Promotion of Insulin Secretion

HDL and apoA1 mediate cholesterol efflux from β-cells. A disturbed basal and glucose-stimulated insulin secretion was reported in apoE-deficient mice which have elevated cholesterol levels in circulation as well as in pancreatic islets [113]. Interestingly, insulin secretion was normalized when cholesterol overload was treated systemically in mice with statins or acutely in islets where cholesterol was depleted with methyl-β-cyclodextrin. In this study, insulin secretion was correlated with the dimerization of neuronal NO synthase and the activity of glucokinase. Additionally, the importance of cholesterol efflux for insulin secretion was demonstrated in a study with mice having a β-cell specific knock-out of ABCA1 [114]. Although these mice had a normal lipoprotein profile, their glucose tolerance was massively deteriorated compared to their control littermates. Presumably, this was caused by a loss of first-phase insulin secretion. Glucose tolerance was further impaired in ABCG1 knock-out mice crossed with the β-cell specific ABCA1 knock-out [115]. Whereas plasma cholesterol levels were not changed in these mice, the defect in insulin secretion was associated with increased islet cholesterol accumulation. Consequences of ABCG1 deficiency alone were mild or not observed in this study. Since insulin secretion in response to potassium chloride was impaired in islets of mice with combined absence of ABCG1 and ABCA1, the authors concluded that the cholesterol accumulation induced a defect in insulin granule exocytosis. Moreover, cholesterol accumulation was associated with IL-1β expression in islets and macrophage infiltration. β-cell specific ABCA1 knock-out mice also showed changes in the organization of cholesterol-enriched membrane microdomains, changes in the Golgi ultrastructure, and impaired insulin processing [116]. It is plausible that these effects were exacerbated by the combined loss of ABCG1 and ABCA1 in β-cells. Whereas acute cholesterol depletion with

methyl-β-cyclodextrin restored insulin granule exocytosis in the absence of ABCA1 [116], methyl-β-cyclodextrin-mediated cholesterol desorption had been shown to decrease the exocytotic response in β-cells in an earlier study [117]. In addition, an intracellular role for ABCG1 was described [118]: ABCG1 deficient mice were less glucose tolerant than wild type controls, whereas total cholesterol content of islets was not changed. However, β-cell ABCG1 was predominantly found in the secretory vesicles, and the subcellular cholesterol distribution was different, with ABCG1 deficient β-cells having less cholesterol in secretory vesicles than wild type β-cells. The authors postulated therefore that ABCG1 is responsible for the regulation of the cholesterol content of secretory vesicles in β-cells. A more recent study with β-cell-specific ABCA1- and ABCG1-deficient mice confirmed the necessity of these two receptors as well as their role in cholesterol homeostasis for proper insulin secretion [119]. Moreover, the decreased insulin secretion caused systemic inflammation and shifted glucose disposal from muscle cells to adipocytes. An elegant study investigated the mere event of insulin granules fusing with the plasma membrane in a full manner or as kiss-and-run event [120]. The authors could demonstrate that cholesterol overload shifts the fusion events towards kiss-and-run events that are far less efficient in insulin release. This could provide an explanation for the defects observed in type 2 DM which are often associated with elevated plasma cholesterol.

An association of HDL-C levels and β-cell secretory function was found in a study of subjects with heterozygous mutations in ABCA1 that have 50% less HDL-C but otherwise a normal lipid profile [121]. Their first-phase insulin secretion was decreased in a hyperglycemic clamp experiment compared to relatives that are non-carriers of the mutation. This finding was challenged by Rickels and colleges who found an association of hetero- or homozygote ABCA1 deficiency with improved insulin secretion [122]. One possible explanation for the contradictory results is the mean age of the study subjects which was 27 years in Rickels' study vs. 54 years in Vergeer's study [123]. It is plausible that the duration for which subjects had been exposed to low HDL levels shifted the cholesterol homeostasis of β-cells from a favorable to a deleterious side. Moreover, infusion of reconstituted HDL (i.e. lipidated apoA1) improved insulin secretion and enforced glucose uptake in healthy individuals [124]. Also in mice, single doses of apoA1 improved glycemic control, possibly by priming of the β-cells for glucose-stimulated insulin secretion [125]. Preincubation of INS-1E cells with an apoA1 derived short peptide (C-terminal domain) or a single dose of this peptide in diet induced obese mice improved glucose induced insulin secretion or insulin secretion in a glucose tolerance test, respectively [126].

CETP inhibitors decrease HDL catabolism and thereby raise HDL levels. This has been shown for five different CETP inhibitors, though the expected decreased risk for cardiovascular disease events has not been established in large randomized trials yet [127]. In healthy individuals, CETP inhibitor treatment increased HDL-C levels within two weeks [128]. This increase in HDL-C was associated with increased postprandial insulin levels. ApoB-depleted plasma of CETP inhibitor-treated subjects stimulated glucose-stimulated insulin secretion from a β-cell line to a larger extent than the apoB-depleted plasma from the placebo-treated group. This effect was probably caused by the increased cholesterol efflux mediated by the CETP inhibitor plasma. Post-hoc analysis of the ILLUMINATE trial revealed lower fasting glucose and insulin levels as well as a decrease in glycated hemoglobin (HbA1c) in the diabetic subgroup of the cohort receiving CETP inhibitor with statin treatment compared to the diabetic subgroup receiving statin only treatment [129]. These effects did not correlate with the increase in HDL-C, however. Therefore, it remains to be clarified how CETP inhibition improved glycemic control.

Besides its role in cholesterol homeostasis, apoA1 – although at supraphysiological doses – was found to increase insulin production by nuclear exclusion of an insulin repressor in INS-1E cells [110].

Several studies found an increased risk for type 2 DM in persons with statin treatment [130]. Statins reduce cholesterol synthesis by inhibition of the HMG-CoAR at the cellular level. In Mendelian randomization studies, loss of function mutations in the HMG-CoAR gene were associated with an increased risk for type 2 DM [131,132]. By contrast, patients with familial hypercholesterolemia were found to have a reduced risk of diabetes notwithstanding their life-long statin treatment. One plausible explanation for this association is the upregulation of LDLR in peripheral cells, including β-cells, and subsequent cholesterol overload of these cells despite low levels of cholesterol in the bloodstream. Statin treatment could affect the fragile cholesterol balance in β-cells and decrease insulin secretion. Moreover, direct effects of statins on Ca^{2+} channels in β-cells have been reported which could explain the defects in insulin secretion associated with statin therapy [133]. Another proposed effect of lipophilic statins on insulin secretion is the cholesterol depletion of β-cells. This disturbs lipid rafts in the cell membrane and thereby interferes with Ca^{2+} channels. Since the authors found an association with body weight as well, it seems well possible that peripheral increased insulin resistance is involved in the elevated risk for type 2 DM.

The effects of proprotein convertase subtilisin/kexin type 9 (PCSK9), which increases the degradation of LDL receptors on hepatocytes and thus rises LDL levels in the blood stream, on glucose metabolism was investigated by several studies [134]. Whereas Langhi et al. could not find a negative effect of PCSK9 deficiency on glucose metabolism in mice, male PCSK9-deficient mice were reported to be hyperglycemic, hypoinsulinemic, and glucose-intolerant at the age of 4 months while their pancreatic islets exhibited decreased insulin content and morphological abnormalities compared to islets of PCSK9-positive mice [135,136]. Mendelian randomization studies on PCSK9 variants found an association between the decreased LDL levels in circulation and an increased risk for type 2 DM [132,137]. Otherwise, Baass et al. even found a positive correlation of PCSK9 levels with fasting insulin levels in children, indicating a negative effect of PCSK9 on glucose homeostasis [138]. To date, clinical studies could not clarify whether PCSK9 inhibition or deficiency results in positive, negative or neutral effects on glucose metabolism [139].

In summary, cholesterol homeostasis of β-cells and their secretory vesicles seems to be important for insulin secretion. HDL which functions as cholesterol donor and/or acceptor depending on the cholesterol status of the cell might stabilize this balance.

4.4.3. Peripheral Insulin Resistance

In obesity, the permanent abundance of nutrients induces several stress-responsive signaling pathways in adipocytes, hepatocytes, and muscle cells. Most of these pathways converge in the inhibition of insulin signaling through serine-phosphroylation of insulin receptor substrate and the promotion of inflammation in the above mentioned tissues [140]. Local inflammation activates resident macrophages that secrete inflammatory cytokines and recruit additional leukocytes. Thus, systemic inflammation, which induces insulin resistance, is sustained in a deleterious feed-forward signaling loop. Since low HDL-C levels were identified as an independent predictor for future insulin resistance in prospective studies [141,142], and since HDL exerts anti-inflammatory effects on macrophages, HDL may serve as an important protector against insulin resistance [143].

In adipocytes, a reduction of chemotactic factors for macrophages (i.e. monocyte chemoattractant protein 1 (MCP-1) and serum amyloid A (SAA) 3) was found after the administration of HDL or apoA1 [144]. These effects were mediated by ABCG1- and SR-BI-, or

ABCA1-dependent cholesterol efflux, respectively. Moreover, in the adipose tissue of mice over-expressing apoA1 on high fat diet, the expression of SAA3, MCP-1, as well as inflammatory cytokines interleukin 6 and TNF-α was reduced compared to wild type mice on high fat diet. By these means, HDL possibly increased insulin sensitivity in adipocytes.

In response to a high-fat diet, mice developed systemic and hepatic inflammation, insulin resistance, and reduced glucose tolerance [145]. These symptoms were prevented by the infusion of apoA1 in mice, whereas cholesterol efflux from hepatocytes mediated by methyl-β-cyclodextrin was not sufficient to reduce inflammation and improve insulin sensitivity. Moreover, an association with the activation of nuclear factor kappa B (NF-κB) was found: NF-κB was upregulated by the high-fat diet, and this up-regulation was attenuated by apoA1 infusion. The same pattern was found for the inflammatory cytokines TNF-α, IL-6, and IFN-γ, which are regulated by NF-κB activation.

In cultured myocytes, an apoA1 derived short peptide (C-terminal domain) induced glucose uptake dose-dependently [126]. A single dose of this peptide in diet induced obese mice or mice with a deficient leptin receptor (db/db mice) significantly improved glucose clearance in a glucose tolerance test, possibly by increased glucose uptake in muscle cells.

4.4.4. AMPK Functions

Besides insulin stimulated glucose uptake, AMP-activated protein kinase (AMPK) mediated glucose uptake in muscle cells and adipocytes seems to be important for glucose homeostasis [143]. In adipocytes, HDL was found to enhance glucose uptake by the increase of glucose transporter GLUT-4 translocation to the cell surface [146]. This facilitated glucose uptake and lowered blood glucose levels. GLUT-4 translocation was associated with AMPK and PI3K signaling which probably was activated by HDL binding on SR-BI.

In muscle cells, apoA1 and HDL stimulated AMPK and increased glucose uptake [124,147]. Since skeletal muscle cells are responsible for the majority of glucose uptake, its stimulation by HDL is important for glucose homeostasis. As for adipocytes, discoidal HDL was described to promote the translocation of glucose transporter GLUT-4 in myocytes [148]. Additionally, glycogen synthesis in muscle cells was stimulated by HDL [146], and glucose oxidation was promoted by apoA1 [149]. By these means, the glycogen storage capacity and utilization was improved.

Also in hepatocytes, where insulin-mediated suppression of gluconeogenesis is lost in insulin resistance, an interaction of HDL and AMPK was found: ApoA1 activated AMPK in hepatocytes which in turn inhibited gluconeogenesis by the downregulation of gluconeogenesis-specific enzymes [147].

4.5. Aim of this Study

At physiological circumstances, hyperglycemia is compensated by an increase in β-cell mass and function. Type 2 diabetes mellitus manifests at the point where this compensation collapses and insulin resistance cannot be counterbalanced. Moreover, pre-diabetic subjects often exhibit a shift in their lipoprotein profile towards low plasma levels of HDL cholesterol, a high TG concentration, and an elevated fraction of small dense LDL. Instead of being a mere consequence of insulin resistance, the decreased HDL levels could expose those people at increased risk for the manifestation of type 2 DM. Several lines of evidence nowadays indicate a causal link between HDL and the pathogenesis of type 2 diabetes mellitus.

During the manifestation of type 2 DM, β-cell apoptosis is a major process. Our lab has previously shown that HDL prevents IL-1β-induced apoptosis of primary human and mouse pancreatic β-cells [88]. Moreover, it was described that apoA1 and S1P could mimic the protective effect of HDL. However, the mechanism behind the protective effects remained largely unknown.

Therefore, the main goals of this thesis are:

1) The confirmation of the described protective components of HDL, and the identification of components of HDL that are responsible for its beneficial effect on β-cell apoptosis.
2) The elucidation of receptors and signaling pathways modulated by HDL in IL-1β-induced apoptosis.

5. Materials and Methods

5.1. Cell Culture

5.1.1. INS-1E Cells

The INS-1 cell line was grown from a radiation-induced rat insulinoma tumor [150]. The clonal INS-1E cell line was selected from the INS-1 cells according to their responsiveness to glucose by Prof. C Wollheim and his group [151]. He kindly provided our lab with these cells.

The INS-1E cells were cultured in 10 cm cell culture plates with RPMI 1640 medium (11.1 mM glucose) supplemented with 10% heat inactivated fetal bovine serum (FBS), 2 mM L-glutamine, 1% PenStrep (i.e. 100 IU/ml Penicillin, 100 μg/ml Streptomycin), 10 mM HEPES, 1 mM NaPyruvate, and 0.05 mM 2-mercaptoethanol (all purchased from Sigma-Aldrich, St. Louis MO, USA) as cell culture medium. Cells were split once per week by gentle trypsinization (Trypsin-EDTA 10x, diluted to 1x with PBS, Sigma-Aldrich) and seeded at 2 to $2.75*10^6$ cells into fresh 10cm-plates. We used the cells between passages 58 and 68. During experiments with HDL, FBS was replaced by delipidated FBS. FBS was delipidated by ultracentrifugation as follows: The density of FBS was adjusted to 1.21 g/ml by the addition of KBr. After 20 hours of centrifugation (59000 rpm; system L90K, Beckman Coulter Inc., Brea CA, USA), the top 1.5 cm liquid were discarded. The lipid-free part was dialyzed (seven steps within 72 hours in 0.9% NaCl solution). The delipidated FBS was filter sterilized (0.22 μm microfilter, Millipore Corporation, Billerica MA, USA) and frozen in aliquots at -80 °C.

5.1.2. Min6 Cells

Min6B1 cells (referred here as Min6) were derived from a mouse insulinoma tumor [152]. They were cultured in 10cm cell culture plates in DMEM medium supplemented with 15% heat-inactivated FBS, 0.06 mM 2-mercaptoethanol and 1% PenStrep (i.e. 100 U/ml Penicillin, 100 μg/ml Streptomycin), all purchased from Sigma-Aldrich. Cells were split 1:5 twice per week by gentle trypsinization.

5.1.3. J774 Cells

The murine macrophage cell line J774 (ATCC, Rockville MD, USA) was cultured in 10 cm bacterial culture plates in RPMI 1640 medium supplemented with 10% FBS and 1% PenStrep (i.e. 100 U/ml Penicillin, 100 μg/ml Streptomycin), all purchased from Sigma-Aldrich. Cells were split once per week 1:2 by removal with 10 mM EDTA in PBS.

5.2. Lipoproteins

5.2.1. Lipoprotein Isolation

Normolipidemic plasma obtained from a blood donor bank (Blutspende Zürich, Schlieren, Switzerland) was used to isolate lipoproteins. HDL (density: 1.063-1.210 g/ml) and LDL (density: 1.019-1.063 g/ml) was isolated by sequential density ultracentrifugation. Potassium bromide (KBr) and ethylenediaminetetraacetic acid (EDTA) were added before each centrifugation step (59000 rpm; system Optima L90K, Beckman Coulter Inc., Brea CA, USA) to adjust the correct density. After isolation, the KBr was removed from lipoprotein fractions by dialysis (five steps within 48h; buffer containing 0.15 M NaCl, 0.3 mM EDTA, pH 7.4). Finally the lipoprotein preparations were filter sterilized (0.22 μm microfilter, Millipore Corporation, Billerica MA, USA). The protein concentration of the isolated HDL and LDL preparations were measured with the DC assay (Bio-Rad, Hercules CA, USA), against a standard-curve with bovine serum albumin. To assess the purity of HDL, the lipoprotein preparation was run in a sodium dodecyl sulfate polyacrylamide gel electrophoresis (SDS-PAGE) with subsequent Coomassie blue staining of the gel. Only HDL preparations without visible contaminations of apoB nor albumin were used for experiments.

From low volume plasma or serum samples of the clinical studies or mouse experiments, HDL was isolated by using 2 ml centrifuge tubes for sequential ultracentrifugation (Optima Max-TL, Beckman Coulter Inc.). According to this protocol, 500μl plasma or serum were combined with 1000 μl 0.150 M NaCl / 1 mM EDTA solution and 500μl 38% KBr solution. This mixture with a density of 1.068 g/cm^3 was filled into the small centrifuge tubes. After 6 hours centrifugation at 120'000 rpm (4 °C), the tubes were cut at 10mm from the bottom. The LDL at the top was collected and the density of the lower fraction was set to 1.21 g/cm^3 by the addition of 900 μl 46.5% KBr solution. After overnight centrifugation at 120'000 rpm (4°C), the tubes were cut at 15 mm from the bottom. The HDL at the top of the tube was collected, dialyzed, and analyzed as described above.

5.2.2. Extraction of HDL Protein and Lipid Moieties

HDL was dialyzed against 0.9% NaCl-solution, lyophilized, and subsequently extracted with an ice-cold chloroform-methanol (2:1, vol:vol) mixture. The dispersion was incubated in an

ultrasonic water bath, and thereafter incubated on ice. Methanol was added to precipitate the HDL protein moiety and the proteins were pelleted by centrifugation.

The supernatant which contained the HDL lipid moiety was transferred to a new tube and the solvents were evaporated under N_2 flow. The dried HDL lipids were dissolved in ethanol before adding to cells.

The protein pellet was washed twice with ice-cold ethanol and centrifuged. The proteins were lyophilized. Before adding the HDL proteins to cells, they were dissolved in guanidinium hydrochloride (5 M) and dialyzed in buffer containing 0.15 M NaCl, 0.3 mM EDTA, pH 7.4.

5.2.3. Apolipoproteins and Lipids

Apolipoprotein A1 (apoA1) was purified from delipidated HDL solubilized in urea (6M) and Tris (10 mM, pH 8) using an anion exchange column (MonoQ) on an Äkta Protein Purification System (GE Healthcare, Life Sciences, Buckinghamshire, UK). Bound HDL proteins were eluted using a gradient of 0 to 150 mM NaCl in 5 M urea, and 10 mM Tris (pH 8), as previously described [153]. The eluted proteins were collected in small fractions. All fractions were dialyzed and analyzed by SDS-PAGE and Coomassie blue staining. The pure apoA1 fractions were pooled. The fractions containing other proteins beside apoA1 were collected for another apoA1 purification cycle, or analyzed for their anti-apoptotic potential.

Purified apolipoprotein C1 (apoC1) and apolipoprotein E (apoE) were purchased from Athens Research & Technology (Athens GA, USA) and reconstituted in deionized water to 2 mg/ml stock concentration. Recombinant apolipoprotein D (apoD, expressed in HEK cells) was purchased from OriGene Technologies (Rockville MD, USA; 0.242 μg/ml stock concentration). Sphingosine-1-phosphate was purchased from Avanti (Avanti Polar lipids, Alabaster AL, USA). It was dissolved in DMSO/1 M HCl (95:5%, vol:vol) and subsequently diluted in 3% BSA/PBS to 1 mM stock concentration.

5.2.4. Lipidation of ApoA1

ApoA1 was lipidated by the cholate dialysis method [154]. Purified apoA1, 2-oleoyl-1-palmitoyl-sn-glycero-3 phosphocholine (POPC, Sigma-Aldrich), and sodium cholate (Sigma-Aldrich) were mixed in a molar ratio of 1/40/80. First, POPC (dissolved in chloroform) was dried in a glass tube under N_2-flow, then it was dissolved in Tris saline buffer (0.01 M Tris, 0.15 M NaCl,

0.1 mM EDTA, pH=8). The POPC-Tris mixture was vortexed thoroughly and incubated 30 minutes on ice. Then, sodium cholate was added and to induce the formation of micelles, this mixture was vortexed every 10 minutes during 30 minutes until the mixture cleared. ApoA1 was added to the micelles in Tris saline buffer and the mixture was incubated 90 minutes on ice. Finally, the mixture was extensively dialyzed in buffer containing 0.15 M NaCl, and 0.3 mM EDTA at pH 7.4 for 48 hours at 4 °C in tubes with a cutoff of 50'000 Da molecular weight to remove free apoA1.

5.2.5. Acetylation of LDL

For the acetylation of LDL, 5 mg LDL protein was diluted with buffer containing 0.15 M NaCl and 0.3 mM EDTA (pH 7.4) to a final volume of 2 ml and mixed with 2 ml ice-cold saturated sodium acetate. After 15 minutes stirring at 4 °C, 80 μl acetic acid was added in portions of 10 μl every 15 minutes. Then, the mixture was incubated 30 minute at 4 °C. The acetylated LDL was dialyzed in four steps within 48 hours against buffer containing 0.15 M NaCl, 0.3 mM EDTA (pH 7.4) at 4 °C.

5.3. RNA Analyses

5.3.1. RNA Isolation with TRI-reagent

INS-1E RNA was isolated from 12- or 6-well dishes containing $4*10^5$ or $1*10^6$ cells per well, respectively. The medium was removed and the cells were lysed with TRI reagent (0.5 ml or 1 ml respectively; Sigma-Aldrich, T9424). The suspension was sheared with a pipette. The lysate was transferred to an Eppendorf tube and mixed with 0.1 or 0.2 ml chloroform. After thorough mixing and incubation on ice, the water and organic phase were separated by centrifugation. The water phase on top was transferred to a fresh tube. To this tube, isopropanol (0.5 ml per ml TRI reagent) was added to precipitate the RNA. After centrifugation, the pellet was washed with 75% ethanol and dried. The pellet was subsequently solubilized in DEPC-treated water and heated 10 minutes at 65 °C to ensure proper dissolving of the RNA. The RNA content was determined with the Nanodrop (ThermoFischer Scientific, Wilmington DE, USA). Finally, RNA was subjected to DNA digestion with DNase (Roche, Basel, Switzerland).

5.3.2. RNA Isolation with Silica-Colums

RNA for gene array analysis was isolated from cells after the induction of apoptosis with the Illustra-Kit (GE Healthcare, Life Sciences, Buckinghamshire, UK). In brief, cells in the 6-well dish ($8*10^5$ cells per well) were washed twice with phosphate buffered saline (PBS). 350 µl provided lysing solution was added and cells were scraped off the well. The lysate was sheared with a syringe and transferred to the silica column. Then the RNA isolation and DNA digestion were performed according to the instructions of the manufacturer. As last step of the isolation, the RNA was eluted in 30 µl RNase-free water.

5.3.3. Reverse Transcription

The transcription of the isolated RNA was done with SuperScript II (LifeTechnologies, Carlsbad CA, USA) or RevertAid (ThermoFischer Scientific, Wilmington DE, USA) according to the manufacturers' protocols.

5.3.4. Polymerase Chain Reaction

The polymerase chain reaction (PCR) was performed with Taq polymerase (Roche, Basel, Switzerland) and the primers described in table 5.1. The PCR products were analyzed by 1% agarose gel electrophoresis.

5.3.5. Quantitative Polymerase Chain Reaction

For the quantification of specific RNAs, the LightCycler system (Roche, Basel, Switzerland) was used. We used the LightCycler mix (Roche, Basel, Switzerland) containing the polymerase enzyme and required dyes. The primers are listed in table 5.1. GAPDH was used for normalization. The data was quantified by using the extended "delta-delta CT" method according to M.W. Pfaffl [155].

5.3.6. RNA Analysis with Agarose Gels

After isolation of RNA with silica columns (see above), the integrity of the isolated RNA was analyzed by electrophoresis on a 1.5% agarose gel. The appearance of distinct 18S and 28S rRNA bands was taken as quality sign for the total isolated RNA. Good quality RNA samples were used for the gene array at the Functional Genomics Center Zürich (FGCZ).

5.3.7. Gene Array

The gene array, including labelling and hybridization of the RNA, was performed by the FGCZ. The SurePrint G3 Rat GE 8x60K Microarray (Agilent Technologies, Santa Clara CA, USA) was chosen for the analysis of the whole gene expression.

The gene array data was normalized and annotated by the FGCZ. Subsequent analyses were done by using the MetaCore^{TM} software (Genego, Thompson Reuters, New York, NY, USA) and the DAVID gene ontology program [156,157].

5.3.8. Primer Specifications

Gene	Direct.	Primer sequence (5' - 3')	Amplicon size (bp)	RT-PCR annealing temperature (°C)
Mouse GAPDH	Fwd	AAG CTG TGG CGT GAT GGC CG	117	60
	Rev	GGC CAT GCC AGT GAG CTT CCC		
Rat ATF6	Fwd	AGA CTG GGA GTC CAC GTT GTT T	152	60
	Rev	GGC TCC ATA TGT CTG ACT CCC		
Rat Bcl-xL	Fwd	GAT GGG GTA AAC TGG GGT CG	182	60
	Rev	TCC ACA AAA GTG TCC CAG CC		
Rat BIM	Fwd	CCG GTC CTC CAG TGG GTA TT	133	60
	Rev	TAT GGA AGC CAT TGC ACT GAG A		
Rat CFLAR	Fwd	GGG ACC TCC TGG ATT GTT TAA GTG	179	60
	Rev	CAG CAG CAC CCT ATA ATC GGA A		
Rat CHOP	Fwd	TTC ACT ACT CTT GAC CCT GCA TC	176	60
	Rev	CAC TGA CCA CTC TGT TTC CGT TTC		
Rat DP5	Fwd	GCC GTG GTG TTA CTT GGA CT	125	60
	Rev	GAT TGT GCC AGA GCT TCA CA		
Rat FAS	Fwd	GGA GGA GTA CAC GGA CAG GA	131	62
	Rev	TTT CTT TGC ACC TGC ACT TG		
Rat IL1R	Fwd	GGC TTG TGA CAT CTT CGG CT	115	60
	Rev	TAC TCC GTG CAT TTG TCG GT		
Rat STAT1	Fwd	AAG CAC CAG AAC CGA TGG AG	88	60
	Rev	GAA GGG TGG ACT TCA GAC ACA		
Rat sXBP1	Fwd	TGC TGA GTC CGC AGC AGG TG	169	60
	Rev	ATT AGC AGA CTC TGG GGA AG		

Table 5.1: Specifications of primers used for PCR and quantitative PCR.

5.4. Protein Analyses

5.4.1. Protein Isolation and Quantification

Cells were grown in 6-well dishes with $1*10^6$ cells per well and stimulated 24 h after seeding. For protein isolation, the cells were washed twice with cold PBS, scraped in PBS and transferred to a tube. After centrifugation, the cells were lysed in 50 µl RIPA buffer (10mM Tris pH 7.4, 150 mM NaCl, 1% NP-40, 1% sodium deoxycholate, 0.1% sodium dodecyl, complete EDTA (Roche, Basel, Switzerland)) with protease inhibitors (Sigma-Aldrich) per well. After 30 minutes incubation, the lysates were centrifuged at 13'000 g to pellet the DNA. The lysates were then transferred to a fresh tube.

To analyze the protein content in the lysates, the colorimetric reaction of the DC protein assay (BioRad) was used with a bovine serum albumin standard curve.

5.4.2. Western Blotting

Proteins from cell lysates were separated according to their size by SDS-PAGE. Thereafter, the proteins were transferred to a PVDF membrane (GE Healthcare) with wet or semi-dry electroblotting systems.

After incubation with the respective antibodies (see table 5.2), the specific proteins were detected with Pierce ECL plus (Thermo Scientific) and subsequent exposure of films (Amersham Hyperfilm ECL, GE Healthcare). Alternatively, western blots incubated with secondary antibodies which emit light in the infrared spectrum, were recorded in the Odyssey infrared image system (LI-COR Biotechnology, Lincoln NE, USA).

5.4.3. Analysis of HDL Protein Composition with Mass-Spectrometry

LC-ESI-MS/MS analyses of the protein composition of the HDL protein fractions were done by my colleague Meliana Riwanto [77]. In brief, the fractions from the FPLC (see above) were digested by trypsin. The peptides were lyophilized and resolubilized in 0.1% trifluoroacetic acid (TFA). Samples were analyzed on a hybrid LTQ-Orbitrap mass spectrometer (ThermoFischer Scientific, Wilmington DE, USA) interfaced with a nanoelectrospray ion source. Chromatographic separation of peptides was achieved on an Eksigent nano LC system

(Eksigent Technologies, Dublin CA, USA). The spectral counts were normalized by using internal standards for known proteins.

5.4.4. ELISA for Apolipoprotein C1

The concentration of apoC1 in plasma, apoB-depleted plasma, and HDL was measured with a commercial apoC1 ELISA (Abnova, Taipei, Taiwan). ApoB was precipitated from serum by the addition of 10% of serum volume sodium dextran sulfate and MgCl (10 g/l Na dextran sulfate, 0.5 M MgCl, pH 7). The mixture was incubated 10 minutes at room temperature. Then, the precipitated apoB was pelleted by 40 minutes centrifugation at 13'000g. ApoC1 was measured in the supernatant, plasma, or HDL according to the manufacturer's protocol.

5.4.5. Antibody Specification

Protein	Source	Antibody type	Host	Dilution
Cleaved Caspase 3	Cell Signaling Technology # 9661	Polyclonal	Rabbit	1:1000
Phospho-PERK (Thr980)	Cell Signaling Technology # 3179	Monoclonal	Rabbit	1:1000
Tubulin (TUB 2.1)	Sigma-Aldrich # T4026	Monoclonal	Mouse	1:5000
Mouse IRDye 800CW	LI-COR Biosciences, # 926-32210	Polyclonal	Goat	1:5000
Rabbit-HRP	Dako / Agilent Technologies # P0448	Polyclonal	Goat	1:5000
Rabbit IRDye 680RD	LI-COR Biosciences # 926-68071	Polyclonal	Goat	1:5000

Table 5.2: Specifications of primary and secondary antibodies used for Western blots.
Cell Signaling Technology, Danvers MA, USA.

5.5. Bioassays for Cell Function and Survival

5.5.1. Cell Death Detection ELISA Plus

Unless otherwise described in the results section, INS-1E cells were pre-incubated in medium with 10% delipidated FBS with or without HDL or the indicated proteins 24 hours after seeding (24-well plates with $2.5*10^5$ cells per well). After this overnight pre-incubation, interleukin 1β (IL-1β) was added for apoptosis induction at 10 ng/ml final concentration in medium. Recombinant rat IL-1β was purchased from PeproTech (PeproTech EC, London, UK) or R&D (R&D Systems, Minneapolis MN, USA) and reconstituted in 5% BSA in PBS to 0.1 mg/ml stock concentration.

24 hours later, apoptosis was quantified in the treated samples and not-treated control samples with the cell death detection ELISA Plus (Roche). For this assay, cells were washed with PBS and lysed in the buffer provided by the manufacturer which preserves the nuclei. Antibodies against DNA and histones detected the cytosolic DNA (a sign of apoptotic cells), but not the DNA in intact nuclei of healthy cells.

Alternatively, apoptosis was stimulated in INS-1E cells after the pre-incubation by the addition of thapsigargin (ThG) at 50 nM final concentration for 8 hours. Thapsigargin (ThG) was purchased from Sigma-Aldrich (T9033) and dissolved in DMSO to 5 mM and 12.5 μM stock solution.

5.5.2. Annexin V / Phosphatidylserine Exposure

In apoptotic cells, phosphatidylserine (PS) molecules are flipped from the inner to the outer membrane. Annexin V binds to this PS molecules on the cell surface of otherwise intact cells. Propidium iodide is used as a marker for necrotic (permeable) cells since it enters the nucleus of necrotic cells and stains the DNA, whereas in intact cells the DNA is not accessible for the propidium iodide.

After apoptosis induction (as described above) in 12- or 24-well dishes (4 or $2.5*\ 10^5$ cells per well, respectively), floating INS-1E cells were collected and attached cells were removed with accutase (Sigma-Aldrich, A6964). Thus, the cells were washed with PBS and incubated with accutase, 5 minutes at 37°C. Then the detached cells were combined with the respective floaters, washed and stained with annexin V (diluted 1:20 in FACS buffer (PBS 1x, 2% FCS,

0.05% NaN_3, 20 mM EDTA), Annexin V labeled with AlexaFluor 647, BioLegend San Diego CA, USA) and propidium iodide (2.5 μg/ml in FACS buffer, Propidium Iodide solution, USBiological, Swampscott MA, USA) in FACS buffer. The stained cells were analyzed by flow cytometry with a 488 nm laser for propidium iodide and a 635 nm laser for annexin V. Thus, cells could be differentiated into healthy cells, necrotic cells, early apoptotic cells and late apoptotic cells.

5.5.3. NF-κB Translocation

INS-1E cells were grown on glass coverslips in 24-well plates with $2.5*10^5$ cells per well. After 16 hours incubation with or without HDL, IL-1β was added to the cells for 5 or 15 minutes, 1, 5, or 24 hours. Afterwards, the cells were fixed with 3.75% paraformaldehyde (PFA) for at least 20 minutes, washed with PBS, and subsequently permeabilized with 0.5% TritonX-100. To visualize the translocation of the transcription factor NF-κB from the cytosol into the nucleus, the fixed cells were incubated with an NF-κB antibody (rabbit-anti-p65, polyclonal, #sc-372, Santa Cruz Biotechnology, Dallas TX, USA), diluted 1:200 in PBS for 1 hour at room temperature. After several washing steps, the cells were incubated with the secondary antibody (donkey-anti-rabbit polyclonal 660, CF660R, #20389, Biotium Inc., Fremont CA, USA), diluted 1:500 in PBS over night at 4°C. Cells were washed and mounted with the Prolong Gold Antifade Reagent with DAPI (LifeTechnologies, Carlsbad CA, USA). The cells were analyzed with a 63x magnification objective at 660 nm (NF-κB) and 355 nm (DAPI).

5.5.4. Pychnotic Nuclei Screening

Min6 cells were treated 24 hours after seeding in 24-well plates ($2.5*10^4$ cells per well) with or without HDL or apoC1, and with or without ThG (0.5 μM, T9033, Sigma-Aldrich) for another 24 hours. After this treatment, the cells were fixed with 4% PFA and the nuclei were visualized with Hoechst stain (94403, Sigma-Aldrich). For analysis, at least 500 cells per condition were screened with a 40x magnification objective at 355 nm.

5.5.5. Active Caspase 3 Detection

For the detection of cleaved/active caspase 3 with the specific antibody (see table 5.2), cells were harvested from a 6 well plate after treatment. Cells were lysed with RIPA buffer and concentration of proteins was determined by DC assay (see section 5.4.1.). 10 μg proteins per sample were loaded for a western blot (see section 5.4.2.).

For the caspase 3 activity assay (CASP3F, Sigma-Aldrich), $2.5*10^4$ INS-1E cells were seeded in 96-well plates. After apoptosis induction with ThG, cells were harvested by centrifugation of the plate (5 min, 1000 rpm, 4°C), subsequent removal of the medium and addition of 100 μl assay buffer. The plates were then covered and frozen at -80 °C. After thawing, 80 μl of the lysate was transferred to a black 96-well plate, mixed with the substrate (a caspase specific peptide conjugated to a fluorescent reporter molecule), and incubated for 60 min at 37°C. After cleavage of the peptide by the caspase, fluorescence was measured at the TECAN Infinite M200 pro series fluorescence reader (excitation at 400 nm and emission at 500 nm, Tecan, Männedorf, Switzerland). The level of the fluorescent signal was directly proportional to the level of active caspase 3 in the cell lysate.

The protein content of the remaining lysate was detected with the Bradford reagent and a standard curve of BSA in assay buffer.

5.5.6. Cholesterol Efflux

For efflux experiments, J774 macrophage cells were seeded into 96-well plates and cultured for 24 hours. Then, the macrophages were loaded with 50 μg/ml acetylated LDL and 2 μCi/ml 3H-cholesterol (Perkin Elmer, Schwerzenbach, Switzerland) in cell culture medium without FBS. 24 hours later, cell were equilibrated in medium containing 0.2% serum albumin supplemented with or without 0.3 mM N6,2'-O-dibutyryladenosine 3',5'-cyclic monophosphate (cAMP; Sigma-Alddrich) to stimulate ATP-binding cassette transporter A1 (ABCA1) expression. The next day, HDL (25 μg protein/ml) were added to the macrophages for the induction of cholesterol efflux. After 6 hours, an aliquot of medium was removed and centrifuged 5 minutes at 13'000 g to pellet cellular debris. The cholesterol [^{3}H]-label in the supernatant was measured by liquid scintillation counting to quantitate the effluxed cholesterol. Meanwhile, the cells were incubated for at least 30 minutes with 0.1 M NaOH at room temperature, whereupon the radioactivity remaining within the cells was determined

by liquid scintillation counting of the cell lysates. Efflux per well was calculated as the percentage of counts released into the medium related to the total dose of radioactivity initially present (counts recovered within the medium added to the counts recovered from the cells). Values obtained from control cells without added HDLs were subtracted to correct for unspecific efflux. Values were normalized to values obtained with HDL isolated from a plasma pool obtained from normolipidemic, healthy controls, which was run with each plate.

5.6. Probands

5.6.1. Healthy Control Plasma Samples

Normolipidemic plasma samples from the blood bank in Zürich (Blutspende Zürich, Schlieren, Switzerland) were used for the isolation of HDL for the set-up of experimental conditions as well as the mechanistic experiments. Blood donors reported their health in a questionnaire. Lipaemic plasma samples were discarded.

5.6.2. VIVIT Cohort

Between September 1999 and October 2000, 750 Caucasian patients were enrolled in a long-term study at the Vorarlberg Institute for Vascular Investigation and Treatment (VIVIT) in Feldkirch, Austria. There, the patients underwent coronary angiography for the evaluation of suspected or established coronary artery disease (CAD) [158]. The study was approved by the Ethics Committee of the University of Innsbruck. All participants gave written informed consent. At baseline, anthropometric data were collected, clinical chemistry laboratory parameters were determined, and coronary angiography (Judkin's technique) was performed on all study participants. Patients were categorized into subgroups without and with CAD (coronary artery stenosis with lumen narrowing of ≥ 50%), and with normal fasting glucose (NFG, <5.6 mmol/L), impaired fasting glucose (IFG, ≥ 5.6 and ≤ 6.9 mmol/L), and type 2 DM (>6.9 mmol/L), according to the WHO criteria. According to the criteria of the National Cholesterol Education Program Adult Treatment Panel III (ATPIII), metabolic syndrome in the patients was assigned if three or more of the following criteria were met: waist circumference >102 cm (♂) or >88 cm (♀), triglycerides ≥1.7 mmol/L, HDL-cholesterol <1.0 mmol/L (♂) or <1.3 mmol/L (♀), blood pressure ≥130/≥85 mmHg, and fasting glucose ≥6.1 mmol/L.

1) Association of ApoC1 Content in HDL with Anti-Apoptotic Activity of HDL

We received 30 plasma samples of patients from the VIVIT cohort with CAD, CAD and metabolic syndrome (CAD+MetS), and CAD and type 2 DM (CAD+T2DM) for our study of the association of the plasma donors' glycemic state with anti-apoptotic activity and apoC1 concentration of HDL. The patient characteristics of the plasma donors are shown in table 5.3.

	CAD+T2DM (n=10)	CAD+MetS (n=10)	CAD (n=10)	p-value
Age (years)	64.27 (±3.58)	63.83 (±4.15)	64.10 (±3.58)	0.5623
Sex (male)	5 (50.00%)	5 (50.00%)	5 (50.00%)	1.0000
Waist circumference (cm)	100.70 (±10.61)	102.40 (±10.01)	94.00 (±8.96)	0.1216
Coronary artery stenosis >50%	10 (100.00%)	10 (100.00%)	10 (100.00%)	n/a
MetS ATP III Definition	8 (80.00%)	10 (100.00%)	0 (0.00%)	**<0.0001**
Type 2 DM (WHO)	10 (100.00%)	0 (0.00%)	0 (0.00%)	**<0.0001**
History of smoking	6 (60.00%)	4 (40.00%)	8 (80.00%)	0.1889
BMI (kg/m^2)	28.64 (±4.27)	28.49 (±1.86)	25.58 (±4.00)	0.1159
Total cholesterol (mmol/L)	4.43 (±1.58)	5.30 (±1.58)	5.18 (±0.75)	0.2013
HDL-cholesterol (mmol/L)	1.12 (±0.27)	1.26 (±0.33)	1.54 (±0.42)*	**0.0271**
LDL-cholesterol (mmol/L)	2.92 (±1.47)	3.68 (±1.45)	3.36 (±0.57)	0.2132
ApoA1 (g/L)	1.31 (±0.24)	1.47 (±0.23)	1.64 (±0.24)**	**0.0104**
ApoB (g/L)	0.80 (±0.33)	0.95 (±0.28)	0.85 (±0.14)	0.3700
Triglycerides (mmol/L)	1.73 (±0.70)	1.70 (±0.79)	1.36 (±0.55)	0.4213
Fasting glucose (mmol/L)	7.49 (±2.44)	5.26 (±0.41)**	5.20 (±0.28)**	**<0.0001**
Glucose 120 min after GTT (mmol/L)	11.60 (±4.51)	6.32 (±1.93)**	6.34 (±1.14)**	**0.0031**
HbA1c (%)	6.79 (±0.98)	5.67 (±0.25)***	5.63 (±0.25)***	**<0.0001**
C-reactive protein (mg/L)	7.18 (±7.91)	4.25 (±2.16)	2.52 (±1.65)	0.2357
Antihypertensive drugs	9 (90.00%)	8 (80.00%)	9 (90.00%)	0.7494
Statins	6 (60.00%)	4 (40.00%)	5 (50.00%)	0.6703
Aspirin	8 (80.00%)	9 (90.00%)	9 (90.00%)	0.7494

Table 5.3: Medical characteristics of coronary artery disease and type 2 diabetes mellitus (CAD+T2DM), CAD and metabolic syndrome (CAD+MetS), and CAD patients.
Values are shown as mean ±SD for the continuous variables and as percentages for the categorical variables. For the continuous clinical variables, p-values were calculated using ANOVA followed by the Bonferroni's post hoc test on the log transformed values. For the categorical variables, p-values were calculated using the X^2 test.
ATPIII: National Cholesterol Education Program Adult Treatment Panel III, BMI: Body mass index, Apo: apolipoprotein, GTT: glucose tolerance test (75 g oral glucose bolus), HbA1c: glycated hemoglobin, Antihypertensive drugs: beta-adrenergic blocking agents and/or angiotensin-converting-enzyme inhibitors.
** represents p<0.05 vs. T2DM, ** represents p<0.001 vs. T2DM, *** represents p<0.0001 vs. T2DM*

2) Association of Apolipoprotein C1 with Incident Diabetes Mellitus

For our study of apoC1 as prognostic marker for future type 2 DM development, 349 patients out of the above mentioned study VIVIT cohort were selected, for which eight years of follow-up data existed. The 111 patients with type 2 DM at baseline were not used for our investigations, and 133 patients were excluded for incomplete follow-up data. The patient

characteristics of the investigated plasma donors (35 patients with and 70 patients without incident type 2 DM during the eight year follow-up period) are shown in table 5.4.

	iT2DM (n=35)	no iT2DM (n=70)	p value
Age (years)	64.49 (±10.31)	61.29 (±9.13)	0.1371
Sex (female)	13 (37.14%)	26 (37.14%)	1.0000
Hypertension (WHO)	21 (60.00%)	28 (40.00%)	0.0528
History of smoking	16 (45.71%)	37 (52.86%)	0.4901
Coronary artery stenosis >50%	23 (65.71%)	38 (54.29%)	0.2632
MetS ATP III Definition	17 (48.57%)	15 (21.43%)	**0.0044**
BMI (kg/m^2)	27.14 (±5.13)	26.42 (±3.32)	0.5310
Waist circumference (cm)	101.00 (±9.61)	99.79 (±6.66)	0.1666
Waist-to-hip ratio	0.95 (±0.10)	0.93 (±0.09)	0.2567
Total cholesterol (mmol/L)	5.80 (±1.30)	5.65 (±1.05)	0.7662
HDL-cholesterol (mmol/L)	1.28 (±0.40)	1.31 (±0.39)	0.6927
LDL-cholesterol (mmol/L)	3.44 (±0.89)	3.48 (±0.80)	0.6523
Triglycerides (mmol/L)	2.20 (±1.62)	1.61 (±0.93)	**0.0186**
Fasting glucose (mmol/L)	6.03 (±1.20)	5.76 (±1.06)	0.1858
HbA1c (%)	6.01 (±0.55)	5.72 (±0.39)	**0.0031**
Fasting insulin (pmol/L)	109.94 (±181.68)	62.37 (±31.98)	0.2212
HOMA-IR	2.89 (±2.20)	2.28 (±1.25)	0.4800
Systolic blood pressure (mmHg)	139.60 (±20.50)	131.60 (±19.09)	0.0510
Diastolic blood pressure (mmHg)	79.85 (±13.62)	76.54 (±10.97)	0.2686
C-reactive protein (mg/L)	7.84 (±14.86)	6.97 (±9.59)	0.7905
Serum Potassium (mmol/L)	1.14 (±0.08)	1.10 (±0.10)	**0.0284**
Creatinine (μmol/L)	108.86 (±88.35)	93.10 (±13.11)	0.2264
eGFR (CKD-EPI, mL/min per 1.73 m^2)	67.19 (±18.07)	70.20 (±13.32)	0.1633
Antihypertensive drugs	35 (100.00%)	57 (81.43%)	**0.0065**
Lipid-lowering drugs	16 (45.71%)	37 (52.86%)	0.4901
Aspirin	28 (80.00%)	54 (77.14%)	0.7386

Table 5.4: Medical characteristics of plasma donors without (no iT2DM) and with incident type 2 DM (iT2DM).

Values are shown as mean ±SD for the continuous variables and as percentages for the categorical variables. For the continuous clinical variables, p-values were calculated using the two-sided Student's t-test on the log transformed values. For the categorical variables, p-values were calculated using the X^2 test.

MetS: Metabolic Syndrome, ATPIII: National Cholesterol Education Program Adult Treatment Panel III, BMI: Body mass index, Apo: apolipoprotein, HbA1c: glycated hemoglobin, HOMA-IR: homeostatic model assessment-insulin resistance, eGFR: estimated glomerular filtration rate (calculated according to CKD-EPI formula [159]), Antihypertensive drugs: beta-adrenergic blocking agents, angiotensin-converting-enzyme inhibitors, angiotensin II receptor antagonists, calcium channel blockers, alpha blockers, thiazides, loop diuretics, potassium sparing diuretics, other diuretics, and/or other antihypertensives; Lipid-lowering drugs: fibrates and/or statins.

	CAD+T2DM (n=15)	CAD+IFG (n=15)	CAD+NFG (n=14)	no CAD+NFG (n=14)	p value
Age (years)	60.83 (±5.35)	60.95 (±5.35)	60.80 (±5.59)	60.83 (±5.66)	0.9998
Sex (male)	15 (100.00%)	15 (100.00%)	14 (100.00%)	14 (100.00%)	n/a
Hypertension (WHO)	12 (80.00%)	13 (86.67%)	9 (64.29%)	11 (78.57%)	0.5332
History of smoking	14 (93.33%)	12 (80.00%)	11 (78.57%)	10 (71.43%)	0.4969
BMI (kg/m^2)	28.80 (±5.05)	26.86 (±2.31)	27.01 (±4.93)	28.56 (±4.80)	0.5894
Total cholesterol (mmol/L)	5.18 (±0.77)	4.97 (±0.80)	6.06 (±1.19)	5.01 (±1.35)	**0.0329**
HDL-C (mmol/L)	1.41 (±0.46)	1.63 (±0.49)	1.61 (±0.46)	1.23 (±0.32)	0.0632
LDL-C (mmol/L)	3.31 (±0.77)	3.25 (±0.75)	4.02 (±1.04)	3.37 (±1.09)	0.1816
ApoA1 (g/L)	1.53 (±0.30)	1.62 (±0.33)	1.60 (±0.24)	1.37 (±0.19)	0.0795
ApoB (g/L)	0.92 (±0.22)	0.82 (±0.16)	0.98 (±0.24)	0.89 (±0.26)	0.3623
Triglycerides (mmol/L)	1.98 (±1.08)	1.19 (±0.51)	1.87 (±1.11)	1.66 (±0.93)	0.1559
Aspartate transaminase (IU/L)	27.00 (±12.77)	32.20 (±22.91)	29.79 (±11.20)	29.29 (±8.20)	0.7420
Alanine transaminase (IU/L)	34.67 (±19.76)	35.13 (±24.11)	29.93 (±13.22)	36.64 (±17.71)	0.7971
Gamma-glutamyl transferase (IU/L)	119.33 (±167.29)	50.33 (±40.92)	42.86 (±29.51)	35.86 (±18.08)	0.1888
Fasting glucose (mmol/L)	9.42 (±2.95)	5.98 (±0.26)*	5.01 (±0.36)*§	5.00 (±0.30)*§	**<0.0001**
HbA1c (%)	7.83 (±1.41)	5.83 (±0.42)*	5.71 (±0.33)*	5.61 (±0.36)*	**<0.0001**
C-reactive protein (mg/L)	3.28 (±2.61)	2.99 (±1.90)	5.74 (±9.93)	4.03 (±6.67)	0.9489
Creatinine (μmol/L)	77.20 (14.36)	79.56 (11.08)	75.14 (14.61)	84.61 (18.90)	0.4603
eGFR (CKD-EPI, mL/min per 1.73 m^2)	90.71 (±13.34)	89.28 (±9.10)	93.20 (±12.78)	84.38 (±16.44)	0.3036
Albumin creatinine ratio	392.79 (±960.66)	44.09 (±92.04)	65.93 (±155.04)	31.31 (±31.03)	0.1656
Antihypertensive drugs	9 (60.00%)	11 (73.33%)	8 (57.14%)	10 (71.43%)	0.7389
Statins	7 (46.67%)	4 (40.00%)	6 (42.86%)	2 (14.29%)	0.2631
Aspirin	9 (60.00%)	8 (53.33%)	10 (71.43%)	7 (50.00%)	0.6684
Diabetes mellitus drugs	10 (66.67%)	0 (0.00%)*	0 (0.00%)*	0 (0.00%)*	**<0.0001**

Table 5.5: Medical characteristics of CAD+T2DM, CAD+IFG, CAD+NFG and no CAD+NFG subjects. Values are shown as mean ±SD for the continuous variables and as percentages for the categorical variables. For the continuous clinical variables, p-values were calculated using ANOVA followed by the Bonferroni's post hoc test on the log transformed values. For the categorical variables, p-values were calculated using the X^2 test.

** represents p<0.0001 vs. T2DM, § represents p<0.05 vs. IFG*

BMI: Body mass index, HDL-C: High density lipoprotein cholesterol, LDL-C: Low density lipoprotein cholesterol, Apo: apolipoprotein, HbA1c: glycated hemoglobin, eGFR: estimated glomerular filtration rate (calculated according to CKD-EPI formula [159]), Antihypertensive drugs: beta-adrenergic blocking agents, angiotensin-converting-enzyme inhibitors, and/or angiotensin II receptor antagonists; Diabetes mellitus drugs: glitazones, meglitinides, biguanide derivatives, sulfonylureas, and/or insulin.

3) Association of Glycemic State with Anti-Apoptotic Functionality of HDL

We used 58 additional samples from the VIVIT cohort to investigate the association of the glycemic state with the anti-apoptotic functionality of HDL. To this end, we isolated HDL from type 2 DM patients with coronary artery disease (CAD+T2DM) and control groups (normal fasting glucose without coronary artery disease (no CAD+NFG), normal fasting glucose with coronary artery disease (CAD+NFG), and impaired fasting glucose with coronary artery disease (CAD+IFG)), The medical characteristics of the HDL donors of this study are shown in table 5.5.

5.6.3. Functionality of HDL from Patients with Diabetes Mellitus Type 1

We obtained plasma samples from 19 young, type 1 diabetic patients and 27 normoglycemic, age-matched control subjects. These samples had been collected in 2011 in the children and youth department of the Landeskrankenhaus in Feldkirch, Austria, at the supervision of Prof. Dr. Burkhard Simma. Dr. Anya Blassnig-Ezeh had been in charge for the patient recruitment and blood collection. All patients, or their parents, gave written informed consent. The subjects' anthropometric data were collected, and clinical chemistry laboratory parameters were determined. The medical characteristics of the HDL donors (type 1 DM and control subjects) are shown in table 5.6.

	T1DM (n=18)	no T1DM (n=27)	p value
Age (years)	15.10 (±2.31)	14.93 (±2.30)	1.0000
Sex (male)	10 (55.56%)	10 (37.04%)	0.2207
BMI (kg/m^2)	20.26 (±3.08)	21.69 (±5.18)	0.2549
Total cholesterol (mmol/L)	4.30 (±0.90)	3.90 (±0.82)	0.1618
HDL-cholesterol (mmol/L)	1.26 (±0.23)	1.04 (±0.30)	**0.0055**
LDL-cholesterol (mmol/L)	2.59 (±0.86)	2.43 (±0.77)	0.6356
nonHDL-cholesterol (mmol/L)	3.04 (±0.92)	2.88 (±0.84)	0.6088
Cholesterol/HDL-Chol. ratio	3.50 (±0.93)	4.00 (±1.30)	0.2099
ApoA1 (g/L)	1.59 (±0.24)	1.39 (±0.23)	**0.0048**
ApoB (g/L)	0.76 (±0.22)	0.69 (±0.24)	0.3265
Triglycerides (mmol/L)	1.00 (±0.41)	0.97 (±0.37)	0.8513
Aspartate transaminase (IU/L)	23.59 (±3.81)	26.10 (±5.76)	0.1718
Alanine transaminase (IU/L)	9.06 (±4.48)	6.75 (±2.80)	**0.0162**
Fasting glucose (mmol/L)	12.18 (±4.62)	4.72 (±1.72)	**0.0001**
HbA1c (%)	9.17 (±1.84)	n/d	n/a
C-reactive protein (mg/L)	4.23 (±3.92)	3.62 (±5.79)	0.1651
Creatinine (μmol/L)	78.00 (±10.17)	72.71 (±11.10)	0.1303
Insulin treatment	18 (100.00%)	n/d	n/a
L-Thyroxin	5 (27.78%)	n/d	n/a
Propanolol	1 (5.56%)	n/d	n/a

Table 5.6: Medical characteristics of T1DM patients and control subjects (no T1DM)
Values are shown as mean ±SD for the continuous variables and as percentages for the categorical variables. For the continuous clinical variables, p-values were calculated using the two-sided Student's t-test on the log transformed values. For the categorical variables, p-values were calculated using the X^2 test.
BMI: Body mass index, Apo: apolipoprotein, HbA1c: glycated hemoglobin.

5.7. Statistical Analyses

Statistical analyses were done with the GraphPad Prism software version 5.00 (GraphPad software Inc., La Jolla CA, USA). Unless otherwise indicated, experiments were done at least in triplicates, and the bar graphs display the mean + one standard error of the mean (SEM) or standard deviation (SD). Scatter dot plots are shown with the median and interquartile ranges (IQR). Continuous patient variables were log-transformed before analysis. The Student's t-test (two-sided) or analysis of variance (ANOVA) with Bonferroni's post hoc test were used to test for significant differences between two or more groups, respectively. The X^2 test was used to compare categorical patient variables. For correlation analyses of patient variables and experimental data, the Pearson's correlation coefficient r, and the p value (two-sided test) were calculated.

6. Results

6.1. Protective Effect of HDL against β-Cell Apoptosis

6.1.1. Effects of HDL and Interleukin-1β on β-Cell Lines

In a first step, we explored if IL-1β was capable to induce apoptosis in the pancreatic β-cell lines INS-1E and Min6. Simultaneously, we investigated if HDL protected the cells from IL-1β-induced apoptosis. The increase in cytosolic DNA after apoptosis stimulation compared to a not treated condition was our indicator for apoptosis.

In Min6 cells, stimulation of apoptosis with IL-1β for 48 hours was mild (1.5-fold) and the presence of HDL did not attenuate the induction of apoptosis (Fig. 6.1A). Thus, Min6 cells were ruled out as an unsuitable model for IL-1β-induced apoptosis. In INS-1E cells, stimulation of apoptosis with IL-1β for 48 hours increased apoptosis by 2.5-fold compared to not treated cells, and HDL attenuated this induction (Fig. 6.1A).

Further experiments with INS-1E cells confirmed that apoptosis was induced by IL-1β stimulation and prevented by HDL in a dose-dependent manner. INS-1E cells were incubated with different concentrations of HDL for 40 hours. The addition of IL-1β during the last 24 hours of the experiment revealed a preventive effect of HDL by 50% and more (Fig. 6.1B). 16 hours of pre-incubation with HDL followed by 24 hours IL-1β stimulation in the absence of HDL ("sequential") revealed a significant anti-apoptotic effect as well (Fig. 6.1C).

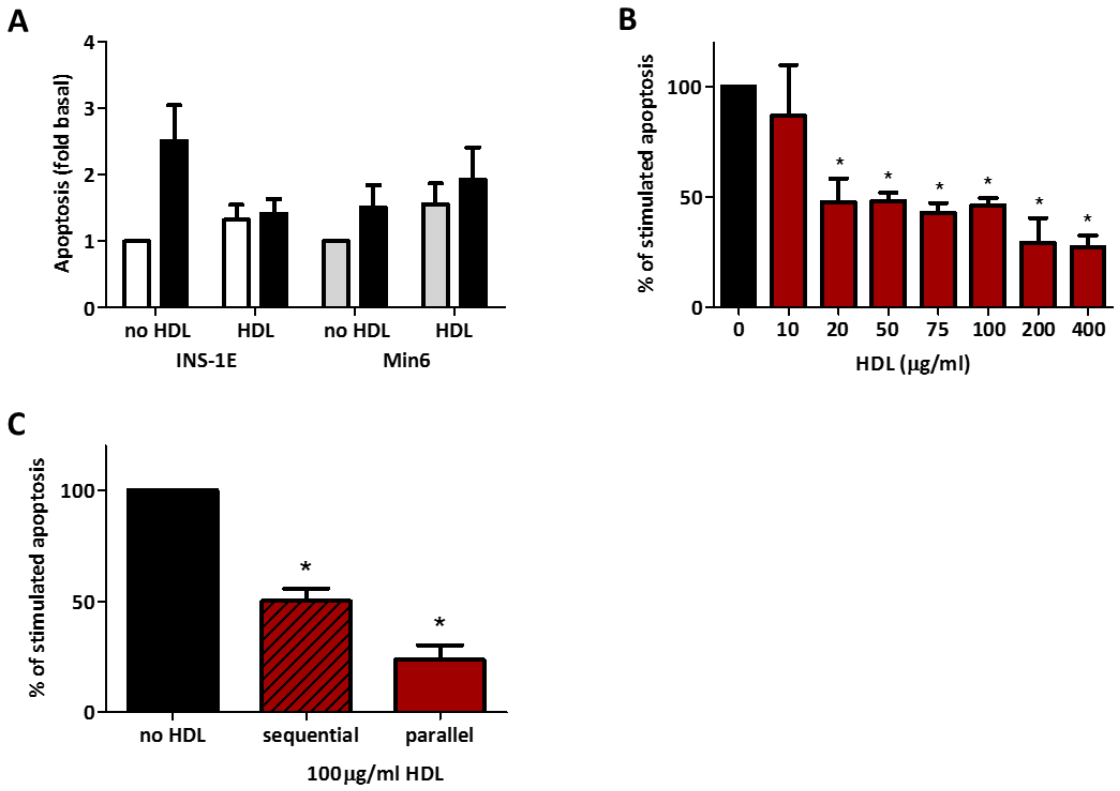

Figure 6.1: Effect of HDL on IL-1β-induced apoptosis in pancreatic β-cells.
A: INS-1E and Min6 cells were cultured for 48 hours in the presence or absence of HDL at a concentration of 20 µg/ml, with and without IL-1β (10 ng/ml) for the stimulation of apoptosis. The white/grey bars indicate basal apoptosis, black bars IL-1β-stimulated apoptosis (n=4).
B: INS-1E cells were cultured for 40 hours in the absence or presence of HDL at the indicated concentrations. During the last 24 hours, IL-1β (10 ng/ml) was added for the stimulation of apoptosis (n=4).
C: INS-1E cells were cultured for 16 hours in the absence (no HDL) or presence of 100 µg/ml HDL (sequential and parallel). The medium was then replaced with medium containing either 10 ng/ml IL-1β alone (no HDL and sequential) or both, 10 ng/ml IL-1β and 100 µg/l HDL (parallel). Apoptosis induction was determined after 24 hours (n=4).
*Bars indicate the mean values +SEM; * represents p<0.05 compared to condition without HDL*

6.1.2. Effects of the HDL Components on Interleukin-1β-Induced Apoptosis

After verifying that HDL prevents IL-1β-induced apoptosis in INS-1E cells, we analyzed the effects of both, the protein and the lipid moieties of HDL, as well as single components of HDL. Incubation with HDL and the protein moiety of HDL prevented apoptosis comparably and effectively (Fig. 6.2A). In contrast, the mild anti-apoptotic effect of the HDL lipid moiety was not significant. The protective effect of the HDL protein moiety was dose-dependent (Fig. 6.2B).

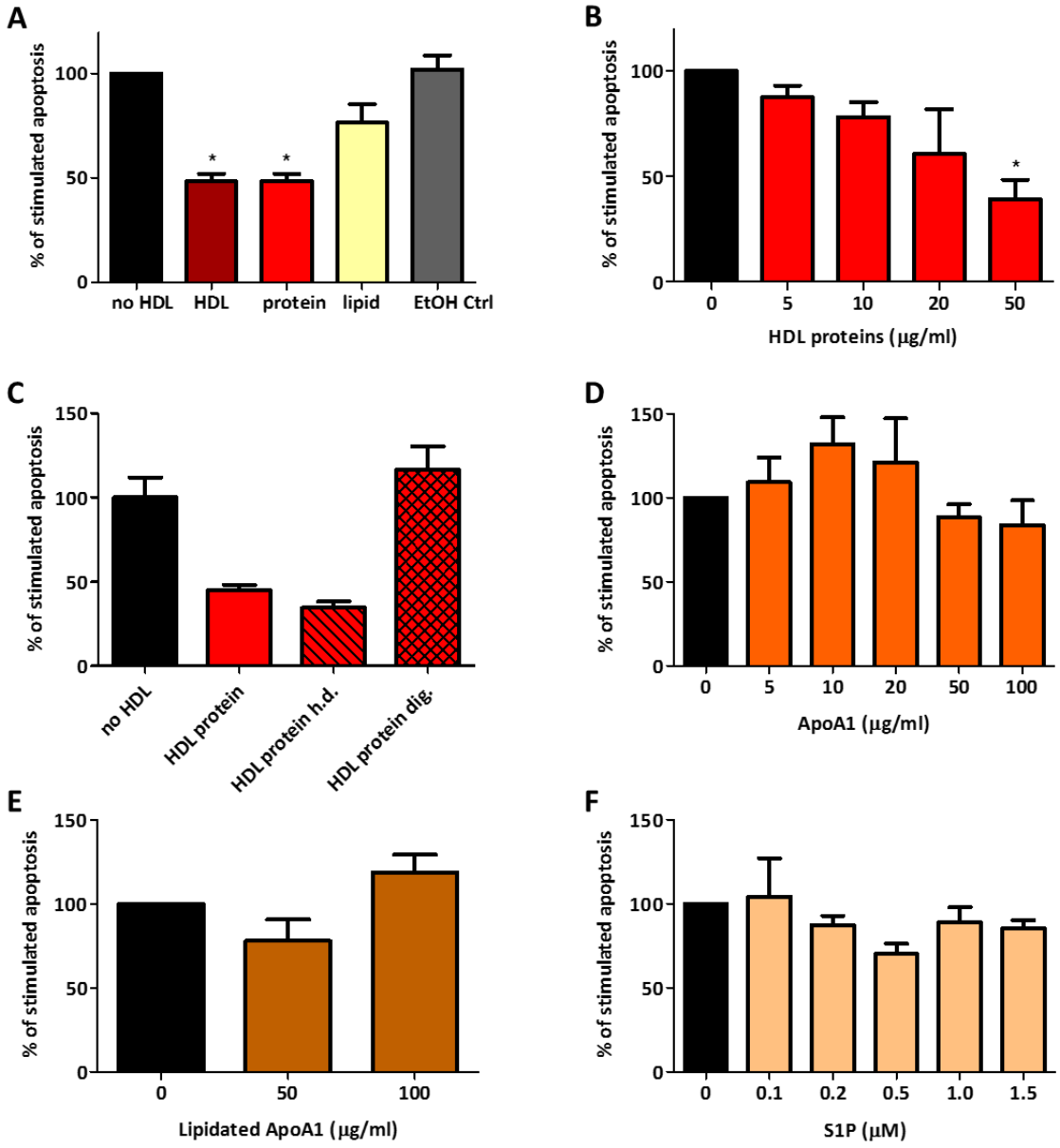

Figure 6.2: Effect of HDL components on IL-1β-induced apoptosis.
INS-1E cells were cultured in the presence of the indicated HDL components. During the last 24 hours, IL-1β (10 ng/ml) was added for the stimulation of apoptosis.
A: INS-1E cells were cultured for 40 hours in the presence or absence of HDL, the HDL protein moiety, the HDL lipid moiety (dissolved in ethanol (EtOH)), or EtOH alone at a concentration corresponding to 50 µg/ml HDL protein (n=8).
B: INS-1E cells were cultured for 40 hours in the presence of the HDL protein moiety at the indicated concentrations (n=3).
C: INS-1E cells were cultured for 40 hours in the presence of the 50 µg/ml HDL protein moiety, heat denatured (h.d.) HDL protein moiety, or the trypsin digested and heat denatured (dig.) HDL protein moiety (n=1).
D: INS-1E cells were cultured for 40 hours in the presence of apoA1 at the indicated concentrations (n=4).
E: INS-1E cells were cultured for 40 hours in the presence of lipidated apoA1 (molar ratio 1:80 apoA1:POPC) at the indicated concentrations (n=8 at 50 µg/ml, n=2 at 100 µg/ml).
F: INS-1E cells were cultured for 40 hours in the presence of S1P at the indicated concentrations (n=3).
*Bars indicate the mean values +SEM; * represents p<0.05 compared to condition without HDL*

The protective effect of the HDL protein moiety against IL-1β-induced apoptosis was abolished by trypsin digestion of the protein moiety, whereas heat denaturation of the protein moiety, which was used for trypsin inactivation, did not affect the protective effect of the HDL protein moiety (Fig. 6.2C).

The HDL protein moiety consists of about 100 different proteins including apolipoprotein A1 (apoA1), which accounts for 70% of the protein mass. Moreover, apoA1 had previously been identified as an anti-apoptotic agent in β-cells of human and murine islets [88]. Therefore, we studied the effect of purified apoA1 in INS-1E cells. The purified apoA1 revealed no significant anti-apoptotic effect (Fig. 6.2D). This negative result was verified with several different apoA1 preparations and over a broad range of concentrations. Lipidation of apoA1 with 1-palmitoyl-2-oleoylphosphatidylcholine (POPC) in the molar ratio of 1:80 (apoA1:POPC) prior to the experiment neither revealed any anti-apoptotic effect for apoA1 (Fig. 6.2E).

The HDL component sphingosine-1-phosphate (S1P) had previously been described to exert anti-apoptotic effects on many cells including β-cells of human or murine islets [88]. However, S1P did not prevent IL-1β-induced apoptosis in INS-1E cells (Fig. 6.2F).

6.1.3. Fractionation of HDL Protein Moiety

Since apoA1 did not prevent IL-1β-induced apoptosis in INS-1E cells, we sought to elucidate which protein(s) of the approximately 100 different proteins identified in HDL particles mediated the anti-apoptotic effect of HDL. For this purpose, the protein moiety was fractionated by liquid chromatography with an anion-exchange column. The fractions were pooled according to the peaks of the chromatogram into five pools (Fig. 6.3A). The different pools were initially analyzed by SDS-PAGE (Fig. 6.3B). All pools contained apoA1 as their major protein component. We analyzed the five pools for their potential to prevent IL-1β-induced apoptosis (Fig. 6.3C). Fractions B and D revealed both some potential to reduce IL-1β-induced apoptosis. Fraction D contained a protein of about 30-35 kDa size, which is characteristic for apolipoprotein E (apoE) (asterisk in Fig. 6.3B), a protein regularly carried by HDL. However, apoE did not prevent IL-1β-induced apoptosis (Fig. 6.3D).

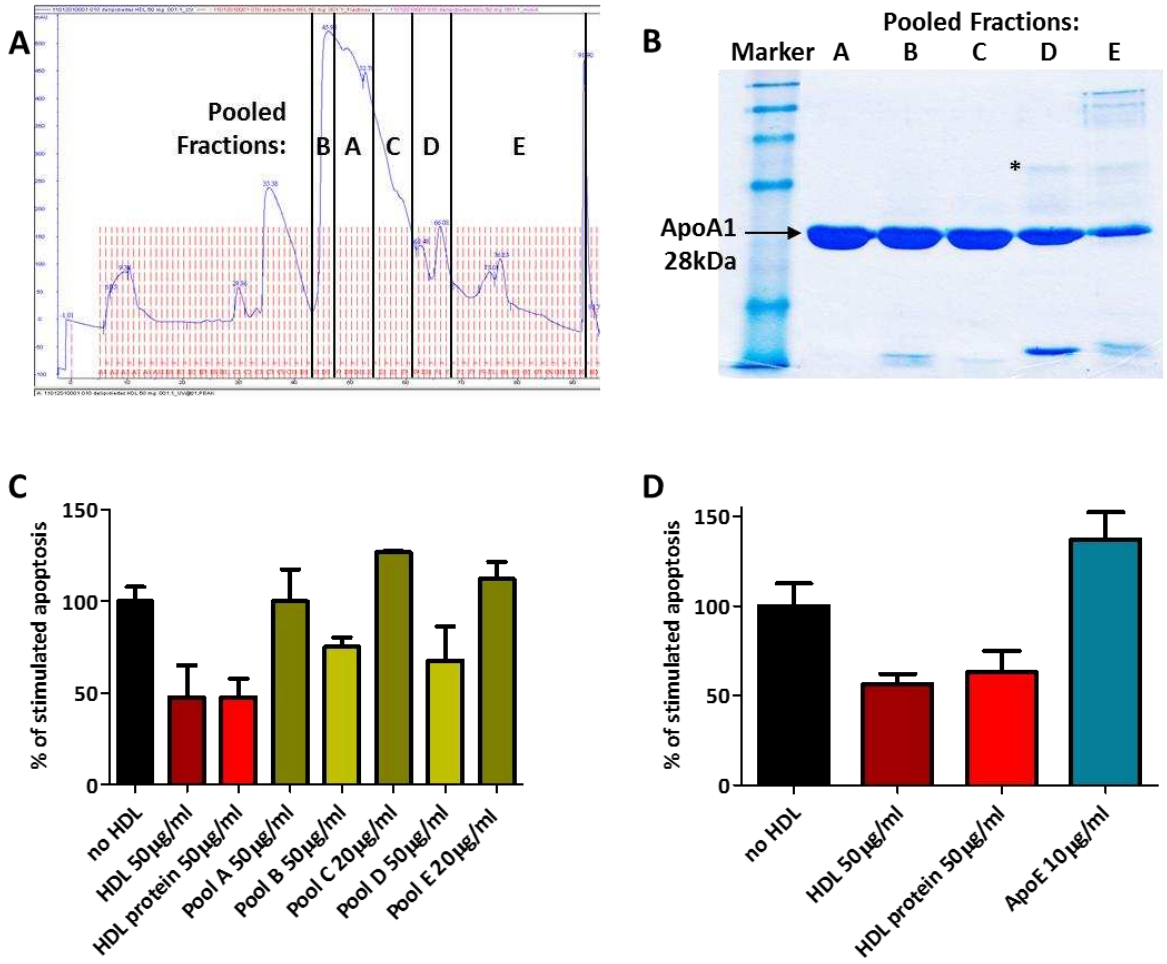

Figure 6.3: Effect of HDL proteins on IL-1β-induced apoptosis.
A: Chromatogram of the anion-exchange chromatography of the HDL protein moiety with the pooled fractions indicated.
B: 12% SDS-PAGE with different fraction pools after Coomassie-blue staining; * indicates a band at about 33 kDa.
C: INS-1E cells were cultured for 40 hours in the presence of HDL, HDL protein moiety, or different pooled HPLC-fractions (A to E) at the indicated concentrations. During the last 24 hours, IL-1β (10 ng/ml) was added for the stimulation of apoptosis (n=1 for pool A, B, C, E; n=2 for others).
C: INS-1E cells were cultured for 40 hours in the presence of HDL, HDL protein moiety, or apoE at the indicated concentrations. During the last 24 hours, IL-1β (10 ng/ml) was added for the stimulation of apoptosis (n=1).
Bars indicate the mean values +SEM

6.1.4. Analysis of HDL Protein Fractions

For further analysis of the protein moiety, we used the collaboration of our group with Meliana Riwanto from the Department of Cardiology [77] to analyze the proteome of the pooled HDL fractions A, B and D. As seen on the SDS-PAGE (Fig. 6.3B), apoA1 was the most abundant protein in all pools (Tab. 5.1). Pool D was characterized by the enrichment of apolipoprotein D (apoD) and apolipoprotein C1 (apoC1), which are otherwise little abundant proteins of HDL.

Pool A		**Pool B**		**Pool D**	
Apolipoprotein	*Abundance rel. to apoA1*	*Apolipoprotein*	*Abundance rel. to apoA1*	*Apolipoprotein*	*Abundance rel. to apoA1*
ApoA1	100.00%	ApoA1	100.00%	ApoA1	100.00%
ApoA2	4.32%	ApoA2	36.10%	**ApoD**	**64.60%**
ApoD	0.63%	ApoC2	6.62%	**ApoC1**	**46.20%**
ApoC3	0.56%	ApoC3	1.80%	ApoC3	6.46%
ApoC2	0.53%	ApoD	0.79%	ApoM	6.46%
ApoL1	0.15%	ApoL1	0.51%	ApoE	4.75%

Table 6.1: Proteomic analysis of pooled HDL protein fractions.
Analysis done by LC-ESI-MS/MS and quantified with internal standards. The abundance of proteins is expressed relative to apoA1.

6.1.5. Effects of Apolipoprotein C1 and Apolipoprotein D

Based on the proteome analysis, we tested if purified apoC1 or recombinant apoD protected the INS-1E cells from IL-1β-induced apoptosis. At the same concentration, apoC1, but not apoD, prevented IL-1β-induced apoptosis (Fig. 6.4A+B). For apoC1, the protective effect was dose-dependent (Fig. 6.4C).

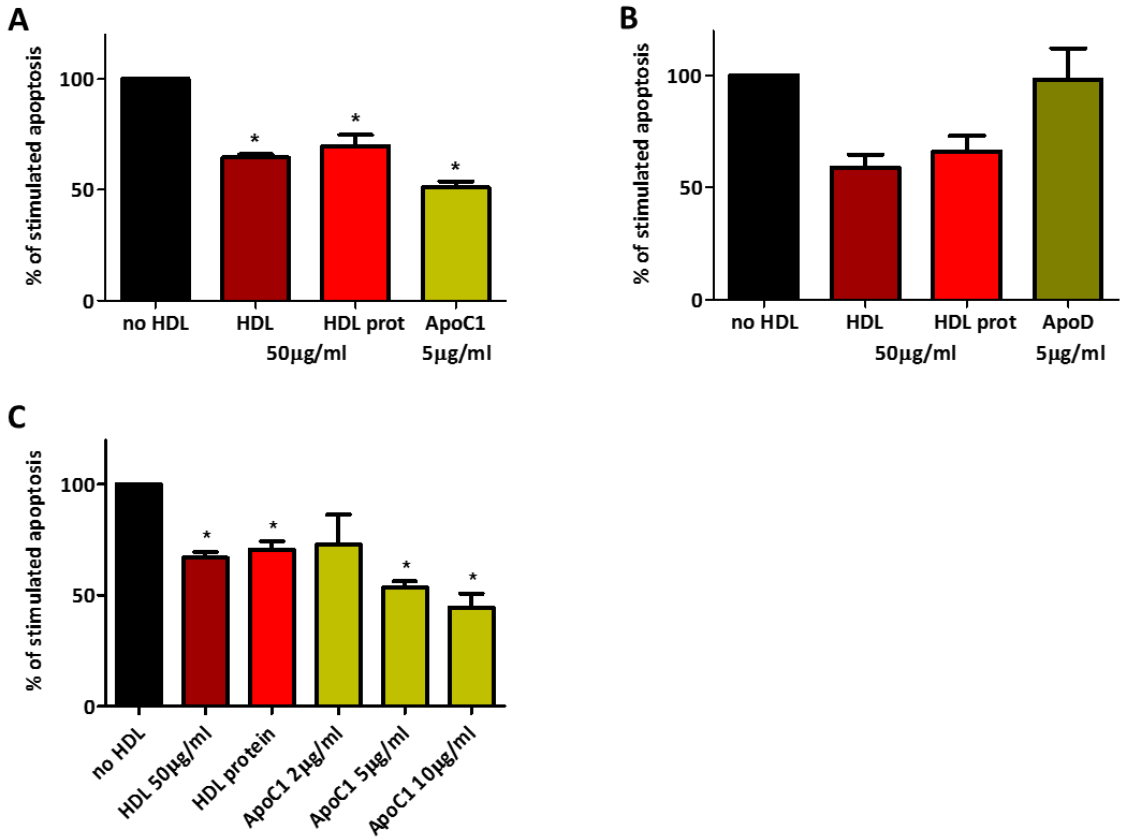

Figure 6.4: Effect of apoC1 and apoD on IL-1β-induced apoptosis.
A+C: INS-1E cells were cultured for 40 hours in the presence of HDL, HDL protein moiety, or apoC1 at the indicated concentrations. During the last 24 hours, IL-1β (10 ng/ml) was added for the stimulation of apoptosis (n=6).
B: INS-1E cells were cultured for 40 hours in the presence of HDL, HDL protein moiety, or apoD at the indicated concentrations. During the last 24 hours, IL-1β (10 ng/ml) was added for the stimulation of apoptosis (n=2).
*Bars indicate the mean values +SEM; * represents p<0.05 compared to condition without HDL*

6.1.6. Effect of Apolipoprotein C1-Deficient Murine HDL

Motivated by the previous finding, we wondered about the protective effect of apoC1-deficient HDL. In collaboration with P. Rensen and J. Berbée from Leiden (NL) [160], we obtained sera from human apoC1 transgene (apoC1Tg), apoC1 deficient (apoC1KO), and control mice to analyze their HDL for the potential to prevent IL-1β-induced apoptosis. Overall, murine HDL revealed a lower anti-apoptotic effect than human HDL (Fig. 6.5). At a concentration of 50 µg/ml, at which human HDL elicit their maximal anti-apoptotic effect (-50%), HDL of wild type mice inhibited apoptosis by 20%, HDL of apoC1KO mice by 0%, and HDL of apoC1Tg mice by 30%. Of note, at a low concentration of 10 µg/ml, where both human and murine HDL (wild type and apoC1Tg) inhibited apoptosis by 20%, HDL of apoC1KO mice had a rather pro-apoptotic effect.

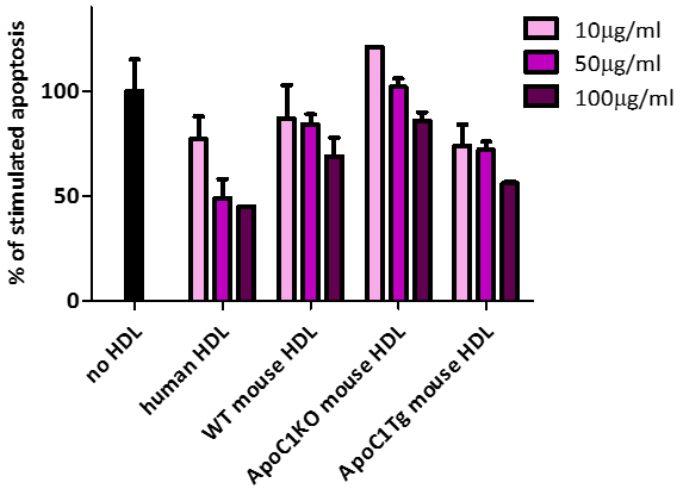

Figure 6.5: Effect of HDL from mice with and without apoC1.

INS-1E cells were cultured for 40 hours in the presence of different mouse HDL or human HDL at the indicated concentrations. During the last 24 hours, IL-1β (10 ng/ml) was added for the stimulation of apoptosis (n=1).
Bars indicate the mean values +SD

6.1.7. Association of Glycemic State with Anti-Apoptotic Activity and ApoC1 Concentration of HDL

Next, we investigated if the glycemic state of human plasma donors was associated with differences in HDL's the anti-apoptotic activity on β-cells and apoC1 content. Therefore, we isolated HDL from plasma samples of 10 patients with coronary artery disease and type 2 DM (CAD+T2DM HDL), 10 CAD patients with metabolic syndrome (CAD+MetS HDL) and 10 CAD patients without metabolic syndrome or diabetes (CAD HDL). The clinical details on the study subjects are listed in table 5.3 (see materials and methods section). According to their diagnosis, subjects differed fasting glucose levels *(7.49 mM (CAD+T2DM) vs. 5.26 mM (CAD+MetS), and 5.20 mM (CAD), p<0.0001)*, glucose levels 120 minutes after a glucose tolerance test *(11.60 mM (CAD+T2DM) vs. 6.32 mM (CAD+MetS), and 6.34 mM (CAD), p=0.0031)*, and glycated hemoglobin percentage (HbA1c, *6.79% (CAD+T2DM) vs. 5.67% (CAD+MetS), and 5.63% (CAD), p=0.0031))*. Further differences with weaker statistical significance though were found in HDL cholesterol levels *(1.12 mM (CAD+T2DM) vs. 1.26 mM (CAD+MetS), and 1.54 mM (CAD), p=0.0271)*, and apoA1 levels *(1.31 g/L (CAD+T2DM) vs. 1.47 g/L (CAD+MetS), and 1.64 g/L (CAD), p=0.0104)*. The other clinical variables were not

significantly different between the patient groups. HDL isolated from healthy blood donors obtained from the blood bank served as control (ctrl HDL).

We did not observe any significant association of the HDL's anti-apoptotic capacity with the glycemic state of the donor (Fig. 6.6A). The anti-apoptotic potential of HDL isolated from the different patients depict a high degree of inter-individual variation though.

The apoC1 levels in HDL did not differ between the patient groups (Fig. 6.6B). However, a significant correlation between the apoC1 content of the HDL samples and their anti-apoptotic effect on INS-1E cells was observed (r=0.4151, Fig. 6.6C). Correlation analysis with the patient's clinical variables revealed significant correlations of the HDL's anti-apoptotic activity with triglyceride levels (r=0.5376) and HDL cholesterol (r=-0.3806, Fig. 6.6D+E, Tab. 6.2). Moreover, the apoC1 concentration in HDL correlated with the patients' age (Tab. 6.2).

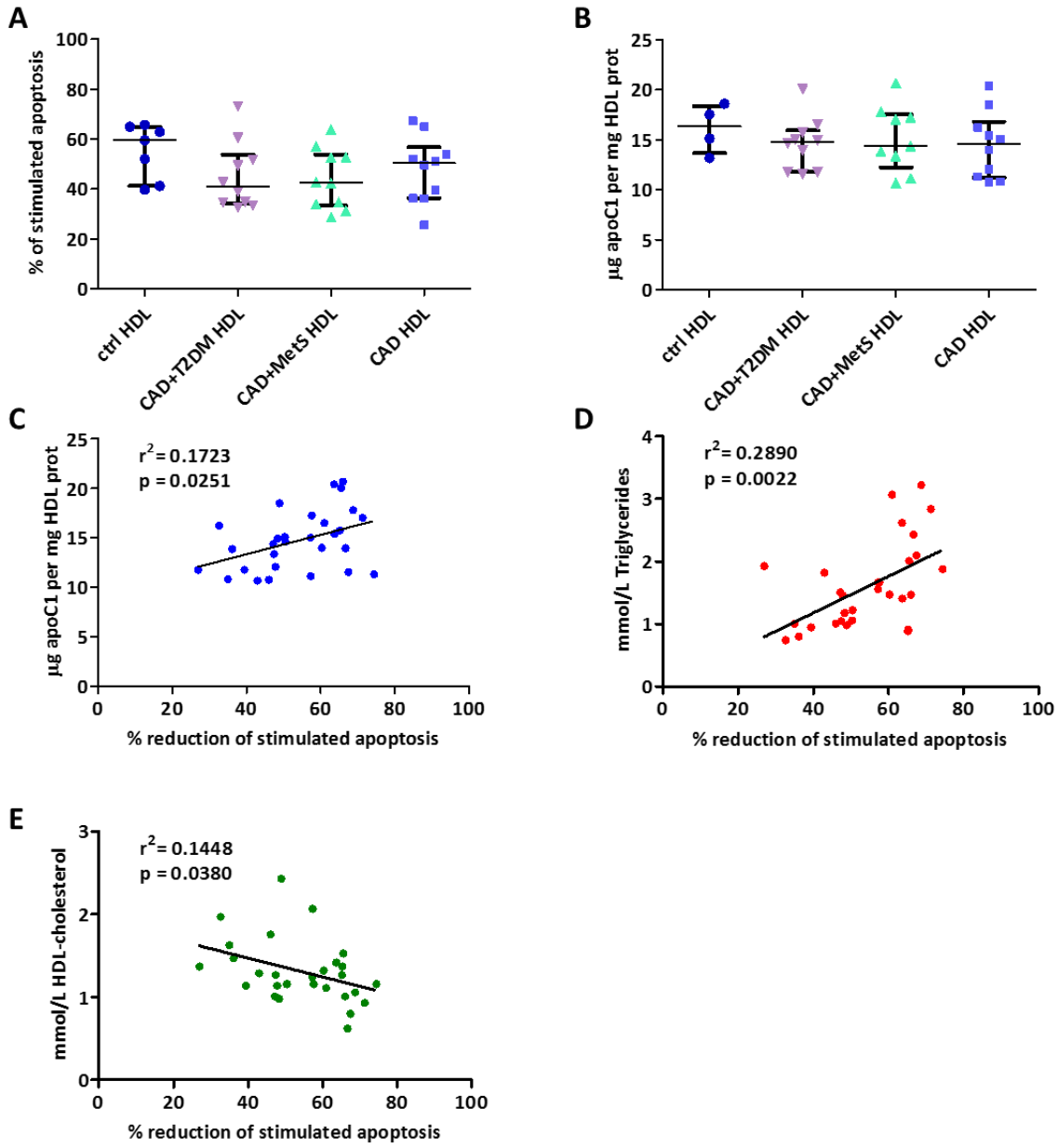

Figure 6.6: Protective effect of HDL is related to apoC1 content.

A: INS-1E cells were cultured for 40 hours in the presence of 50 µg/ml HDL from healthy control subjects (ctrl HDL, n=7) or patient donors with coronary artery disease and type 2 diabetes (CAD+T2DM, n=10), CAD and metabolic syndrome (CAD+MetS, n=10) or CAD (n=10). During the last 24 hours, IL-1β (10 ng/ml) was added for the stimulation of apoptosis.

B: ApoC1 content of the HDL samples described in 6A normalized to total HDL protein content.

C: Correlation analysis of the data of the apoptosis experiments shown in 6A and the respective apoC1 content (relative to HDL protein content) shown in 6B.

D+E: Correlation analysis of apoptosis reduction in β-cells shown in 6A and triglyceride levels (D), or HDL-cholesterol levels (E) of the respective HDL donor.

Scatter dot plots (A+B) are displayed with the median ± IQR.

The regression line (C-F) is shown for better visibility of the graph.

Clinical variables	reduction of stim. apoptosis		ApoC1 content	
	Pearson r	*p value*	*Pearson r*	*p value*
Age	0.0237	0.9010	0.4867	**0.0074**
Sex (male)	-0.2104	0.2645	0.1366	0.4798
History of smoking	-0.1095	0.5645	0.1748	0.3646
BMI	0.2449	0.1921	-0.0190	0.9221
Waist circumference	0.2621	0.1618	0.1871	0.3311
Triglycerides	0.5376	**0.0022**	0.2855	0.1333
Total cholesterol	0.1257	0.5081	0.2298	0.2305
LDL-cholesterol	0.1515	0.4242	0.1754	0.3627
HDL-cholesterol	-0.3806	**0.0380**	0.0163	0.9331
ApoA1	-0.1274	0.5100	0.1132	0.5664
ApoB	0.2308	0.2284	0.2186	0.2638
Fasting glucose	0.3117	0.0936	0.0472	0.8080
Glucose tolerance test (120min)	-0.1773	0.3863	-0.1230	0.5581
HbA1c	0.1140	0.5485	-0.1001	0.6055
C-reactive protein	0.0832	0.6620	0.0157	0.9354
Antihypertensive drugs	0.0191	0.9203	-0.0162	0.9334
Statins	0.3513	0.0569	-0.0481	0.8043
Aspirin	0.2601	0.1651	0.2200	0.2515

Table 6.2: Correlation analysis between the patient's clinical variables and the reduction of stimulated apoptosis by HDL, or the apoC1 concentration in HDL, respectively.
The Pearson's correlation coefficient r and p values (two-tailed test) are indicated.
BMI: Body mass index, Apo: apolipoprotein, HbA1c: glycated hemoglobin, Antihypertensive drugs: beta-adrenergic blocking agents and/or angiotensin-converting-enzyme inhibitors.

6.1.8. Association of Apolipoprotein C1 with Incident Diabetes Mellitus

We investigated in a prospective study if apoC1 levels are associated with incident type 2 DM. ApoC1 levels were measured in total and apoB-depleted plasma (a surrogate for HDL) of 105 patients of the VIVIT cohort who were normoglycemic at baseline. During eight years follow up, 35 persons out of the 105 had developed type 2 diabetes mellitus (Fig. 6.7A). The clinical variables of the study subjects are listed in table 5.4 (see materials and methods section). At baseline, the study subjects with incident type 2 DM differed from the study subjects without incident type 2 DM by significantly higher triglyceride levels *(2.20 mM vs. 1.61 mM, p=0.0186)*, higher HbA1c levels *(6.01% vs. 5.72%, p=0.0031)*, higher serum potassium levels *(1.14 mM vs. 1.10 mM, p=0.0284)*, as well as by higher prevalence of metabolic syndrome *(48.57% vs. 21.43%, p=0.0044)*, and antihypertensive drug treatment *(100.00% vs 81.43%, p=0.0065)*.

Otherwise, the clinical variables were not significantly different between the subjects with and without incident type 2 DM.

No differences in apoC1 plasma levels were found between persons developing type 2 diabetes and persons not developing type 2 diabetes neither in the total plasma (Fig. 6.7B) samples nor in the apoB-depleted plasma (Fig. 6.7C). ApoC1 levels in both, total and apoB-depleted plasma, correlated significantly with plasma levels of triglycerides (r=0.5117 / r=0.6207) and cholesterol (r=0.3598 / r=0.4792, Fig. 6.7D+E, Tab. 6.3). The waist circumference of the patients was correlated weakly with the apoC1 content of their plasma (r=0.2101, p=0.0432, Tab. 6.3). Moreover, patients with aspirin treatment, had slightly lower apoC1 levels in their plasma samples compared to patients without aspirin treatment (88.27 μg/ml (no aspirin) vs. 78.31 μg/ml (with aspirin), p=0.0405, Tab. 6.3).

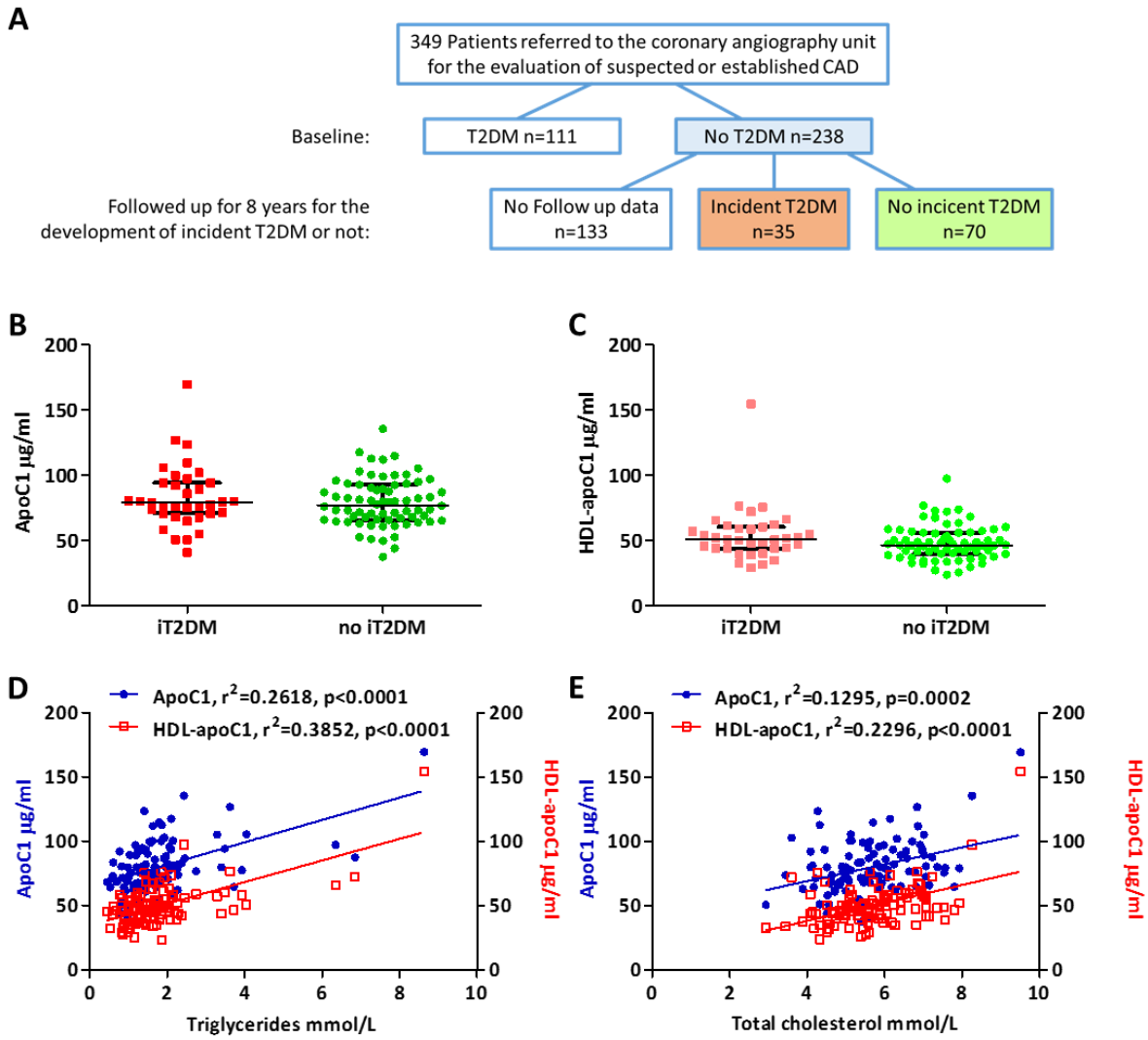

Figure 6.7: Prospective study with apoC1 levels in future type 2 DM patients.
A: Overview on study samples
B: ApoC1 content of plasma samples from patients developing type 2 DM (iT2DM) and control subjects (no iT2DM) during the eight year follow up period
C: ApoC1 content of apoB-depleted plasma samples (HDL-apoC1) from the same donors
D-G: Correlation analysis of apoC1 content, or apoC1 content of apoB-depleted plasma samples (HDL-apoC1) shown in 7 B+C and triglyceride levels (D), total cholesterol levels (E).
The regression line is shown for better visibility of the graph.
Scatter dot plots (B+C) are displayed with the median ± IQR

Clinical variables	ApoC1 content		HDL-apoC1 content	
	Pearson r	*p value*	*Pearson r*	*p value*
Age	0.0077	0.9381	0.0253	0.7979
Sex (female)	0.1263	0.1993	0.1079	0.2735
Hypertension (WHO)	0.0069	0.9447	-0.0737	0.4548
History of smoking	-0.0445	0.6522	-0.0652	0.5085
Coronary artery stenosis >50%	-0.0832	0.3988	-0.0158	0.8727
MetS ATP III Definition	0.1224	0.2134	0.1662	0.0902
BMI	0.0273	0.7836	-0.1147	0.2463
Waist circumference	0.2101	**0.0432**	0.1998	0.0548
Waist-to-hip ratio	0.0593	0.5723	0.0120	0.9092
Triglycerides	0.5117	**<0.0001**	0.6207	**<0.0001**
Total cholesterol	0.3598	**0.0002**	0.4792	**<0.0001**
LDL-cholesterol	0.1365	0.1735	0.1661	0.0969
HDL-cholesterol	-0.0792	0.4286	-0.1023	0.3065
Fasting glucose	0.0676	0.4935	0.0074	0.9402
HbA1c	-0.0017	0.9861	0.0714	0.4694
Fasting insulin	0.1990	0.0533	0.0634	0.5415
HOMA-IR	0.1706	0.1002	0.1403	0.1775
Systolic blood pressure	0.1076	0.2793	0.0466	0.6401
Diastolic blood pressure	-0.0273	0.7850	-0.0814	0.4161
C-reactive protein	-0.0696	0.4917	-0.0300	0.7668
Serum Potassium	-0.0408	0.6883	0.0352	0.7295
Creatinine	-0.1601	0.1080	-0.1204	0.2281
eGFR (CKD-EPI)	0.0371	0.7109	-0.0242	0.8095
Antihypertensive drugs	0.1164	0.2369	0.0659	0.5043
Lipid-lowering drugs	0.0209	0.8327	0.0506	0.6083
Aspirin	-0.2003	**0.0405**	-0.1905	0.0516

Table 6.3: Correlation analysis between the patient's clinical variables and the apoC1 concentration of the patient's plasma, or the apoC1 concentration in the HDL fraction of the patient's plasma, respectively.

The Pearson's correlation coefficient r and p values (two-tailed test) are indicated.
MetS: Metabolic Syndrome, ATPIII: National Cholesterol Education Program Adult Treatment Panel III, BMI: Body mass index, Apo: apolipoprotein, HbA1c: glycated hemoglobin, HOMA-IR: homeostatic model assessment-insulin resistance, eGFR: estimated glomerular filtration rate (calculated according to CKD-EPI formula [159]), Antihypertensive drugs: beta-adrenergic blocking agents, angiotensin-converting-enzyme inhibitors, angiotensin II receptor antagonists, calcium channel blockers, alpha blockers, thiazides, loop diuretics, potassium sparing diuretics, other diuretics, and/or other antihypertensives; Lipid-lowering drugs: fibrates and/or statins.

6.2. Apoptotic Signaling Analysis

We performed a genome-wide expression analysis at the Functional Genomics Center Zürich (FGCZ) to unravel the signaling cascades by which HDL inhibits IL-1β-induced apoptosis of pancreatic β-cells. For this purpose, the gene expression of INS-1E cells treated with and without IL-1β in the presence or absence of HDL was compared, and two different IL-1β-incubation times were analyzed: 24 hours and 12 hours (Fig. 6.8A).

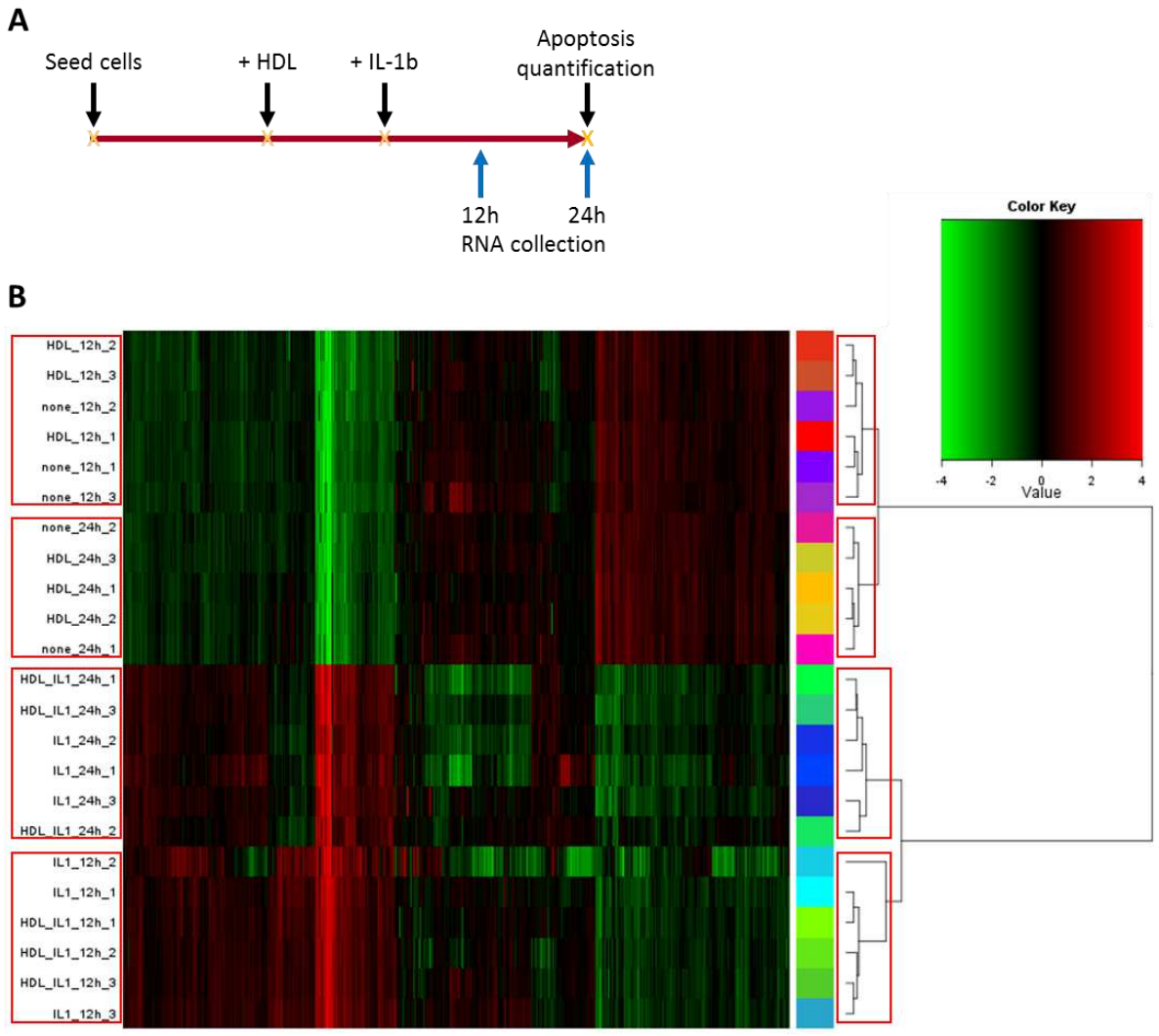

Figure 6.8: Gene expression analysis.
A: Experimental set-up for gene expression analysis
B: Cluster analysis of the 2000 probes with the highest standard deviation, threshold for standard deviation of log2 signal across samples: 0.504

A cluster analysis of the 2000 genes with the highest variance revealed a massive effect of IL-1β treatment on gene expression (Fig. 6.8B). Moreover, the two chosen incubation times

induced the formation of subclusters (red frames), although these differences were smaller. Unfortunately, the effect of HDL was minor or not consistent: The absence or presence of HDL did not induce the formation of clusters, neither with, nor without IL-1β stimulation.

6.2.1. Effects of Interleukin-1β on Gene Transcription

12 hours of IL-1β stimulation upregulated 1993 genes (log 2 ratio > 0.5), and downregulated 1968 genes (log 2 ratio < -0.5) with a p-value < 0.05% and false discovery rate (FDR) < 0.1267 (Fig. 6.9A). 24 hours of IL-1β stimulation upregulated 1392 genes (log 2 ratio > 0.5), and downregulated 1708 genes (log 2 ratio < -0.5) with a p-value < 0.05% and false discovery rate (FDR) < 0.1237 (Fig. 6.9B).

Gene ontology analysis [156,157] of upregulated genes after 12 hours and 24 hours IL-1β stimulation (orange dots in Fig. 6.9A+B) depicted functional annotation clusters related to immune and inflammatory responses, cell death, and the regulation of cytokine production (Tab. 6.4). The enrichment score is based on the p-values of the gene ontology terms within the respective cluster: a high enrichment score correlates with low p-values and vice versa. Gene ontology analysis of downregulated genes after 12 hours and 24 hours IL-1β stimulation revealed functional annotation clusters related to cell cycle regulation and protein biosynthesis.

12h IL-1β stimulated/not treated cells; upregulated genes		**24h IL-1β stimulated/not treated cells; upregulated genes**	
Annotation Cluster	*Enrichment Score*	*Annotation Cluster*	*Enrichment Score*
Immune response	7.71	Immune response	9.88
Translation	4.34	Inflammatory response	6.98
Inflammatory response	4.02	Antigen processing and presentation	4.97
Nucleotide binding	3.87	Response to bacterium	4.23
Response to bacterium	3.60	Cell death	4.04
Protein dimerization activity	3.30	Lytic vacuole	3.93
Induction of apoptosis	3.25	Regulation of cytokine production	3.77
Cell death	3.05	Cell activation	3.60
Regulation of programmed cell death	3.09	positive regulation of immune response	3.31
Regulation of cytokine production	2.95	DEATH-like	3.04
Response to organic substance	2.88	Cytokine activity	2.90
Cation binding	2.76	Regulation of leukocyte migration	2.86
12h IL-1β stimulated/not treated cells; downregulated genes		**24h IL-1β stimulated/not treated cells; downregulated genes**	
Annotation Cluster	*Enrichment Score*	*Annotation Cluster*	*Enrichment Score*
Chromosome	10.61	Endoplasmic reticulum	7.43
Cell cycle	7.50	Cell fraction	4.80
Cellular response to stress	5.81	Cytoplasmic vesicle	4.80
Condensed chromosome	5.77	Regulation of secretion	4.78
Non-membrane-bounded organelle	5.55	Cell-cell signaling	4.00
Membrane-enclosed lumen	5.38	Response to unfolded protein	3.49
Microtubule cytoskeleton	4.82	Response to carbohydrate stimulus	3.24
Ubiquitin-like protein conjugation	4.61	Protein dimerization activity	3.10
Regulation of cell cycle	4.26	Cellular homeostasis	2.81
Nucleotide binding	4.19	GTP-binding	2.78
Protein dimerization activity	3.50	Nucleotide binding	2.65
Response to hormone stimulus	3.31	Sterol metabolic process	2.49

Table 6.4: Annotation Clusters of up- or downregulated genes in response to 12 hours or 24 hours IL-1β stimulation compared to not treated cells.

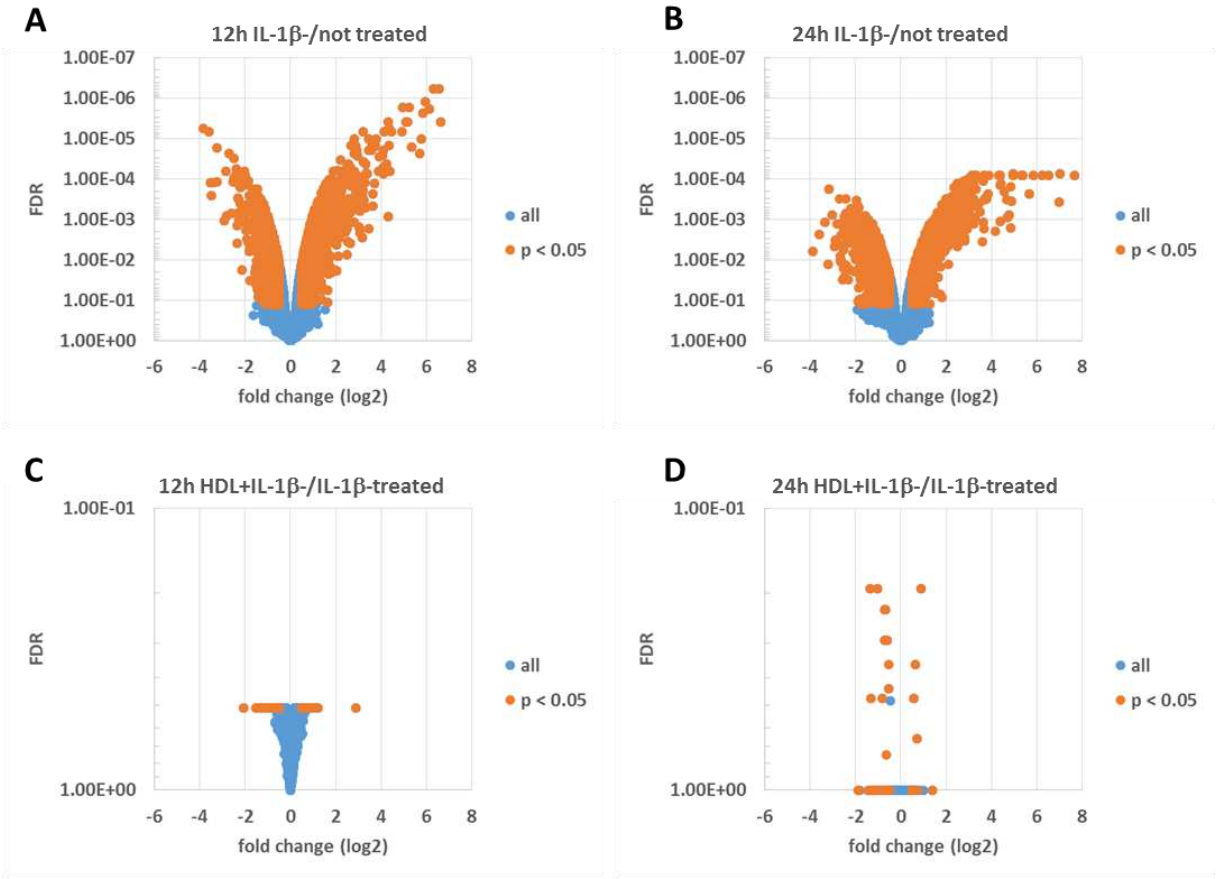

Figure 6.9: Expression data displayed in volcano plots.
A-D: Each blue point represents the ratio of the expression data of the ratio of a single gene and the respective false discovery rate (FDR). Orange points represent the values which have log2 ratios of <-0.5 or >0.5 and p-values <0.05.
A: Comparison of the gene expression of 12 hours IL-1β-treated (10 ng/ml) cells (n=3) with not treated cells (n=3)
B: Comparison of the gene expression of 24 hours IL-1β-treated (10 ng/ml) cells (n=3) with not treated cells (n=2)
C: Comparison of the gene expression of 30 hours HDL (50 μg/ml) plus 12h IL-1β-treated (10 ng/ml) cells (n=3) with 12 hours IL-1β-treated (10 ng/ml) cells (n=3)
D: Comparison of the gene expression of 40 hours HDL (50 μg/ml) plus 24 hours IL-1β-treated (10 ng/ml) cells (n=3) with 24 hours IL-1β-treated (10 ng/ml) cells (n=3)

6.2.2. Effects of HDL on Gene Transcription

The absence or presence of HDL in addition to 12 h IL-1β stimulation led to differential expression of 456 genes (log 2 ratio > 0.5 or < -0.5, respectively) with a p-value < 0.05. However, the false discovery rate (FDR) of 0.5105 indicates more than 50% risk of false positives among these genes (Fig. 6.9C). The same comparison at 24 h IL-1β stimulation in the presence or absence of HDL disclosed 16 genes which were differentially regulated (log 2 ratio > 0.5 or < -0.5) with a p-value < 0.05 and a FDR < 0.7469 (Fig. 6.9D). The expression data of the

latter conditions (24 h IL-1β stimulation +/- HDL) were not investigated beyond this point, because of the high rate of false positives.

Genes which were up- or downregulated by 12 h IL-1β stimulation and attenuated by the presence of HDL (orange dots in Fig. 6.9C) were used for functional annotation clustering analysis. (Tab. 6.5). These clusters include the regulation of transcription factors (NF-κB among others), the endoplasmic reticulum stress response, protein biosynthesis, and the induction of apoptosis.

Furthermore, functional annotation clustering analysis revealed that genes which were downregulated by 12 h IL-1β stimulation and attenuated by HDL, clustered with lipid biosynthetic processes, glucose metabolism, the response to hormone and cytokine stimuli, and cellular development.

12h HDL+IL-1β stimulation/IL-1β stimulation; genes upregulated by IL-1β, attenuated by HDL		**12h HDL+IL-1β stimulation/IL-1β stimulation; genes downregulated by IL-1β, atten. by HDL**	
Annotation Cluster	*Enrichment Score*	*Annotation Cluster*	*Enrichment Score*
Cation binding	1.76	Lipid biosynthetic process	1.46
Regulation of transcription factor activity	1.53	SH3 domain	1.38
Endoplasmic reticulum unfolded protein response	1.44	Monosaccharide metabolic process	1.36
Intracellular organelle lumen	1.05	Phospholipid biosynthesis	1.35
RNA processing	1.04	Response to hormone stimulus	1.15
Regulation of transcription	1.02	Response to cytokine stimulus	1.11
BTB/POZ fold	1.02	Nucleotide binding	0.97
Leucine-rich repeat	0.99	DNA metabolic process	0.97
Protein dimerization activity	0.98	DNA packaging	0.82
Transport	0.96	Cellular homeostasis	0.81
Transcription regulation	0.88	Regulation of hormone secretion	0.77
Positive regulation of apoptosis	0.85	Regulation of cell development	0.73

Table 6.5: Annotation Clusters of up- or downregulated genes in response to 12h IL-1β stimulation in the absence or presence of HDL.

Given the relatively low enrichment scores (the enrichment score correlates inversely with the p-values of the gene ontology terms within the respective cluster) and high false discovery rates, though, these analyses must be interpreted with caution. Nevertheless, we decided to investigate the NF-κB signaling and the ER stress response with independent experiments.

6.2.3. Validation of Candidate Genes with Quantitative PCR

We selected several genes for validation out of the apoptotic pathways, which had been differentially regulated by IL-1β and HDL in the gene array (red circles in Fig. 6.10). These genes were located in the ER stress pathway, in the intrinsic or extrinsic apoptotic pathway. Additional time points were analyzed to better resolve the effects of IL-1β and HDL for quantitative real-time PCR (qPCR) analyses. Thus, we used RNA samples which were collected in two independent experiments from cells either exposed to IL-1β for 8, 12 and 16 hours, or 3, 6, 10, 16 and 24 hours, in the presence or absence of HDL. Gene expression changes and the time of the maximal fold change are listed in table 6.6. Similarly to the results of the gene array, the validation experiments revealed major effects of IL-1β treatment in the transcription of the tested genes when compared to not treated cells (left side of table 6.6). The presence of HDL in addition to IL-1β treatment only induced a minor attenuation of up- or downregulation of these genes (right side of table 6.6).

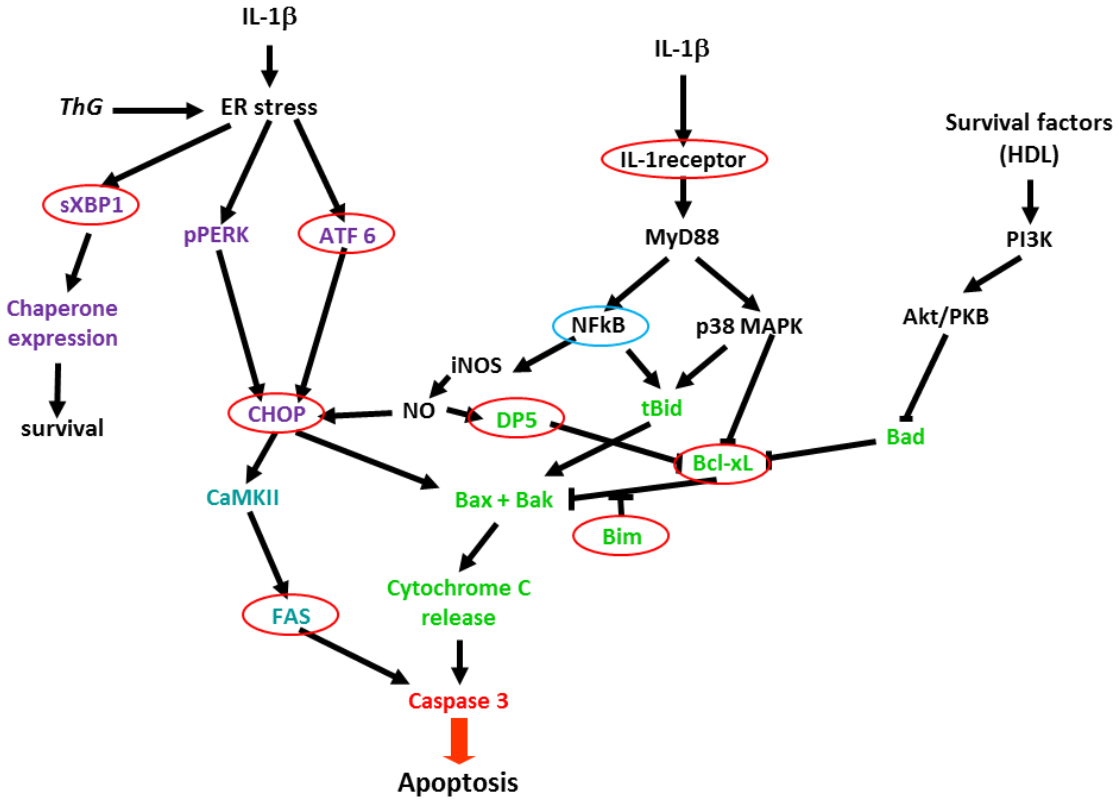

Figure 6.10: Network of genes, transcription factors, enzymes, and signalling molecules involved in β-cell apoptosis.
Genes of the apoptotic pathway which were selected for validation by quantitative PCR (red circles).

Gene	IL-1β treated vs. not treated cells		IL-1β + HDL treated vs. not treated cells	
	Fold change	*peak at*	*Fold change*	*peak at*
DP5	6.3x	10-12h	6.5x	10-12h
Bcl-xL	1.6x	10h	1.6x	10h
BIM	0.3x	6-8h	0.4x	6-8h
STAT1	3.3x	8+16h	3.3x	8+16h
IL-1R	1.8x/1.9x	3+24h	2.2x/1.6x	3+24h
CHOP	7.4x	10-12h	5.6x	10-12h
sXBP1	1.9x/1.8x	3+16h	2.3x/1.6x	3+16h
ATF6	3.5x	16h	3.4x	16h
CFLAR/FLIP	2.2x	6h	2.1x	3h
FAS	26.8x	3h	32.6x	3h

Table 6.6: Fold changes of gene expression in response to IL-1β or IL-1β + HDL treatment compared to not treated cells, including time of maximal up- or downregulation of the gene.
DP5: death protein 5; B-cell lymphoma extra Large; Bim: Bcl-2-like protein 11; STAT1: signal transducer and activator of transcription 1; IL-1R: Interleukin 1 receptor; CHOP: C/EBP homologous protein; sXBP1: spliced X-box binding Protein 1; ATF6: activating transcription factor 6; CFLAR/FLIP: CASP8 and FADD-like apoptosis regulator / FLICE-like inhibitory protein

6.2.4. Translocation of Transcription Factor NF-κB

Several of the differentially expressed genes, which were found in the gene array, are linked to the transcription factor NF-κB, which is related to cell survival (Fig. 6.11). Therefore, the involvement of NF-κB was analyzed by studying the subcellular location of its subunit p65 by fluorescence microscopy. INS-1E cells were treated with IL-1β for different times in the absence or presence of HDL. After fixing and staining, the inspection at the microscope revealed a drastic translocation of NF-κB into the nucleus after 15 and 60 minutes of IL-1β treatment (Fig. 6.11). Interestingly, at 5 minutes stimulation with IL-1β, NF-κB was still in the cytoplasm, and after 5 h the NF-κB was relocated back into the cytoplasm. The presence of HDL did not modify the NF-κB translocation.

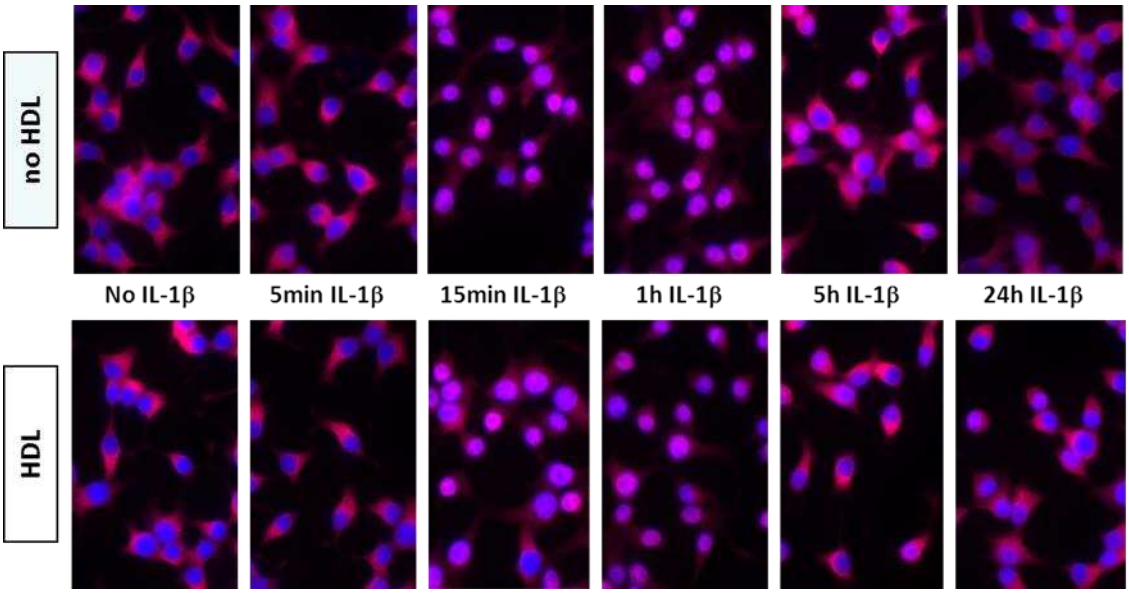

Figure 6.11: Effect of IL-1β on the translocation of p65 NF-κB into the nucleus.
Location of the p65 subunit of NF-κB (pink) after the indicated stimulation time with IL-1β (10 ng/ml) in the absence or presence of HDL (100 μg/ml), blue=DAPI.

6.2.5. Involvement of ER Stress

IL-1β had been found to upregulate several genes involved in ER stress (Fig. 6.11) which, according to the gene array, was partially prevented by the presence of HDL. Therefore, we sought to confirm this link between HDL and ER-stress, and started a collaboration with Christian Widmann's group in Lausanne. This group had published that HDL prevents apoptosis and ER stress in primary human β-cells as well as in Min6 cells induced by thapsigargin, a drug which inhibits the sarco/endoplasmic reticulum Ca^{2+} ATPase (SERCA) [109,111]. Christian Widmann, a member of my PhD committee, invited me to join his group for a few experiments.

We investigated if apoC1 mimicked the protective effect of HDL against ER stress-induced apoptosis in Min6 cells. The cells were treated with HDL or apoC1, and thapsigargin (ThG) for 24 h. The expression of CHOP (a marker of ER stress) was consistently upregulated by ThG treatment and blocked by HDL, but unfortunately not by apoC1 (Fig. 6.12A). For the phosphorylation of PERK, the data were not as clear. PERK phosphorylation was induced by ThG, as expected. In the presence of either HDL or apoC1 the effect of ThG was attenuated, however, to a lesser degree by apoC1 as compared to HDL. Finally, the number of pycnotic nuclei revealed clearly less apoptosis after ThG treatment in the presence of either 1mM HDL-C or 20 μg/ml apoC1 (Fig. 6.12B+C).

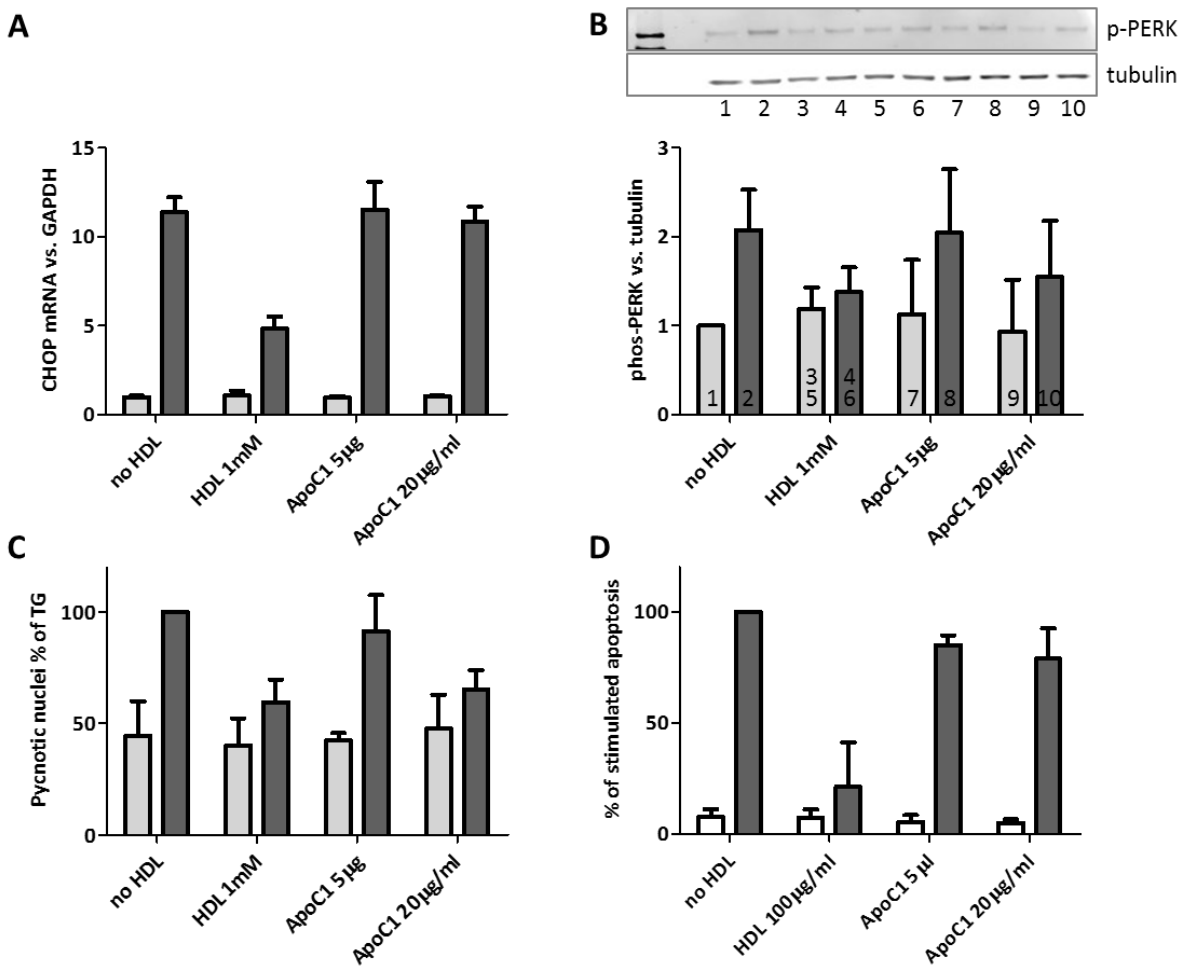

Figure 6.12: Effect of HDL or apoC1 on thapsigargin-induced ER stress.
A-C: Min6 cells were cultured for 24 hours with or without thapsigargin (0.5 μM, dark grey bars) in the presence or absence of HDL (two preparations) or apoC1 at indicated concentrations.
A: RNA was harvested after 24 h of treatment and the gene expression levels of CHOP were determined by qPCR
B: Proteins were harvested after 24 h of treatment and the phosphorylation of PERK (170 kDa) was analyzed using specific antibodies. Tubulin (55 kDa) was used as loading control. The graph displays the averaged quantification of three western blots. The numbers within the bars correspond to the columns in the western blot.
C: After the treatment, Min6 cells were fixed with PFA and the nuclei were stained with Hoechst stain. The pychnotic nuclei were counted carefully (at least 500 cells per condition in triplicates).
D: INS-1E cells were cultured for 40 hours in the presence of HDL or apoC1 at indicated concentrations. During the last 16 hours, thapsigargin (25 nM, dark grey bars) was added in order to induce apoptosis.
Bars indicate the mean values +SD

To further investigate the role of apoC1 in ER stress-induced apoptosis, the experiments were rerun in INS-1E cells. ThG-induced apoptosis in INS-1E cells, and the ThG-induced apoptosis was reduced by HDL but not by apoC1 at either of the tested concentrations (5 μg/ml and 20 μg/ml) (Fig. 6.12D). Compared to Min6 cells, the concentration optimum of ThG to induce

apoptosis was twenty times lower in INS-1E cells (0.5 μM in Min6 cells vs. 25 nM in INS-1E cells). Likewise, the HDL concentration which prevented ThG-induced apoptosis was about ten times lower in INS-1E cells (1 mM HDL-cholesterol in Min6 cells vs. 100 μg/ml HDL-protein in INS-1E cells).

Thapsigargin-induced apoptosis was found with two additional assays: annexin V / propidium iodide staining (Fig. 6.13B+C) and caspase 3 activation (Fig. 6.13D+E). Since apoC1 was not preventing ThG-induced apoptosis, we could not exploit this model to delineate the mechanisms by which apoC1 interfered with apoptosis.

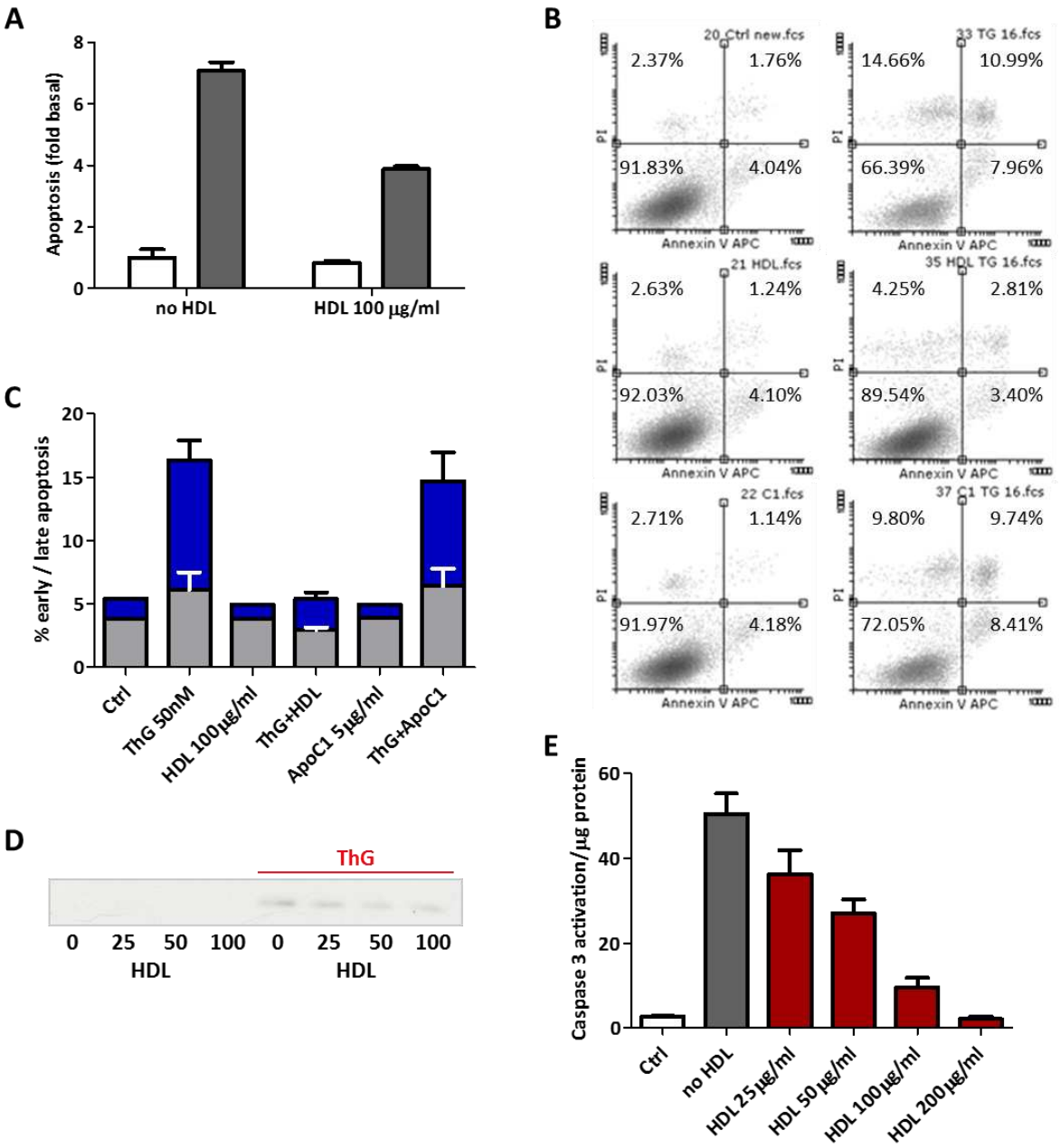

Figure 6.13: Alternative methods for apoptosis detection after stimulation with thapsigargin.
A: INS-1E cells were cultured for 40 hours in the presence or absence of HDL. Thapsigargin (ThG, 50 nM, grey bars) was added for the stimulation of apoptosis during the last 16 hours. Apoptosis was determined with the cell death detection ELISA (n=1).
B+C: INS-1E cells were cultured for 40 hours in the presence or absence of HDL (100 µg/ml) or apoC1 (50 µg/ml). Thapsigargin (ThG, 50 nM) was added for the stimulation of apoptosis during the last 16 hours.
B: Scatterplot of flow cytometry with annexin V- versus Propidium iodine (PI)-staining (n=1).
C: Average percentage of early apoptotic (annexin V positive, PI negative, grey) and late apoptotic (annexin V and PI positive, blue) cells (n=1).
D+E: INS-1E cells were cultured for 40 (D) or 24 (E) hours in the absence or presence of HDL at the indicated concentrations. During the last 16 (D) or 8 (E) hours, ThG (50 nM) was added for the stimulation of apoptosis except in the not treated control (Ctrl) condition.
D: Cleaved caspase 3 (17 kDa) was detected in proteins which were harvested from INS-1E cells.
E: Apoptosis was determined by the caspase 3 activity assay (n=1).
Bars indicate the mean values +SD

6.3. Clinical Studies on the Impact of Diabetes on HDL Functionality

To investigate further components of HDL, which might interfere with ThG-induced apoptosis, we used an approach, which our lab previously applied in collaboration with the group of Ulf Landmesser (Department of Cardiology) for the identification of HDL-components, which protect endothelial cells from apoptosis. In that study [77], HDL of coronary artery disease patients and healthy controls differed by anti-apoptotic activity, functional parameters of endothelial cells (i.e. the stimulation of nitric oxide (NO) production and the inhibition of stimulated VCAM-1 expression), and protein composition. For β-cells, no comparable study had been done. Therefore, we measured effects of HDL from healthy and diabetic adolescent and adult study subjects on the survival of β-cells. We also analyzed the cholesterol efflux capacity of HDL isolated from the adolescents, because HDL can elicit cellular responses by altering the cellular cholesterol homeostasis.

The detailed clinical variables of the study subjects are listed in tables 5.5 and 5.6 (see materials and methods section). The adolescents with type 1 DM differed from the age-matched control subjects by significantly higher fasting glucose levels *(12.18 mM vs. 4.72 mM, p=0.0001)* (Tab. 5.6), alanine transaminase (ALT) activity *(9.06 IU/L vs. 6.75 IU/L, p=0.0162)*, HDL cholesterol *(1.26 mM vs. 1.04 mM, p=0.0055)*, and apoA1 levels *(1.59 g/L vs. 1.39 g/L, p=0.0048)*. Otherwise, the clinical variables were not significantly different between the type 1 DM subjects and control subjects.

By definition, the adult patients with coronary artery disease and type 2 DM (CAD+T2DM), impaired fasting glucose (CAD+IFG) and euglycemia (CAD+NFG and no CAD+NFG)) differed by fasting glucose *(p<0.0001)*, HbA1c *(p<0.0001)*, and treatment for type 2 DM *(p<0.0001)* (Tab. 5.5). Moreover, total cholesterol levels differed slightly between the groups *(p=0.0329)*: subjects with normal fasting glucose and coronary artery disease (CAD+NFG) had the highest cholesterol levels *(6.06 mM vs. 5.18 mM (CAD+T2DM), 4.97 mM (CAD+IFG), and 5.01 mM (no CAD+NFG))*. Otherwise, the clinical variables were not significantly different between the four groups.

6.3.1. Protective Effects in β-Cells

Apoptosis of INS-1E cells was stimulated by ThG-treatment. Activated caspase 3 was measured as a surrogate for apoptosis in this study. HDL from type 1 diabetic adolescents had slightly less anti-apoptotic potential on INS-1E cells than HDL from healthy adolescents (p=0.3535, Fig. 6.14A). However, this difference was not significant. Neither was the glycemic state of adult patients associated with any significant differences of their HDLs' anti-apoptotic activity (Fig. 6.14B).

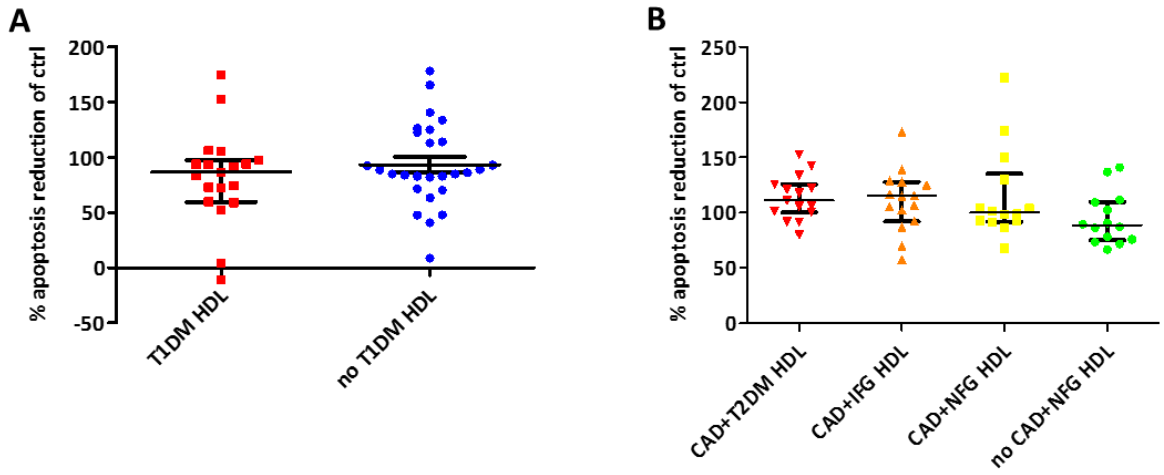

Figure 6.14: Anti-apoptotic effects of HDL from type 1 and type 2 DM patients.
A: INS-1E cells were cultured for 24 hours in the presence of HDL samples (100 μg/ml) collected from type 1 DM adolescents (T1DM HDL, n=19) or healthy, age-matched adolescents (no T1DM HDL, n=27). During the last 8 hours, ThG (50 nM) was added for the stimulation of apoptosis. Apoptosis was determined by the caspase 3 activity assay. The apoptosis reduction of the internal control HDL compared with ThG-stimulated apoptosis without HDL was set as 100% apoptosis reduction.
B: INS-1E cells were treated as described in A. HDL samples were isolated from patients with type 2 DM and coronary artery disease or impaired fasting glucose and CAD (CAD+T2DM or CAD+IFG HDL, respectively, n=15 each), or euglycemic subjects with or without CAD (CAD+NFG HDL or no CAD+NFG HDL, respectively, n=14 each).
Scatter dot plots are displayed with median values ±IQR

6.3.2. Cholesterol Efflux from Macrophages

HDL isolated from patients with type 1 DM differed from HDL of control subjects by a slightly reduced potential to induce cholesterol efflux from J774 macrophages, which had previously been loaded with acetylated LDL and cholesterol (Fig. 6.15A+B). However, neither for the macrophages, in which ABCA1 expression had been stimulated with cyclic adenosine monophosphate (cAMP, Fig. 6.15B), nor for the macrophages without cAMP stimulation (Fig. 6.15A) this difference was significant (p=0.0971 and p=0.5040, respectively).

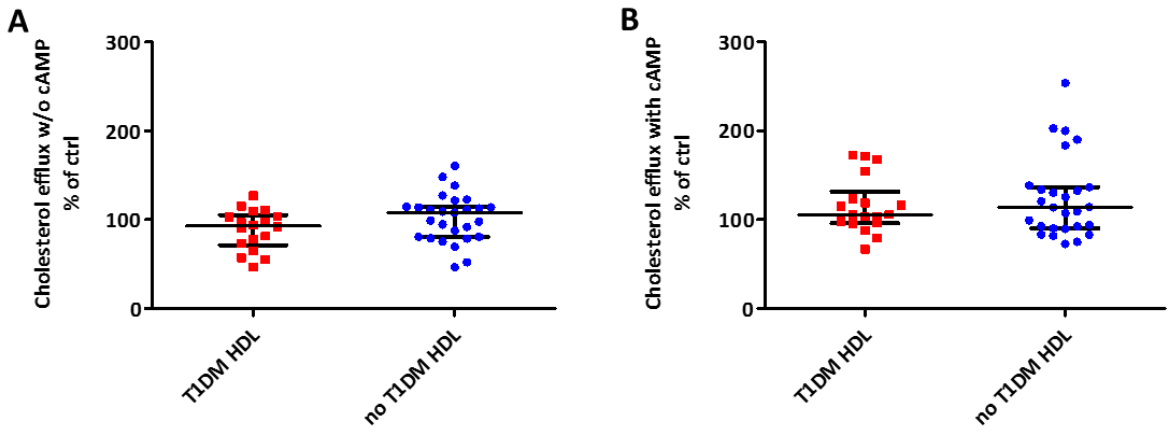

Figure 6.15: Functionality of HDL from type 1 and type 2 DM patients towards macrophages.
A+B: J774 macrophage cells were loaded with cholesterol for 24 hours, followed by the induction of ABCA1 expression with cAMP (B) or not (A). Cholesterol efflux induced by HDL from subjects with or without type 1 DM (25 µg/ml) is shown as % of the internal control HDL.
Scatter dot plots are displayed with median values ±IQR.

6.3.3. Correlation Analysis between Functionality of HDL and the Clinical Variables of Study Participants

Correlation analysis between the functionality of HDL towards β-cells and macrophages, and the clinical variables of the study subjects with type 1 DM and control subjects revealed significant, negative correlations of the potential of HDL to reduce thapsigargin-stimulated apoptosis with LDL cholesterol levels (r=-0.3204), non-HDL cholesterol levels (r=-0.3066), the cholesterol-to-HDL cholesterol ratio (r=-0.3131), and apoB levels (r=-0.2963, Tab. 6.7). Moreover, the potential of HDL to induce cholesterol efflux from macrophages without ABCA1 expression stimulation by cyclic adenosine monophosphate (cAMP) was positively correlated to total cholesterol levels (r=0.3922), LDL cholesterol levels (r=0.3554), non-HDL cholesterol levels (r=0.3244) and the activity of aspartate transaminase (r=0.3573) in the subjects with type 1 DM (Tab. 6.7). When the ABCA1 expression was stimulated by 24 hours of incubation with medium containing cAMP, cholesterol efflux from macrophages correlated positively with the total cholesterol levels (r=0.3411) and apoB concentrations (r=0.3663) of the plasma donors (Tab. 6.7). As expected, a positive correlation was found between the HDL-induced cholesterol efflux from macrophages with and without prior incubation with cyclic adenosine monophosphate (r=0.6409, Tab. 6.8). The other functionality tests for HDL or patient variables were not correlated to each other.

Clinical variables	apoptosis reduction in β-cells		Cholesterol efflux without cAMP from macrophages		Cholesterol efflux with cAMP from macrophages	
	r	*p value*	*r*	*p value*	*r*	*p value*
Age	-0.1211	0.4334	-0.2639	0.0834	-0.1313	0.3957
Sex (male)	0.1855	0.2225	-0.1777	0.2429	-0.0980	0.5219
BMI	-0.1963	0.2247	0.0682	0.6759	0.1391	0.3921
Total cholesterol	-0.2469	0.1149	0.3922	**0.0102**	0.3411	**0.0271**
HDL-cholesterol	0.1887	0.2313	0.1865	0.2370	0.1812	0.2508
LDL-cholesterol	-0.3204	**0.0386**	0.3554	**0.0209**	0.2702	0.0835
nonHDL-cholesterol	-0.3066	**0.0483**	0.3244	**0.0361**	0.2754	0.0775
Cholesterol/HDL-chol. ratio	-0.3131	**0.0435**	0.1265	0.4248	0.1103	0.4869
ApoA1	0.1300	0.3948	0.2680	0.0751	0.2015	0.1844
ApoB	-0.2963	**0.0481**	0.2744	0.0682	0.3663	**0.0133**
Triglycerides	-0.0948	0.5503	0.0006	0.9971	0.1594	0.3134
Aspartate transaminase	0.1463	0.3808	0.3573	**0.0277**	0.2530	0.1253
Alanine transaminase	0.0100	0.9497	-0.0164	0.9181	0.0465	0.7700
Fasting glucose	0.0605	0.7037	-0.0384	0.8095	0.1183	0.4555
HbA1c	-0.0611	0.8158	-0.2457	0.3417	-0.0649	0.8044
C-reactive protein	0.0436	0.7838	0.0473	0.7662	0.0912	0.5655

Table 6.7: Correlation analysis in T1DM patients and control subjects between the patient's clinical variables, and the HDL functionality data % apoptosis reduction of control HDL in β-cells, or cholesterol efflux with and without cAMP from macrophages.
The Pearson's correlation coefficient r and p values (two-tailed test) are indicated.
cAMP: cyclic adenosine monophosphate, BMI: body mass index, Apo: apolipoprotein, HbA1c: glycated hemoglobin.

		apoptosis reduction in β-cells	Cholesterol efflux without cAMP from macrophages
Cholesterol efflux with cAMP from macrophages	*Pearson r*	-0.0998	0.6409
	p value	0.5144	**<0.0001**
Cholesterol efflux without cAMP from macrophages	*Pearson r*	-0.0586	
	p value	0.7024	

Table 6.8: Correlation analysis in T1DM patients and control subjects between HDL functionality data % apoptosis reduction of control HDL in β-cells and cholesterol efflux (expressed as % of control HDL) from macrophages with and without prior cyclic adenosine monophosphate (cAMP) stimulation.
The Pearson's correlation coefficient r and p values (two-tailed test) are indicated.

Correlation analysis of the functionality of type 2 DM patients' and their controls' HDL with their clinical variables revealed a positive and significant correlation between the ability of these HDL to reduce thapsigargin-stimulated apoptosis and HDL cholesterol (r=0.2772) as well as apoA1 levels (r=0.3173, Tab. 6.9). Otherwise, none of the tested variables correlated with the potential of the patient's HDL to reduce ThG-stimulated apoptosis in INS-1E cells.

	apoptosis reduction in β-cells	
Clinical variables	*Pearson r*	*p value*
Age	0.1980	0.1362
Sex (male)	n/a	n/a
Hypertension (WHO)	0.0529	0.6934
History of smoking	0.0770	0.5659
BMI	0.0553	0.6802
Total cholesterol	0.1513	0.2571
HDL-Cholesterol	0.2772	**0.0351**
LDL-Cholesterol	0.0832	0.5345
ApoA1	0.3173	**0.0152**
ApoB	0.0607	0.6510
Triglycerides	0.0115	0.9316
Aspartate transaminase	0.0627	0.6400
Alanine transaminase	0.0006	0.9967
Gamma-glutamyl transferase	0.0339	0.8008
Fasting glucose	0.1283	0.3372
HbA1c	0.0452	0.7362
C-reactive protein	-0.2095	0.1145
Creatinine	-0.1051	0.4325
eGFR (CKD-EPI)	0.0381	0.7762
Albumin creatinine ratio	0.0867	0.5897
Antihypertensive drugs	-0.0172	0.8979
Statins	-0.1789	0.1791
Aspirin	-0.2229	0.0926
Diabetes mellitus drugs	0.0463	0.7298

Table 6.9: Correlation analysis in T2DM, CAD, CAD+IFG patients and control subjects between the patient's clinical variables, and the HDL functionality data % apoptosis reduction of control HDL in β-cells.

The Pearson's correlation coefficient r and p values (two-tailed test) are indicated.
BMI: Body mass index, Apo: apolipoprotein, HbA1c: glycated hemoglobin, eGFR: estimated glomerular filtration rate (calculated according to CKD-EPI formula [159]), Antihypertensive drugs: beta-adrenergic blocking agents, angiotensin-converting-enzyme inhibitors, and/or angiotensin II receptor antagonists; Diabetes mellitus drugs: glitazones, meglitinides, biguanide derivatives, sulfonylureas, and/or insulin.

7. Discussion

7.1. Protective Effect of HDL against β-Cell Apoptosis

Type 2 DM has been misunderstood as a disease of insulin resistance for some time. However, during the last two decades it has been established that insulin resistance is not sufficient for the manifestation of type 2 DM [15,16,26]. The transition from normal glucose tolerance to impaired glucose tolerance and finally type 2 DM is driven by the cumulative loss of β-cell function and mass in the background of peripheral insulin resistance [20,27].

Tissue inflammation, which is often found in patients with metabolic diseases, is likely to induce β-cell apoptosis [56]. The human lipoproteins HDL, LDL, and VLDL are possible modulators of β-cell function and survival [107]. In this context, the precursor PhD project of this thesis investigated the influence of HDL and LDL on β-cell apoptosis, proliferation and function in primary pancreatic islets of human and murine origin [88]. These studies found a protective effect of HDL against high glucose- and IL-1β-induced apoptosis. The anti-apoptotic effects were found to be exerted by both, the protein and lipid moieties of HDL, as well as by isolated apoA1 and S1P.

The goal of the follow-up project, which is presented here, was to elucidate the mechanism underlying the protective effects of HDL and its components in β-cells. Since we were specifically interested in effects which happen in the β-cells we chose to work with a β-cell line. With IL-1β-induced apoptosis in INS-1E cells (Fig.6.1A), we established a suitable model to study the protective effects of HDL and its components.

7.1.1. Protective Effects of HDL and its Components

The physiological HDL concentration in human plasma ranges between 1 and 2 mmol/l cholesterol. This is equivalent to 1 to 2 mg/ml total protein. Since the vasculature of pancreatic islets is fenestrated, the concentration of HDL around β-cells in vivo presumably lies in the range of the HDL plasma concentration [91]. Interestingly, the anti-apoptotic effect of HDL started to become relevant at a protein concentration as low as 20 μg/ml in our experiments with IL-1β-induced apoptosis (Fig 6.1B). This corresponds to maximally 2% of the normal plasma concentration.

HDL is a good scavenger for amphiphilic molecules, e.g. lipopolysaccharide [161]. Therefore, we investigated if HDL simply neutralizes IL-1β when it prevents apoptosis. For this purpose, INS-1E cells were pre-incubated with HDL followed by IL-1β stimulation in the absence of HDL (Fig 6.1C). The significant anti-apoptotic effect that was detected indicates that HDL did not scavenge the cytokine, but rather activated a sustained, protective program in the β-cells.

A profound and dose-dependent protective effect was found for the HDL protein moiety in the INS-1E β-cell line (Fig 6.2A+B). Interestingly, this effect was abolished when the HDL protein moiety was digested with trypsin before the incubation with the INS-1E cells (Fig 6.2C). In contrast to our previous findings in murine and human islets [88], we found protective effects of neither apoA1 nor S1P in INS-1E cells (Fig 6.2D-F). It cannot be excluded that these molecules had induced indirect protective effects on β-cells within the pancreatic islets in those experiments, i.e. by interaction with non-β cells. Moreover, recent work has claimed that S1P is only able to exert anti-inflammatory effects on endothelial cells once it is bound to apoM [162,163]. It is well possible that complexing with albumin as done by us (but also other laboratories) did not allow S1P to inhibit the IL-1β-induced apoptosis of INS-1E cells. However, the loss of protective HDL effects on INS-1E cells upon digestion of HDL proteins indicate that HDL protein(s) other than apoA1 specifically protect β-cells from IL-1β-induced apoptosis.

In order to identify candidate proteins among the more than 100 proteins found in HDL [67], the protein moiety was fractionated by liquid chromatography with an anion-exchange column (Fig 6.3A+B). Five pools of fractions revealed different anti-apoptotic features (Fig 6.3C). Since we could not identify single proteins with this technique, we used the collaboration of our group with Meliana Riwanto from the Department of Cardiology to analyze the proteome of three protective HDL fractions with LC-ESI-MS/MS [77]. The apolipoproteins apoC1 and apoD were found to be enriched in the most anti-apoptotic pool (pool D) compared to the regular HDL protein composition (Tab 6.1). Further analyses of these two proteins revealed a significant and dose-dependent anti-apoptotic effect for apoC1 in β-cells when apoptosis was stimulated with IL-1β (Fig 6.4A-C). Thus, apoC1 was selected for more detailed follow-up experiments.

7.1.2. Effects of Apolipoprotein C1 on β-Cells

Several interesting functions of apoC1 have been described – beneficial and adverse. ApoC1 activates LCAT and inhibits CETP as well as hepatic lipase [80–82]. Moreover, apoC1 inhibits the selective uptake of cholesteryl esters from HDL into hepatocytes mediated by SR-BI [82]. The combination of these apoC1 functions increases HDL stability. Otherwise, apoC1 was reported to increase VLDL levels. It reduces lipoprotein lipase activity as well as apoE-mediated binding to the LDL receptor or the LDL receptor related protein by inducing conformational changes of VLDL and chylomicrons [80,164]. Interesting findings arose from apoC1 transgenic and apoC1-deficient mice: ApoC1 transgenic (apoC1Tg) mice in an ob/ob background were reported to be protected from obesity and impaired glucose tolerance [160]. Moreover, apoC1 deficient mice displayed elevated CE and TG content in the liver, as well as decreased plasma levels of HDL [165].

The published information on apoC1 effects together with our previous finding (Fig 6.4) motivated us to investigate the role of apoC1 in HDL in the context of β-cell apoptosis. For this purpose, we received sera from human apoC1 transgene (apoC1Tg), apoC1 deficient (apoC1KO) and control mice from P. Rensen and J. Berbée (Leiden, NL). Unfortunately, the results were equivocal and the limited amount of available mouse sera impeded any replication of the experiment. The anti-apoptotic effect of murine (WT) HDL on β-cells was considerably weaker (-20% for 50 μg/ml; Fig 6.5) than the anti-apoptotic effect of human HDL (-50% for 50 μg/ml) which limits the comparability to human HDL. Furthermore, at a low concentration of 10 μg/ml HDL of apoC1KO mice elicited a rather pro-apoptotic effect that disappeared at higher concentrations. Thus, our hypothesis that apoC1 acts as a potent anti-apoptotic protein in HDL was neither rejected nor supported by our analysis of HDL from genetic mouse models.

7.1.3. Clinical Studies on the Associations between ApoC1, Anti-Apoptotic Activity and Glycemic State

Since the results with murine HDL were not conclusive, we sought to investigate the anti-apoptotic activity of apoC1 towards β-cells in human HDL. Humans with an apoC1-deficiency are not known. However, it had been reported that the apoC1 concentration in HDL of patients with diabetes mellitus was lower compared to HDL of healthy subjects [93]. We therefore

compared HDL from coronary artery disease (CAD) patients differing by the presence or absence of metabolic syndrome or type 2 DM towards their anti-apoptotic potential on IL-1β stimulated INS-1E cells and their apoC1 content. Unfortunately, neither the anti-apoptotic capacity nor the apoC1 content of the tested HDL was associated with the glycemic state of the plasma donors (Fig 6.6A+B). However, we found a significant correlation between the apoC1 content of the HDL samples and their anti-apoptotic effect on INS-1E irrespective of the glycemic state of the plasma donors (Fig 6.6C).

β-cell apoptosis is particularly relevant during the manifestation of type 2 DM. We therefore hypothesized that – if apoC1 had anti-apoptotic properties on β-cells – individuals with low levels of apoC1 would be predisposed to develop type 2 DM. In a prospective study of CAD patients, we investigated whether baseline apoC1 levels are associated with incident type 2 DM. During eight years follow up, 35 persons out of our 105 patients who were normoglycemic at the baseline examination, developed type 2 DM (Fig 6.7A). In this cohort our lab previously identified atypical sphingolipids and some circulating microRNAs as biomarkers of incident diabetes [166,167]. However, no differences in baseline apoC1 plasma levels were detected between the samples from persons with incident diabetes and persons not developing diabetes neither in total (Fig 6.7B) nor in apoB-depleted plasma, the latter of which was used as a surrogate for HDL (Fig 6.7C).

A potentially important limitation of both, the cross-sectional and the longitudinal study, is the fact that we investigated CAD patients. In a recent proteomics study, my lab found a decreased apoC1 content in HDL of patients with type 2 DM and/or CAD compared to HDL from healthy control subjects [168]. However, the apoC1 content did not differ between CAD patients with or without type 2 DM. In addition, other studies found decreased apoC1 levels in HDL of CAD patients and a correlation between the risk for CAD with low apoC1 levels [169–171]. Thus, the analysis of CAD patients may have been inappropriate to unravel any association of the glycemic state of the plasma donors with the apoC1 content and the anti-apoptotic activity of HDL.

At first sight paradoxically, HDL from subjects with higher TG or lower HDL-C plasma levels protected INS-1E cells better against IL-1β-induced apoptosis (Fig 6.6D+E). We found no significant correlation between TG and the apoC1 content of the respective HDL in the cross-sectional study (r=0.2855, p=0.1333, Tab 6.2) but a significant positive correlation between TG levels and apoC1 in both total and apoB-depleted plasma in the longitudinal study (r=0.5117,

p<0.0001; r=0.6207, p<0.0001, Tab 6.3). A correlation of plasma apoC1 and TG concentration was described in a study of men suffering from metabolic syndrome [172]. The authors explained their findings with the fact that apoC1 inhibits the lipoprotein lipase and stabilizes VLDL. Moreover, it has been described that apoC1 increases VLDL levels as it interferes with the removal of TG-rich lipoproteins by LDL receptor, Low density lipoprotein receptor-related protein 1 (LRP1) and VLDL receptor [80,164]. Thus, the higher TG levels and the better anti-apoptotic protection of the respective HDL could both be a consequence of higher apoC1 levels. Otherwise, apoC1 inhibits CETP and thereby stabilizes HDL particles. This inhibitory effect was found to be attenuated by glycation of apoC1 that occurs typically in type 1, or type 2 DM [173]. Since the majority of the study subjects had an impaired glucose tolerance (metabolic syndrome or type 2 DM), such an impaired CETP inhibition by glycated apoC1 seems plausible in our cohort. Relatively high CETP action combined with high VLDL levels will load HDL with TG, increase HDL clearance and thus lower HDL-C levels. As for our experiments HDL was dosed according to its protein concentration and as HDL-C is not necessarily a good predictor of HDL quality [79], the inverse correlation of HDL-C and anti-apoptotic potential is not contradictory.

In summary, the significant correlation between the apoC1 content and the anti-apoptotic potential of the HDL samples in the cross-sectional study supports an anti-apoptotic role of apoC1 in humans. However, our data from the longitudinal study is insufficient to show whether apoC1 reduces the risk to develop type 2 DM.

7.1.4. Problems with Apoptosis Induction and Prevention

Additional experiments had been planned for the analysis of the anti-apoptotic effect of apoC1. However, in the beginning of 2013 two major problems made it impossible to continue. Apoptosis induction in INS-1E cells with IL-1β worked robustly and was prevented by 50% and more by HDL (50 μg/ml) or apoC1 (5 μg/ml) for more than three years in our hands (as in Fig. 7.1A). However, these effects were getting considerably weaker and unstable in spring 2013: First, we had problems to prevent apoptosis by more than 30% (as in Fig. 7.1B). The replacement of different cell culture components (plates, media, HDL and apoC1, using cells frozen down at a lower passage number, replacing the INS-1E cells with isolates obtained from C. Wollheim and P. Maechler in Geneva (who originally isolated the INS-1E clone from

INS-1 cells [151]), did not solve these problems. Instead, we suddenly faced the loss of the IL-1β effect by the end of April 2013 (as in Fig. 7.1C). Whereas the apoptosis induced by 24 hours of IL-1β-treatment had been usually in the range of fourfold to even 20-fold, the effect of the same treatment was then often below twofold induction of apoptosis. The use of other IL-1β preparations did not restore the effect. Neither could we solve the problem by the use of alternative assays for the recording of apoptosis, for example by caspase-3 activity, or annexin V / propidium iodide staining in flow cytometry (data not shown). A summary of all experiments done between February and August 2013 illustrates the inconsistency of the experiments (Fig. 7.1D).

Despite extensive efforts, we could not identify the culprit. Possibly, we had recorded effects on a small number of cells with our apoptosis assay that measured the fold induction of apoptosis instead of a percentage of apoptotic cells. Hence, the effect would have been very fragile.

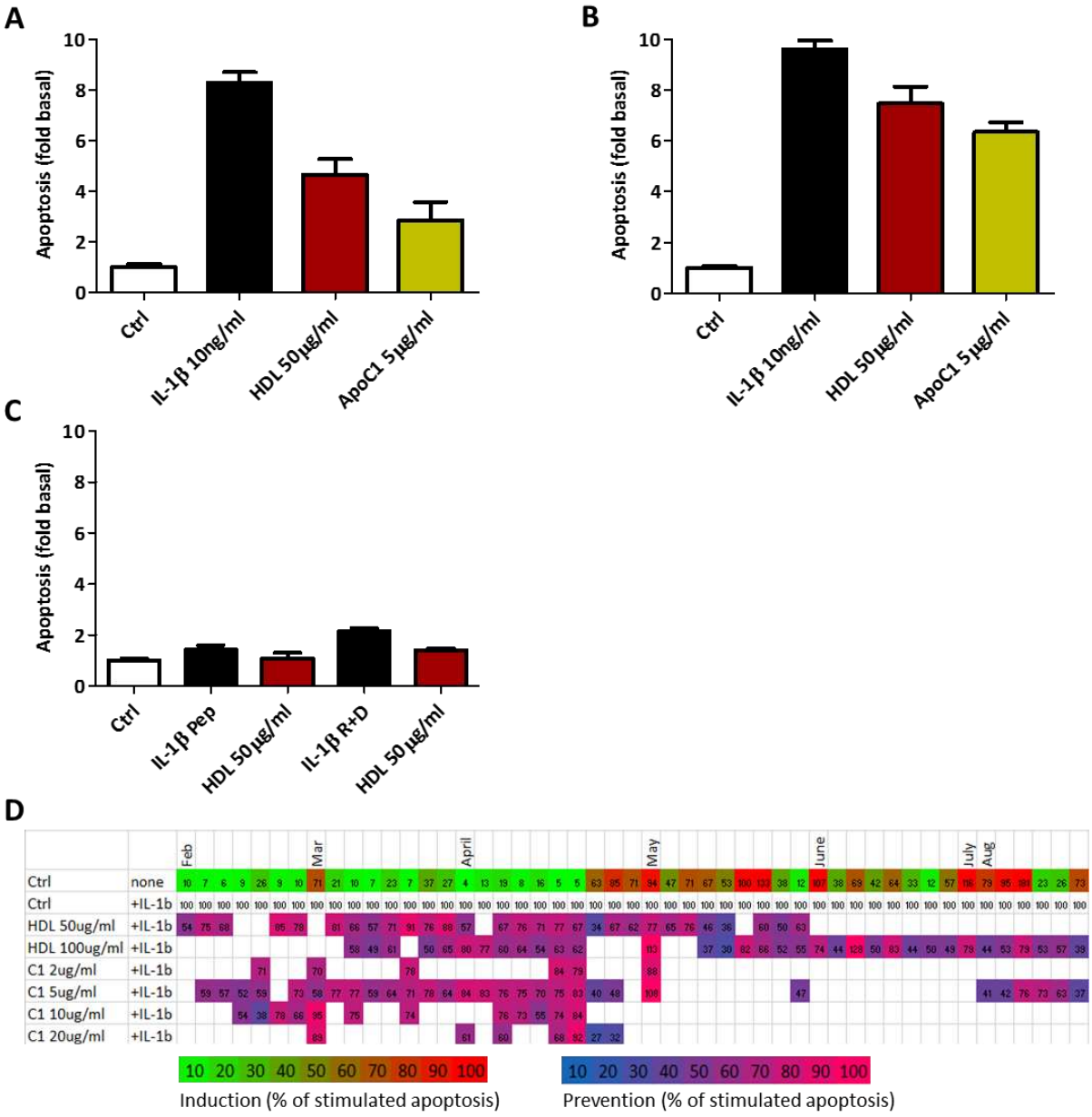

Figure 7.1: Problems with apoptosis prevention and induction.
A: Experiment of 19th of October 2012 (typical experiment): INS-1E cells were cultured for 40 hours in the presence of HDL or apoC1 at the indicated concentrations. During the last 24 hours, IL-1β (10 ng/ml) was added for the stimulation of apoptosis except in the not treated control (Ctrl) condition.
B: Experiment of 28th of February 2013: INS-1E cells were treated as described in A
C: Experiment of 17th of May 2013: INS-1E cells were treated as described in A, IL-1β from our usual supplier (Pep for Peprotech) was compared to IL-1β from R&D (each at 10 ng/ml).
D: Overview of all experiments done between February and August 2013
Bars indicate the mean values + SD

7.2. Apoptotic Signaling Analysis

Several gene expression studies have been undertaken to investigate the effect of IL-1β in pancreatic β-cells – mostly in combination with interferon γ (IFNγ) or other cytokines [44,174,175]. Also on the protein level, a previous study identified differentially regulated proteins in response to IL-1β treatment in pancreatic islets [176]. The modulation of apoptotic pathways by HDL has been explored only by one study of Pétremand and collegues in β-TC3 cells subjected to serum deprivation and incubation with or without 1mM HDL-C [109]. Thus, we performed a genome-wide expression analysis at the Functional Genomics Center Zürich (FGCZ) and several follow-up experiments to elucidate the signaling cascades by which HDL inhibited IL-1β-induced apoptosis of pancreatic β-cells in INS-1E cells.

7.2.1. Effects of Interleukin-1β and HDL on Gene Transcription

The cluster analysis revealed that the effect of IL-1β on transcription outraged the consequences of HDL treatment on gene expression by far (Fig 6.8). The changes in gene expression in response to the respective treatments were summarized in functional annotation clusters. After 12 h and 24 h IL-1β stimulation, these annotation clusters indicated massive changes in immune and inflammatory responses, cell death, regulation of cytokine production, cell cycle regulation, and protein biosynthesis (Tab 6.4). The results of our gene array analysis were thus similar to the findings of the Eizirik group who had identified differentially regulated genes and pathways in response to cytokine treatment [44,174]. In contrast to our data however, Eizirik and colleagues stated repeatedly that IL-1β does not trigger β-cell apoptosis on its own [44,174,177,178]. Larsen and colleagues described differentially expressed proteins in response to IL-1β-exposure in primary rat islets [176]. After separation with high-resolution 2D-gel electrophoresis, proteins belonging to energy transduction; the glycolytic pathway; protein synthesis, chaperones, and protein folding; and signal transduction, regulation, differentiation, and apoptosis were identified with mass spectrometry.

Unfortunately, genes differentially regulated by IL-1β and HDL had high false discovery rates in our study (> 0.5101). The subsequent search for annotation clusters of differentially regulated genes yielded considerably lower enrichment scores (Tab 6.5). These clusters

included the regulation of transcription factors (NF-κB among others), the endoplasmic reticulum stress response, protein biosynthesis, the induction of apoptosis, lipid biosynthetic processes, glucose metabolism, the response to hormone and cytokine stimuli, and cellular development. Given the relatively low enrichment scores and high false discovery rates, this data was interpreted with caution. A possible explanation for the poor outcome in the search for differentially regulated genes is the timing of the experiments. Since RNA transcription adapts within hours to certain stimuli, our collection times after 12 h and 24 h IL-1β incubation might have missed essential changes in expression which could have increased the survival of the HDL treated cells.

Thus, ten candidate genes of the apoptotic pathway that had been slightly differentially regulated by IL-1β and HDL in the gene array were re-analyzed by quantitative real-time PCR (qPCR) at additional time points, i.e. after 3 to 24 h IL-1β incubation in the presence or absence of HDL. The selected genes were located in the ER stress pathway, in the intrinsic or extrinsic apoptotic pathway (Fig 6.10). Although considerable changes in expression over time were detected for some genes, the differences between IL-1β treated cells with and without HDL on the gene expression level were minor compared to the pronounced effect of IL-1β- versus not treated cells (Tab 6.6). These results corroborated a massive effect of IL-1β stimulation on gene expression in INS-1E cells. More importantly, they affirmed our previous notion that the primary protective action of HDL against IL-1β-induced apoptosis might not be found at the transcription level. We therefore sought to investigate the NF-κB signaling and the ER stress response with independent experiments.

7.2.2. Investigation of NF-κB

The transcription factor NF-κB – among other functions – is important for the expression of genes related to cell survival and apoptosis [179]. NF-κB is involved in the progression of several metabolic diseases [180]. The inhibition of NF-κB by salicylates resulted in the amelioration of glucose homeostasis and insulin resistance in a mouse model. Overexpression of IκBα, an inhibitor of NF-κB, protected pancreatic islet cells from IL-1β-induced cell death [181]. In pancreatic β-cells, NF-κB translocation (i.e. activation) in response to short-term IL-1β exposure had protective effects whilst it induced apoptosis when IL-1β stimulation

persisted [182]. Moreover, an NF-κB blockade resulted in β-cell protection against diabetogenic agents in vitro and in vivo [183].

As expected, we observed a reversible translocation of NF-κB (subunit p65) into the nucleus in response to IL-1β treatment in INS-1E cells (Fig 6.11). Unfortunately, the presence of HDL did not modify the NF-κB translocation under the tested conditions (i.e. 0, 5, 15 and 60 minutes, and 5 and 24 hours of IL-1β incubation). Additional time points might have revealed a different translocation pattern in cells treated with and without HDL. However, HDL was neither found to alter the distribution of NF-κB in another β-cell line [109]. Thus, there is good reason to assume that HDL interferes with apopotosis independently of the NF-κB pathway. We therefore focused on the investigation of other ER stress related pathways.

7.2.3. Investigation of ER Stress

Several genes of the ER stress response pathway were found to be differentially regulated by IL-1β and HDL in our gene array analysis. Moreover, it was described beforehand that IL-1β (partly in combination with other cytokines) induces ER stress in pancreatic β-cells [38,44,46,184]. Christian Widmann's group previously demonstrated that HDL resolves ER stress and ER stress related apoptosis in Min6 cells and primary beta cells [109,111]. Thus, in a collaboration with Christian Widmann's group we investigated whether HDL and especially its component apoC1 reduced ER stress and ER stress-induced apoptosis in Min6 cells. Whereas the activation of PERK and subsequent apoptosis by the ER stressor thapsigargin (ThG) were partially prevented by HDL and the higher dose of apoC1, the ThG-stimulated expression of CHOP was clearly reduced by HDL but not apoC1 (Fig 6.12A-C). Experiments in INS-1E cells confirmed a protective role of HDL against ThG-induced apoptosis for β-cells. However, no protective effect of apoC1 was found in these experiments (Fig 6.12D). Albeit IL-1β stimulation triggers ER stress, we conclude that the mechanism by which ThG induces ER stress and subsequent apoptosis differs from the IL-1β-induced apoptosis pathway. Any protective effect of apoC1 seems to be exerted on a pathway that is not modified by ThG. This is similar to an observation of the Widmann group, who described earlier that HDL protected β-cells against different stressors by diverse means [109]. Meanwhile, my laboratory found that HDL prevents ThG-induced apoptosis of INS-1E cells by a mechanism which involves the mobilization of sterols, and which requires exclusively apoA1/phospholipid particles [185]. This finding further

underscores the assumption that HDL elicits different anti-apoptotic mechanisms by different pathways and components. Specifically, cytokine- and ER-stress-induced apoptosis of INS-1E cells are inhibited by HDL through different mechanisms with different structural requirements.

7.2.4. Problems with Apoptosis Induction and Prevention

The problems described in section 7.1.5 hampered the investigation in IL-1β- and HDL-modulated signaling pathways as well. In contrast to IL-1β-induced apoptosis, ThG-induced apoptosis was continuously and robustly working: apoptosis was detected with two additional assays (annexin V / propidium iodide (PI) staining and caspase 3 activation, Fig 6.13A+B). Since apoC1 did not prevent ThG-induced apoptosis however, we could not use this model to investigate the mechanism(s) by which apoC1 interfered with β-cell apoptosis.

7.3. Clinical Studies on the Impact of Diabetes on HDL Functionality

Since our analyses on the anti-apoptotic effect of apoC1 in INS-1E cells could not proceed, we investigated the components of HDL that might interfere with ThG-induced apoptosis of pancreatic β-cells. By case-control studies, we sought to investigate the impact of type 1 and type 2 DM on the ability of HDL to protect INS-1E cells from ThG-induced apoptosis. In addition, the potential of HDL to stimulate cholesterol efflux from macrophages, as well as to regulate NO production, adhesion molecule expression and starvation-induced apoptosis in endothelial cells were investigated. These comprehensive studies aimed to check whether type 1 and type 2 DM share dysfunctions, and whether the different functionalities of HDL correlate with each other. The cholesterol homeostasis of β-cell membranes is known to play an important role in the regulation of insulin secretion [113,114,116,120]. Moreover, recent studies of my lab provided evidence that the protection of INS-1E cells by HDL from ThG-induced apoptosis involves the mobilization of sterols [185].

To rule out any interference of CAD (see 7.1.3) we compared the protective effects of HDL from patients with or without CAD, normal or impaired fasting glucose or type 2 DM. Unfortunately, no differences in ThG-induced apoptosis reduction were detected for these HDL samples (Fig 6.14B). Correlation analysis of the apoptosis reduction with the clinical parameters of the study subjects did not reveal any significant associations once we adjusted for multiple testing (Tab 6.9). The HDL samples from the different groups differed neither by their abilities to protect human aortic endothelial cells (HAECs) from starvation induced apoptosis nor to elicit NO production in bovine aortic endothelial cells (data not shown). At first sight, the negative findings suggest that the anti-apoptotic effect of HDL towards pancreatic β-cells is robust and not affected by disease. However, the endothelial functions of HDL were found to be adversely affected by diabetes and CAD by several groups [77,95,186–189]. The negative findings also question the arguments of our discussion on the negative findings in the case-control study on IL-1β-induced apoptosis (see 6.1.7 and 7.1.3), namely that the presence of CAD hides any differences between diabetic and non-diabetic subjects. However, the control subjects (without established coronary artery disease and with normal fasting glucose) were neither healthy. Most of them received treatment for hypertension (beta blockers, ACE inhibitors), aspirin or statins (Tab 5). In conjunction with the relatively high analytical variation of the bioassays and the rather small sample number, our study may have

not been powered enough to find any significant differences between the control subjects and the patient groups. In fact, previous studies from our lab compared CAD patients and very healthy blood donors, for example towards the endothelial functionality of HDL [77,95,189]. In a recent very comprehensive systems biology study, my lab compared HDL of 50 healthy volunteers with HDL of 100 patients with either diabetes, CAD or both [168]. In this study, the ability of HDL to protect INS-1E cells from ThG-induced apoptosis was impaired in CAD patients whereas the ability of the HDL to prevent starvation-induced apoptosis of HAECs was impaired in diabetic patients compared to HDL from healthy subjects. In line with this difference, the two activities were found to have different structural determinants.

Type 2 DM patients often suffer from comorbidities such as obesity, hypertension, macro- and microvascular diseases, chronic kidney disease, depression, and/or cognitive decline [24,190]. It has been demonstrated before that several diseases – including type 2 DM – change the composition and functionality of HDL [67,77,93–95,191]. However, because many comorbidities are present already at the time point of diagnosis and because many of them cause structural and functional changes of HDL, it is difficult to resolve structure-function-disease relationships of HDL in type 2 DM. It was therefore particularly interesting to investigate the protective effects of HDL from adolescent type 1 DM patients towards β-cell apoptosis, because comorbidities presumably had not evolved at this early stage of disease. Thus, any changes in anti-apoptotic activity of HDL from adolescents with type 1 DM could be assigned to type 1 DM-related HDL remodeling. In fact, two studies found evidence for disturbed HDL function in type 1 diabetes, i.e. a decreased HDL-apoA1 exchange rate and an impaired cholesterol efflux capacity, respectively [192,193].

HDL isolated from diabetic adolescents had slightly but not significantly less anti-apoptotic potential on INS-1E cells compared to HDL isolated from age-matched, healthy adolescents ($p=0.3535$, Fig 6.14A). Cholesterol efflux experiments from J774 macrophages with and without previous cAMP-stimulation of the ABCA1 receptor expression revealed a similar picture. In both conditions, HDL from adolescents with type 1 DM induced slightly less cholesterol efflux (Fig 6.15A+B). The differences were not significant though ($p=0.0971$ without cAMP stimulation, $p=0.5040$ with cAMP stimulation).

As expected, cholesterol efflux from macrophages with prior cAMP stimulation correlated with cholesterol efflux without prior cAMP stimulation (Tab 6.8). Otherwise, correlation

analysis of the functional tests with the clinical parameters of the study subjects did not reveal any significant associations after adjustment for multiple testing (Tab 6.7).

Further experiments of coworkers with the same HDL samples in endothelial cells likewise yielded little and mostly insignificant differences between patients with type 1 DM and healthy controls: HDL from adolescents with type 1 DM was a less potent stimulator of NO release from bovine aortic endothelial cells than HDL from the age-matched healthy control subjects *(76.60% ± 6.785% vs. 100.5% ± 8.238%, p=0.0409)*. HDL from the type 1 diabetic donors was but slightly less active than HDL from control subjects to protect human aortic endothelial cells against starvation-induced apoptosis *(81.55% ± 4.903% vs. 88.29% ± 5.866%, p=0.4108) or* stimulated VCAM-1 expression *(91.91% ± 3.278% vs. 87.09% ± 3.015%, p=0.3063)*.

These results did not motivate further experiments to investigate the quality and composition of the tested HDL samples. A higher sample number could have possibly unraveled significant differences between HDL of adolescents with or without type 1 DM. Thus, we cannot assess whether the small deteriorations in the function of our HDL samples from adolescents with type 1 DM mirror the early and persistent decreases in HDL function of type 1 diabetic adolescents described by Heier and Gourgari [192,193].

7.4. Conclusion

The first aim of this PhD project was to identify HDL components with anti-apoptotic effects on pancreatic β-cells. This issue was addressed in INS-1E cells, a rat pancreatic β-cell line, with interleukin-1β (IL-1β)-induced apoptosis. Whereas the previously described anti-apoptotic components apoA1 and S1P [88] did not reduce apoptosis significantly in our β-cell model, apoC1 was found protect INS-1E cells against IL-1β-induced apoptosis (see section 7.1.1.). With apoC1-deficient murine HDL, we sought to estimate the relevance of apoC1 within HDL for its anti-apoptotic effect (see section 7.1.2.). However, the differences between the effects of murine and human HDL on β-cells overrode the magnitude of apoC1's anti-apoptotic effects. Since apoC1 levels were described to be lower in subjects with metabolic diseases [93], we decided to investigate this question by testing the effect of HDL from different patient groups (see 7.1.3.). The glycemic state of the study subjects did not associate with the anti-apoptotic activity of the tested HDL samples on INS-1E cells, but we observed a positive correlation between the apoC1 content and the ability of the respective HDL to reduce apoptosis in all of the study samples. However, we did not find any association of apoC1 plasma levels with the presence or incidence of diabetes, possibly because we investigated CAD patients who are also known to have lower apoC1 levels in HDL [169–171] (see 7.1.4.).

To identify receptors and signaling pathways, by which HDL and apoC1 interfere with IL-1β-induced apoptosis, we performed a genome-wide expression analysis. In contrast to the massive gene expression changes in response to IL-1β treatment, the presence or absence of HDL induced but minor differential gene regulation (see 7.2.1.). These differentially regulated pathways included the transcription factor NF-κB and the response to ER stress. The validation experiments confirmed that IL-1β promotes the NF-κB translocation from the cytosol into the nucleus but did not provide any evidence that HDL interferes with this (see 7.2.2.). Unfortunately, the collapse of our apoptosis model hampered further experiments to characterize any mechanism by which apoC1-may interfere with IL-1β-induced apoptois of INS-1E cells (see 7.1.5.).

We therefore started the investigation of another model of β-cell apoptosis, namely ER-stress related apoptosis induced by thapsigargin [109,111]. We confirmed the protective effect of HDL in INS-1E cells. However, apoC1 did not mimic the protective effect of HDL against thapsigargin-induced apoptosis (see 7.2.3.). We thus assume that the protective effect of

apoC1 against IL-1β-induced apoptosis lies in a branch of the apoptotic pathway that is not modified by the ER stressor thapsigargin. With HDL samples from different patient groups, we sought to identify protective HDL components against ER stress-related apoptosis induced by ThG. Regrettably, neither type 2 DM nor type 1 DM was associated with any difference in the ability of HDL to protect INS-1E cells from ThG-induced apoptosis (see 7.3). Because of the high variation of the bioassay and because of confounding, we cannot rule out that our studies had too little statistical power to unravel any significant difference between the groups.

We found some evidence that apoC1 contributes to the ability of HDL to protect pancreatic β-cells from IL-1β-induced apoptosis but not to the ability of HDL to inhibit ER-stress. Otherwise, recent studies of my lab found that the protection of INS-1E cells by HDL from ThG-induced apoptosis involves the mobilization of sterols [185]. Moreover, coworkers from my lab discovered that HDL from CAD patients was less able to protect INS-1E cells from ThG-induced apoptosis whereas the ability of the HDL to prevent starvation-induced apoptosis of HAECs was impaired in diabetic patients compared to HDL from healthy subjects [168]. Interestingly, the two features were found to have different structural determinants.

In conclusion, different structural determinants and mechanisms seem to account for the ability of HDL to protect INS-1E cells from IL-1β- and ThG-/ER-stress-induced apoptosis. Unfortunately, our in vitro findings on the anti-apoptotic activities of HDL and apoC1 could not be translated into bioassays and biomarkers that help to identify patients with increased risk of diabetes.

8. References

1. WHO. *Definition, Diagnosis and Classification of Diabetes Mellitus and its Complications Part1: Diagnosis and Classification of Diabetes Mellitus*. (1999).
2. Diabetes Treatment History. Available at: http://worldhistoryproject.org/topics/diabetes-treatment-history. (Accessed: 9th September 2019)
3. Laios, K., Karamanou, M., Saridaki, Z. & Androutsos, G. Aretaeus of Cappadocia and the first description of diabetes. *Hormones* **11**, 109–113 (2012).
4. Minkowski, O. Untersuchungen über den Diabetes mellitus nach Exstirpation des Pankreas. *Arch. für Exp. Pathol. und Pharmakologie* **31**, 85–189 (1893).
5. Minkowski, O. Historical development of the theory of pancreatic diabetes. *Diabetes* **38**, 1–6 (1989).
6. Banting, F. G., Best, C. H., Collip, J. B., Campbell, W. R. & Fletcher, A. A. Pancreatic extracts in the treatment of diabetes mellitus. 1922. *Indian J. Med. Res.* **125**, 141–146 (2007).
7. Himsworth, H. P. Diabetes mellitus: its differentiation into insulin-sensitive and insulin-insensitive types. 1936. *Int. J. Epidemiol.* **42**, 1594–1598 (2013).
8. Yalow, R. S. & Berson, S. A. Immunoassay of Endogenous Plasma Insulin in Man. *J. Clin. Invest.* **39**, 1157–1175 (1960).
9. Bray, G. A. Methods and obesity research: the radioimmunoassay of insulin. *Obes. Res.* **4**, 579–582 (1996).
10. Karam, J. H., Grodsky, G. M. & Forsham, P. H. Excessive insulin response to glucose in obese subjects as measured by Immunochemical Assay. *Diabetes* **12**, 197–204 (1963).
11. Lin, Y. & Sun, Z. Current views on type 2 diabetes. *J. Endocrinol.* **204**, 1–11 (2010).
12. Thorens, B. & Mueckler, M. Glucose transporters in the 21st Century. *Am. J. Physiol. - Endocrinol. Metab.* **298**, 141–145 (2010).
13. Butler, P. C., Meier, J. J., Butler, A. E. & Bhushan, A. The replication of β cells in normal physiology, in disease and for therapy. *Nat. Clin. Pract. Endocrinol. Metab.* **3**, 758–768 (2007).
14. Ogilvie, R. F. The islands of langerhans in 19 cases of obesity. *J. Pathol. Bacteriol.* **37**, 473–481 (1933).
15. Prentki, M. & Nolan, C. J. Islet b cell failure in type 2 diabetes. *J. Clin. Invest.* **116**, 1802–1812 (2006).
16. Lee, Y. C. & Nielsen, J. H. Regulation of beta cell replication. *Mol. Cell. Endocrinol.* **297**, 18–27 (2009).
17. Chen, C., Cohrs, C. M., Stertmann, J., Bozsak, R. & Speier, S. Human beta cell mass and function in diabetes: Recent advances in knowledge and technologies to understand disease pathogenesis. *Mol. Metab.* **6**, 943–957 (2017).
18. Yoneda, S. *et al.* Predominance of β-cell neogenesis rather than replication in humans with an impaired glucose tolerance and newly diagnosed diabetes. *J. Clin. Endocrinol. Metab.* **98**, 2053–2061 (2013).
19. Steiner, D. F. The Biosynthesis of Insulin. in *Pancreatic Beta Cell in Health and Disease* (eds. Seino, S. & Bell, G. I.) 31–49 (Springer, Tokyo, 2008). doi:https://doi.org/10.1007/978-4-431-75452-7_3
20. Guillausseau, P.-J. *et al.* Abnormalities in insulin secretion in type 2 diabetes mellitus. *Diabetes Metab.* **34**, S43–S48 (2008).

21. Komatsu, M., Takei, M., Ishii, H. & Sato, Y. Glucose-stimulated insulin secretion: A newer perspective. *J. Diabetes Investig.* **4**, 511–516 (2013).
22. Lemaire, K. & Schuit, F. Integrating insulin secretion and ER stress in pancreatic β-cells. *Nat. Cell Biol.* **14**, 979–981 (2012).
23. Polonsky, K. S., Given, B. D. & Van Cauter, E. Twenty-four-hour profiles and pulsatile patterns of insulin secretion in normal and obese subjects. *J. Clin. Invest.* **81**, 442–448 (1988).
24. WHO. Global report on diabetes. *WHO Press* (2016).
25. Nam Han Cho (chair) dkk. *IDF Diabetes Atlas Eighth edition 2017*. *IDF Diabetes Atlas, 8th edition* (2017). doi:http://dx.doi. org/10.1016/S0140-6736(16)31679-8.
26. Kahn, S. E., Hull, R. L. & Utzschneider, K. M. Mechanisms linking obesity to insulin resistance and type 2 diabetes. *Nature* **444**, 840–846 (2006).
27. Butler, A. E. *et al.* Humans With Type 2 Diabetes. *Diabetes* **52**, 102–110 (2003).
28. Melloul, D., Marshak, S. & Cerasi, E. Regulation of insulin gene transcription. *Diabetologia* **45**, 309–326 (2002).
29. Cnop, M., Ladrière, L., Igoillo-Esteve, M., Moura, R. F. & Cunha, D. A. Causes and cures for endoplasmic reticulum stress in lipotoxic β-cell dysfunction. *Diabetes, Obes. Metab.* **12**, 76–82 (2010).
30. Donath, M. Y. & Shoelson, S. E. Type 2 diabetes as an inflammatory disease. *Nat. Rev. Immunol.* **11**, 98–107 (2011).
31. Lodish, H. *et al.* Cell Death and Its Regulation. in *Molecular Cell Biology* 936–948 (W. H. Freeman, 2007).
32. Galluzzi, L. *et al.* Molecular definitions of cell death subroutines: Recommendations of the Nomenclature Committee on Cell Death 2012. *Cell Death Differ.* **19**, 107–120 (2012).
33. Berchtold, L. A., Prause, M., Størling, J. & Mandrup-Poulsen, T. Cytokines and Pancreatic β-Cell Apoptosis. *Adv. Clin. Chem.* **75**, 99–158 (2016).
34. Donath, M. Y. & Ehses, J. A. Type 1, type 1.5, and type 2 diabetes: NOD the diabetes we thought it was. *Proc. Natl. Acad. Sci. U. S. A.* **103**, 12217–12218 (2006).
35. Wali, J., Masters, S. & Thomas, H. Linking Metabolic Abnormalities to Apoptotic Pathways in Beta Cells in Type 2 Diabetes. *Cells* **2**, 266–283 (2013).
36. Meyerovich, K., Ortis, F., Allagnat, F. & Cardozo, A. K. Endoplasmic reticulum stress and the unfolded protein response in pancreatic islet inflammation. *J. Mol. Endocrinol.* **57**, R1–R17 (2016).
37. McKenzie, M. D. *et al.* Glucose induces pancreatic islet cell apoptosis that requires the BH3-only proteins bim and puma and multi-BH domain protein bax. *Diabetes* **59**, 644–652 (2010).
38. Eizirik, D. L., Cardozo, A. K. & Cnop, M. The role for endoplasmic reticulum stress in diabetes mellitus. *Endocr. Rev.* **29**, 42–61 (2008).
39. Cunha, D. A. *et al.* Initiation and execution of lipotoxic ER stress in pancreatic β-cells. *J. Cell Sci.* **121**, 2308–2318 (2008).
40. Cunha, D. A. *et al.* Death protein 5 and p53-upregulated modulator of apoptosis mediate the endoplasmic reticulum stress-mitochondrial dialog triggering lipotoxic rodent and human β-cell apoptosis. *Diabetes* **61**, 2763–2775 (2012).
41. Maedler, K. *et al.* Glucose-induced b cell production of IL-1 b contributes to glucotoxicity in human pancreatic islets. *J. Clin. Invest.* **110**, 851–860 (2002).
42. Ehses, J. A. *et al.* Increased Number of Islet-Associated Macrophages in Type 2 Diabetes. *Diabetes* **56**, 2356–2370 (2007).

43. Böni-Schnetzler, M. *et al.* β Cell-Specific Deletion of the IL-1 Receptor Antagonist Impairs β Cell Proliferation and Insulin Secretion. *Cell Rep.* **22**, 1774–1786 (2018).
44. Cnop, M., Welsh, N., Jonas, J., Jo, A. & Lenzen, S. Many Differences, Few Similarities. *Am. Diabetes Assoc.* 97–107 (2005).
45. Thomas, H. E., McKenzie, M. D., Angstetra, E., Campbell, P. D. & Kay, T. W. Beta cell apoptosis in diabetes. *Apoptosis* **14**, 1389–1404 (2009).
46. Cardozo, A. K. *et al.* Cytokines Downregulate the Sarcoendoplasmic Endoplasmic Reticulum Ca2þ, Leading to Induction of Reticulum Pump Ca2þ ATPase 2b and Deplete Endoplasmic Reticulum Stress in Pancreatic -Cells. **54**, (2005).
47. Chan, J. Y. *et al.* The balance between adaptive and apoptotic unfolded protein responses regulates β-cell death under ER stress conditions through XBP1, CHOP and JNK. *Mol. Cell. Endocrinol.* **413**, 189–201 (2015).
48. Brozzi, F. *et al.* Cytokines induce endoplasmic reticulum stress in human, rat and mouse beta cells via different mechanisms. *Diabetologia* **58**, 2307–2316 (2015).
49. Jurgens, C. A. *et al.* β-Cell loss and β-cell apoptosis in human type 2 diabetes are related to islet amyloid deposition. *Am. J. Pathol.* **178**, 2632–2640 (2011).
50. Subramanian, S. L. *et al.* CJUN N-terminal kinase (JNK) activation mediates islet amyloid-induced beta cell apoptosis in cultured human islet amyloid polypeptide transgenic mouse islets. *Diabetologia* **55**, 166–174 (2012).
51. Westwell-Roper, C. *et al.* IL-1 Blockade Attenuates Islet Amyloid Polypeptide-Induced Proinflammatory Cytokine Release and Pancreatic Islet Graft Dysfunction. *J. Immunol.* **187**, 2755–2765 (2011).
52. Hui, Q. *et al.* Amyloid formation disrupts the balance between interleukin-1β and interleukin-1 receptor antagonist in human islets. *Mol. Metab.* **6**, 833–844 (2017).
53. Maedler, K. *et al.* Glucose Induces β-Cell Apoptosis Via Upregulation of the Fas Receptor in Human Islets. *Diabetes* **50**, 1683–1690 (2001).
54. Romeo, G. R., Lee, J. & Shoelson, S. E. Metabolic syndrome, insulin resistance, and roles of inflammation- mechanisms and therapeutic targets. *Arterioscler. Thromb. Vasc. Biol.* **32**, 1771–1776 (2012).
55. Goldfine, A. B. *et al.* Salicylate (Salsalate) in Patients With Type 2 Diabetes. *Ann. Intern. Med.* **159**, 1 (2013).
56. Donath, M. Y. Multiple benefits of targeting inflammation in the treatment of type 2 diabetes. *Diabetologia* **59**, 679–682 (2016).
57. Mastandrea, L. *et al.* Etanercept Treatment in Children With New-Onset Type 1 Diabetes. *Diabetes Care* **32**, 1244–1249 (2009).
58. Stanley, T. L. *et al.* TNF-α Antagonism with Etanercept Decreases Glucose and Increases the Proportion of High Molecular Weight Adiponectin in Obese Subjects with Features of the Metabolic Syndrome. *J. Clin. Endocrinol. Metab.* **96**, E146–E150 (2011).
59. Di Prospero, N. A. *et al.* CCR2 antagonism in patients with type 2 diabetes mellitus: a randomized, placebo-controlled study. *Diabetes, Obes. Metab.* **16**, 1055–1064 (2014).
60. Larsen, C. M. *et al.* Interleukin-1-receptor antagonist in type 2 diabetes mellitus. *N. Engl. J. Med.* **356**, 1517–1526 (2007).
61. Larsen, C. M. *et al.* Sustained Effects of Interleukin-1 Receptor Antagonist Treatment in Type 2 Diabetes. *Diabetes Care* **32**, 1663–1668 (2009).
62. Goldfine, A. B. & Shoelson, S. E. Therapeutic approaches targeting inflammation for diabetes and associated cardiovascular risk. *J. Clin. Invest.* **127**, 83–93 (2017).

63. van Poppel, P. C. M. *et al.* The interleukin-1 receptor antagonist anakinra improves first-phase insulin secretion and insulinogenic index in subjects with impaired glucose tolerance. *Diabetes, Obes. Metab.* **16**, 1269–1273 (2014).
64. Everett, B. M. *et al. Anti-Inflammatory Therapy With Canakinumab for the Prevention and Management of Diabetes*. *Journal of the American College of Cardiology* **71**, (American College of Cardiology Foundation, 2018).
65. Ikonen, E. Cellular cholesterol trafficking and compartmentalization. *Nat. Rev. Mol. Cell Biol.* **9**, 125–138 (2008).
66. Fielding, C. J. & Fielding, P. E. Dynamics of lipoprotein transport in the circulatory system. in *Biochemistry of Lipids, Lipoproteins and Membranes* (eds. Vance, D. E. & Vance, J. E.) 533–554 (Elsevier B.V., 2008).
67. Annema, W. & Von Eckardstein, A. High-density lipoproteins - Multifunctional but vulnerable protections from atherosclerosis. *Circ. J.* **77**, 2432–2448 (2013).
68. Jonas, A. & Phillips, M. C. Lipoprotein structure. in *Biochemistry of Lipids, Lipoproteins and Membranes* (eds. Vance, D. E. & Vance, J. E.) 485–506 (Elsevier B.V., 2008).
69. Williams, K. J. Science in medicine Molecular processes that handle — and mishandle — dietary lipids. *J. Clin. Invest.* **118**, 3247–3259 (2008).
70. Goldstein, J. L. & Brown, M. S. Expression of the familial hypercholesterolemia gene in heterozygotes: model for a dominant disorder in man. *Trans. Assoc. Am. Physicians* **87**, 120–131 (1974).
71. Kontush, A. *et al.* Structure of HDL: Particle Subclasses and Molecular Components. in *Handbook of experimental pharmacology* **224**, 3–51 (2015).
72. Rye, K. A. & Barter, P. J. Regulation of high-density lipoprotein metabolism. *Circ. Res.* **114**, 143–156 (2014).
73. Zannis, V. I. *et al.* HDL Biogenesis, Remodeling, and Catabolism. in *Handbook of experimental pharmacology* **224**, 53–111 (2015).
74. Rader, D. J. Molecular regulation of HDL metabolism and function: implications for novel therapies. **116**, 3090–3100 (2006).
75. Rader, D. J. & Daugherty, A. Translating molecular discoveries into new therapies for atherosclerosis. *Nature* **451**, 904–913 (2008).
76. Camont, L. *et al.* Small, dense high-density lipoprotein-3 particles are enriched in negatively charged phospholipids: relevance to cellular cholesterol efflux, antioxidative, antithrombotic, anti-inflammatory, and antiapoptotic functionalities. *Arterioscler. Thromb. Vasc. Biol.* **33**, 2715–23 (2013).
77. Riwanto, M. *et al.* Altered activation of endothelial anti-and proapoptotic pathways by high-density lipoprotein from patients with coronary artery disease: Role of high-density lipoprotein-proteome remodeling. *Circulation* **127**, 891–904 (2013).
78. Davidson, W. S. *et al.* Proteomic analysis of defined hdl subpopulations reveals particle-specific protein clusters: Relevance to antioxidative function. *Arterioscler. Thromb. Vasc. Biol.* **29**, 870–876 (2009).
79. Von Eckardstein, A. & Rohrer, L. HDLs in crises. *Curr. Opin. Lipidol.* **27**, 264–273 (2016).
80. Shachter, N. S. Apolipoproteins C-I and C-III as important modulators of lipoprotein metabolism. *Curr. Opin. Lipidol.* **12**, 297–304 (2001).
81. Gautier, T. *et al.* Human apolipoprotein C-I accounts for the ability of plasma high density lipoproteins to inhibit the cholesteryl ester transfer protein activity. *J. Biol. Chem.* **275**, 37504–37509 (2000).
82. de Haan, W. *et al.* Apolipoprotein CI inhibits scavenger receptor BI and increases plasma HDL levels in vivo. *Biochem. Biophys. Res. Commun.* **377**, 1294–1298 (2008).

83. Fitzgerald, M. L., Mujawar, Z. & Tamehiro, N. ABC transporters, atherosclerosis and inflammation. *Atherosclerosis* **211**, 361–370 (2010).
84. Ishigami, M. *et al.* Temporary sequestration of cholesterol and phosphatidylcholine within extracellular domains of ABCA1 during nascent HDL generation. *Sci. Rep.* **8**, 2–11 (2018).
85. Nofer, J.-R. Signal Transduction by HDL: Agonists, Receptors, and Signaling Cascades. in *Handbook of experimental pharmacology* **224**, 229–256 (2015).
86. Robert, J. *et al.* Interleukin 6 stimulates endothelial binding and transport of high-density lipoprotein through induction of endothelial lipase. *Arterioscler. Thromb. Vasc. Biol.* **33**, 2699–2706 (2013).
87. Laychock, S. G., Sessanna, S. M., Lin, M. H. & Mastrandrea, L. D. Sphingosine 1-phosphate affects cytokine-induced apoptosis in rat pancreatic islet β-cells. *Endocrinology* **147**, 4705–4712 (2006).
88. Rütti, S. *et al.* Low- and high-density lipoproteins modulate function, apoptosis, and proliferation of primary human and murine pancreatic β-cells. *Endocrinology* **150**, 4521–4530 (2009).
89. Chahil, T. J. & Ginsberg, H. N. Diabetic dyslipidemia. *Endocrinol. Metab. Clin. North Am.* **35**, 491–510, vii–viii (2006).
90. Goldberg, I. J., Vanni-Reyes, T., Ramakrishnan, S., Holleran, S. & Ginsberg, H. N. Circulating lipoprotein profiles are modulated differently by lipoprotein lipase in obese humans. *J. Cardiovasc. Risk* **7**, 41–7 (2000).
91. von Eckardstein, A. & Widmann, C. High-density lipoprotein, beta cells, and diabetes. *Cardiovasc. Res.* **103**, 384–394 (2014).
92. Zhang, Y. *et al.* Adipocyte modulation of high-density lipoprotein cholesterol. *Circulation* **121**, 1347–1355 (2010).
93. Davidsson, P., Hulthe, J., Fagerberg, B. & Camejo, G. Proteomics of apolipoproteins and associated proteins from plasma high-density lipoproteins. *Arterioscler. Thromb. Vasc. Biol.* **30**, 156–163 (2010).
94. O'Neill, F. *et al.* Structural and functional changes in HDL with low grade and chronic inflammation. *Int. J. Cardiol.* **188**, 111–116 (2015).
95. Speer, T. *et al.* Abnormal high-density lipoprotein induces endothelial dysfunction via activation of toll-like receptor-2. *Immunity* **38**, 754–768 (2013).
96. Mao, J. Y. *et al.* Serum amyloid A enrichment impairs the anti-inflammatory ability of HDL from diabetic nephropathy patients. *J. Diabetes Complications* **31**, 1538–1543 (2017).
97. Glomset, J. A. The plasma lecithins:cholesterol acyltransferase reaction. *J. Lipid Res.* **9**, 155–167 (1968).
98. Miller, G. J. & Miller, N. E. Plasma-High-Density-Lipoprotein Concentration and Development of Ischæmic Heart-Disease. *Lancet* **305**, 16–19 (1975).
99. Rohrer, L. *et al.* High-density lipoprotein transport through aortic endothelial cells involves scavenger receptor BI and ATP-binding cassette transporter G1. *Circ. Res.* **104**, 1142–1150 (2009).
100. Perisa, D., Rohrer, L., Kaech, A. & Von Eckardstein, A. Itinerary of high density lipoproteins in endothelial cells. *Biochim. Biophys. Acta - Mol. Cell Biol. Lipids* **1861**, 98–107 (2016).
101. Haffner, S. M., Stern, M. P., Hazuda, H. P., Mitchell, B. D. & Patterson, J. K. Cardiovascular Risk Factors in Confirmed Prediabetic Individuals: Does the Clock for Coronary Heart Disease Start Ticking Before the Onset of Clinical Diabetes? *JAMA J.*

Am. Med. Assoc. **263**, 2893–2898 (1990).
102. Von Eckardstein, A., Schulte, H. & Assmann, G. Risk for diabetes mellitus in middle-aged Caucasian male participants of the PROCAM study: Implications for the definition of impaired fasting glucose by the American Diabetes Association. *J. Clin. Endocrinol. Metab.* **85**, 3101–3108 (2000).
103. Haase, C. L., Tybjærg-Hansen, A., Nordestgaard, B. G. & Frikke-Schmidt, R. HDL Cholesterol and Risk of Type 2 Diabetes: A Mendelian Randomization Study. *Diabetes* **64**, 3328–3333 (2015).
104. White, J. *et al.* Lipid Fractions and Contrasting Risks of Coronary Artery Disease and Diabetes. *JAMA Cardiol.* **1**, 692–699 (2016).
105. Fall, T. *et al.* Using Genetic Variants to Assess the Relationship Between Circulating Lipids and Type 2 Diabetes. *Diabetes* **64**, 2676–2684 (2015).
106. Liu, J. *et al.* A Mendelian Randomization Study of Metabolite Profiles, Fasting Glucose, and Type 2 Diabetes. *Diabetes* **66**, 2915–2926 (2017).
107. Roehrich, M. E. *et al.* Insulin-secreting β-cell dysfunction induced by human lipoproteins. *J. Biol. Chem.* **278**, 18368–18375 (2003).
108. Abderrahmani, A. *et al.* Human high-density lipoprotein particles prevent activation of the JNK pathway induced by human oxidised low-density lipoprotein particles in pancreatic beta cells. *Diabetologia* **50**, 1304–1314 (2007).
109. Pétremand, J. *et al.* Involvement of 4E-BP1 in the protection induced by HDLs on pancreatic β-cells. *Mol. Endocrinol.* **23**, 1572–1586 (2009).
110. Cochran, B. J. *et al.* Apolipoprotein A-I increases insulin secretion and production from pancreatic β-cells via a G-protein-cAMPPKA-FoxO1-dependent mechanism. *Arterioscler. Thromb. Vasc. Biol.* **34**, 2261–2267 (2014).
111. Pétremand, J. *et al.* HDLs protect pancreatic β-cells against ER stress by restoring protein folding and trafficking. *Diabetes* **61**, 1100–1111 (2012).
112. Puyal, J., Pétremand, J., Dubuis, G., Rummel, C. & Widmann, C. HDLs protect the MIN6 insulinoma cell line against tunicamycin-induced apoptosis without inhibiting ER stress and without restoring ER functionality. *Mol. Cell. Endocrinol.* **381**, 291–301 (2013).
113. Hao, M., Head, W., Gunawardana, S. & Hasty, A. Direct Effect of Cholesterol on Insulin Secretion. *Diabetes* **56**, (2007).
114. Brunham, L. R. *et al.* β-cell ABCA1 influences insulin secretion, glucose homeostasis and response to thiazolidinedione treatment. *Nat. Med.* **13**, 340–347 (2007).
115. Kruit, J. K. *et al.* Loss of both ABCA1 and ABCG1 results in increased disturbances in islet sterol homeostasis, inflammation, and impaired β-cell function. *Diabetes* **61**, 659–664 (2012).
116. Kruit, J. K. *et al.* Islet cholesterol accumulation due to loss of ABCA1 leads to impaired exocytosis of insulin granules. *Diabetes* **60**, 3186–3196 (2011).
117. Vikman, J., Jimenez-Feltström, J., Nyman, P., Thelin, J. & Eliasson, L. Insulin secretion is highly sensitive to desorption of plasma membrane cholesterol. *FASEB J.* **23**, 58–67 (2009).
118. Sturek, J. M. *et al.* An intracellular role for ABCG1-mediated cholesterol transport in the regulated secretory pathway of mouse pancreatic β cells. *J. Clin. Invest.* **120**, 2575–2589 (2010).
119. Cochran, B. J. *et al.* Impact of perturbed pancreatic β-cell cholesterol homeostasis on adipose tissue and skeletal muscle metabolism. *Diabetes* **65**, 3610–3620 (2016).
120. Xu, Y., Toomre, D. K., Bogan, J. S. & Hao, M. Excess cholesterol inhibits glucose-stimulated fusion pore dynamics in insulin exocytosis. *J. Cell. Mol. Med.* **21**, 2950–

2962 (2017).
121. Vergeer, M. *et al.* Carriers of loss-of-function mutations in ABCA1 display pancreatic β-cell dysfunction. *Diabetes Care* **33**, 869–874 (2010).
122. Rickels, M. R. *et al.* Loss-of-function mutations in ABCA1 and enhanced β-cell secretory capacity in young adults. *Diabetes* **64**, 193–199 (2015).
123. Patankar, J. V., Brunham, L. R. & Hayden, M. R. Comment on Rickels et al. Loss-of-Function Mutations in *ABCA1* and Enhanced β-Cell Secretory Capacity in Young Adults. Diabetes 2015;64:193–199. *Diabetes* **64**, e25–e26 (2015).
124. Drew, B. G. *et al.* High-density lipoprotein modulates glucose metabolism in patients with type 2 diabetes mellitus. *Circulation* **119**, 2103–2111 (2009).
125. Stenkula, K. G. *et al.* Single injections of apoA-I acutely improve in vivo glucose tolerance in insulin-resistant mice. *Diabetologia* **57**, 797–800 (2014).
126. Edmunds, S. J. *et al.* ApoAI-derived peptide increases glucose tolerance and prevents formation of atherosclerosis in mice. *Diabetologia* **62**, 1257–1267 (2019).
127. Barter, P. J. & Rye, K. A. Cholesteryl ester transfer protein inhibition is not yet dead - Pro. *Arterioscler. Thromb. Vasc. Biol.* **36**, 439–441 (2016).
128. Siebel, A. L. *et al.* Effects of high-density lipoprotein elevation with cholesteryl ester transfer protein inhibition on insulin secretion. *Circ. Res.* **113**, 167–175 (2013).
129. Barter, P. J. *et al.* Effect of torcetrapib on glucose, insulin, and hemoglobin a1c in subjects in the investigation of lipid level management to understand its impact in atherosclerotic events (Illuminate) Trial. *Circulation* **124**, 555–562 (2011).
130. Yu, Q., Chen, Y. & Xu, C. B. Statins and new-onset diabetes mellitus: LDL receptor may provide a key link. *Front. Pharmacol.* **8**, 1–5 (2017).
131. Swerdlow, D. I. *et al.* HMG-coenzyme A reductase inhibition, type 2 diabetes, and bodyweight: Evidence from genetic analysis and randomised trials. *Lancet* **385**, 351–361 (2015).
132. Ference, B. A. *et al.* Variation in PCSK9 and HMGCR and risk of cardiovascular disease and diabetes. *N. Engl. J. Med.* **375**, 2144–2153 (2016).
133. Brault, M., Ray, J., Gomez, Y. H., Mantzoros, C. S. & Daskalopoulou, S. S. Statin treatment and new-onset diabetes: A review of proposed mechanisms. *Metabolism.* **63**, 735–745 (2014).
134. Filippatos, T. D., Kei, A., Rizos, C. V. & Elisaf, M. S. Effects of PCSK9 Inhibitors on Other than Low-Density Lipoprotein Cholesterol Lipid Variables. *J. Cardiovasc. Pharmacol. Ther.* **23**, 3–12 (2018).
135. Mbikay, M. *et al.* PCSK9-deficient mice exhibit impaired glucose tolerance and pancreatic islet abnormalities. *FEBS Lett.* **584**, 701–706 (2010).
136. Langhi, C. *et al.* PCSK9 is expressed in pancreatic δ-cells and does not alter insulin secretion. *Biochem. Biophys. Res. Commun.* **390**, 1288–1293 (2009).
137. Schmidt, A. F. *et al.* PCSK9 monoclonal antibodies for the primary and secondary prevention of cardiovascular disease. *Cochrane Database Syst. Rev.* **4**, CD011748 (2017).
138. Baass, A. *et al.* Plasma PCSK9 Is Associated with Age, Sex, and Multiple Metabolic Markers in a Population-Based Sample of Children and Adolescents. *Clin. Chem.* **55**, 1637–1645 (2009).
139. Filippatos, T. D. *et al.* PCSK9 and carbohydrate metabolism: A double-edged sword. *World J. Diabetes* **8**, 311 (2017).
140. Odegaard, J. I. & Chawla, A. Pleiotropic Actions of Insulin Resistance and Inflammation in Metabolic Homeostasis. *Science (80-.).* **339**, 172–177 (2013).

141. Risérus, U., Ärnlöv, J. & Berglund, L. Long-Term Predictors of Insulin Resistance. *Diabetes Care* **30**, 2928–2933 (2007).
142. Wilson, P. W. F., D'Agostino, R. B., Fox, C. S., Sullivan, L. M. & Meigs, J. B. Type 2 diabetes risk in persons with dysglycemia: The Framingham Offspring Study. *Diabetes Res. Clin. Pract.* **92**, 124–127 (2011).
143. Drew, B. G., Rye, K. A., Duffy, S. J., Barter, P. & Kingwell, B. A. The emerging role of HDL in glucose metabolism. *Nat. Rev. Endocrinol.* **8**, 237–245 (2012).
144. Umemoto, T. *et al.* Apolipoprotein AI and high-density lipoprotein have anti-inflammatory effects on adipocytes via cholesterol transporters: ATP-binding cassette A-1, ATP-binding cassette G-1, and scavenger receptor B-1. *Circ. Res.* **112**, 1345–1354 (2013).
145. McGrath, K. C. *et al.* High density lipoproteins improve insulin sensitivity in high-fat diet-fed mice by suppressing hepatic inflammation. *J. Lipid Res.* **55**, 421–430 (2014).
146. Zhang, Q. *et al.* High density lipoprotein (HDL) promotes glucose uptake in adipocytes and glycogen synthesis in muscle cells. *PLoS One* **6**, 4–11 (2011).
147. Han, R. *et al.* Apolipoprotein A-I stimulates AMP-activated protein kinase and improves glucose metabolism. *Diabetologia* **50**, 1960–1968 (2007).
148. Dalla-Riva, J., Stenkula, K. G., Petrlova, J. & Lagerstedt, J. O. Discoidal HDL and apoA-I-derived peptides improve glucose uptake in skeletal muscle. *J. Lipid Res.* **54**, 1275–1282 (2013).
149. Lehti, M. *et al.* High-density lipoprotein maintains skeletal muscle function by modulating cellular respiration in mice. *Circulation* **128**, 2364–2371 (2013).
150. Asfari, M. *et al.* Establishment of 2-mercaptoethanol-dependent differentiated insulin-secreting cell lines. *Endocrinology* **130**, 167–178 (1992).
151. Merglen, A. *et al.* Glucose Sensitivity and Metabolism-Secretion Coupling Studied during Two-Year Continuous Culture in INS-1E Insulinoma Cells. *Endocrinology* **145**, 667–678 (2004).
152. Miyazaki, J.-I. *et al.* Establishment of a Pancreatic β Cell Line That Retains Glucose-Inducible Insulin Secretion: Special Reference to Expression of Glucose Transporter Isoforms. *Endocrinology* **127**, 126–132 (1990).
153. Brown, W. V., Levy, R. I. & Fredrickson, D. S. Studies of the proteins in human plasma very low density lipoproteins. *J. Biol. Chem.* **244**, 5687–5694 (1969).
154. Lorenzi, I., von Eckardstein, A., Radosavljevic, S. & Rohrer, L. Lipidation of apolipoprotein A-I by ATP-binding cassette transporter (ABC) A1 generates an interaction partner for ABCG1 but not for scavenger receptor BI. *Biochim. Biophys. Acta - Mol. Cell Biol. Lipids* **1781**, 306–313 (2008).
155. Pfaffl, M. W. A new mathematical model for relative quantification in real-time RT-PCR. *Nucleic Acids Res.* **29**, e45 (2001).
156. Huang, D. W., Sherman, B. T. & Lempicki, R. A. Systematic and integrative analysis of large gene lists using DAVID bioinformatics resources. *Nat. Protoc.* **4**, 44–57 (2009).
157. Huang, D. W., Sherman, B. T. & Lempicki, R. A. Bioinformatics enrichment tools: Paths toward the comprehensive functional analysis of large gene lists. *Nucleic Acids Res.* **37**, 1–13 (2009).
158. Drexel, H. *et al.* Is atherosclerosis in diabetes and impaired fasting glucose driven by elevated LDL cholesterol or by decreased HDL cholesterol? *Diabetes Care* **28**, 101–107 (2005).
159. Levey, A. S. *et al.* A new equation to estimate glomerular filtration rate. *Ann. Intern. Med.* **150**, 604–612 (2009).

160. Jong, M. C. *et al.* Protection From Obesity and Insulin Resistance in Mice Overexpressing Human Apolipoprotein C1. *Diabetes* **50**, 2779–85 (2001).
161. Pajkrt, D. *et al.* Antiinflammatory effects of reconstituted high-density lipoprotein during human endotoxemia. *J. Exp. Med.* **184**, 1601–1608 (1996).
162. Galvani, S. *et al.* HDL-bound sphingosine 1-phosphate acts as a biased agonist for the endothelial cell receptor S1P1 to limit vascular inflammation. *Sci. Signal.* **8**, (2015).
163. Ruiz, M. *et al.* High-density lipoprotein-associated apolipoprotein M limits endothelial inflammation by delivering sphingosine-1-phosphate to the sphingosine-1-phosphate receptor 1. *Arterioscler. Thromb. Vasc. Biol.* **37**, 118–129 (2017).
164. Berbée, J. F. P., Van Der Hoogt, C. C., Sundararaman, D., Havekes, L. M. & Rensen, P. C. N. Severe hypertriglyceridemia in human APOC1 transgenic mice is caused by apoC-I-induced inhibition of LPL. *J. Lipid Res.* **46**, 297–306 (2005).
165. Gautier, T. *et al.* Hepatic lipid accumulation in apolipoprotein C-I-deficient mice is potentiated by cholesteryl ester transfer protein. *J. Lipid Res.* **48**, 30–40 (2007).
166. Othman, A. *et al.* Plasma 1-deoxysphingolipids are predictive biomarkers for type 2 diabetes mellitus. *BMJ Open Diabetes Res. Care* **3**, 1–10 (2015).
167. Jaeger, A. *et al.* Circulating microRNAs -192 and -194 are associated with the presence and incidence of diabetes mellitus. *Sci. Rep.* **8**, 1–14 (2018).
168. Cardner, M. *et al.* Structure–function relationships of HDL in diabetes and coronary heart disease. *JCI Insight* **5**, (2019).
169. Yan, L. R. *et al.* A pro-atherogenic HDL profile in coronary heart disease patients: An iTRAQ labelling-based proteomic approach. *PLoS One* **9**, (2014).
170. Natarajan, P. *et al.* Association of an HDL Apolipoproteomic Score With Coronary Atherosclerosis and Cardiovascular Death. *J. Am. Coll. Cardiol.* **73**, 2135–2145 (2019).
171. Jin, Z. *et al.* Development and validation of apolipoprotein AI-associated lipoprotein proteome panel for the prediction of cholesterol efflux capacity and coronary artery disease. *Clin. Chem.* **65**, 282–290 (2019).
172. Van Der Ham, R. L. M. *et al.* Plasma apolipoprotein CI and CIII levels are associated with increased plasma triglyceride levels and decreased fat mass in men with the metabolic syndrome. *Diabetes Care* **32**, 184–186 (2009).
173. Bouillet, B. *et al.* Glycation of apolipoprotein C1 impairs its CETP inhibitory property: Pathophysiological relevance in patients with type 1 and type 2 diabetes. *Diabetes Care* **37**, 1148–1156 (2014).
174. Cardozo, A. K. *et al.* A Comprehensive Analysis of Cytokine-induced and Nuclear Factor-κB-dependent Genes in Primary Rat Pancreatic β-Cells. *J. Biol. Chem.* **276**, 48879–48886 (2001).
175. Ortis, F. *et al.* Cytokines Interleukin-1beta and Tumor Necrosis Factor-alpha Regulate Different Transcriptional and Alternative Splicing Networks in Primary beta-Cells. *Diabetes* **59**, 358–374 (2010).
176. Larsen, P. M. *et al.* in Protein Expression in Rat Islets of Langerhans. **50**, (2001).
177. Eizirik, D. L. & Mandrup-Poulsen, T. A choice of death - The signal-transduction of immune-mediated beta-cell apoptosis. *Diabetologia* **44**, 2115–2133 (2001).
178. Eizirik, D. L. *et al.* The human pancreatic islet transcriptome: Expression of candidate genes for type 1 diabetes and the impact of pro-inflammatory cytokines. *PLoS Genet.* **8**, (2012).
179. Hayden, M. S. & Ghosh, S. Signaling to NF-kappaB. *Genes Dev.* 2195–2224 (2004). doi:10.1101/gad.1228704
180. Baker, R. G., Hayden, M. S. & Ghosh, S. NF-κB, inflammation, and metabolic disease.

Cell Metab. **13**, 11–22 (2011).
181. Giannoukakis, N., Rudert, W. A., Trucco, M. & Robbins, P. D. Protection of human islets from the effects of interleukin-1β by adenoviral gene transfer of an IκB repressor. *J. Biol. Chem.* **275**, 36509–36513 (2000).
182. Papaccio, G., Graziano, A., D'Aquino, R., Valiante, S. & Naro, F. A biphasic role of nuclear transcription factor (NF)-κB in the islet β-cell apoptosis induced by interleukin (IL)-1β. *J. Cell. Physiol.* **204**, 124–130 (2005).
183. Eldor, R. *et al.* Conditional and specific NF-κB blockade protects pancreatic beta cells from diabetogenic agents. *Proc. Natl. Acad. Sci. U. S. A.* **103**, 5072–5077 (2006).
184. Chan, J. Y., Biden, T. J. & Laybutt, D. R. Cross-Talk between the unfolded protein response and nuclear factor-kappaB signalling pathways regulates cytokine-mediated beta cell death in MIN6 cells and isolated mouse islets. *Diabetologia* **55**, 2999–3009 (2012).
185. Yalcinkaya, M. *et al.* HDL inhibits endoplasmic reticulum stress-induced apoptosis of pancreatic β-cells in vitro by activation of Smoothened. *J. Lipid Res.* (2020).
186. Annema, W. & von Eckardstein, A. Dysfunctional high-density lipoproteins in coronary heart disease: implications for diagnostics and therapy. *Transl. Res.* **173**, 30–57 (2016).
187. Lüscher, T. F., Landmesser, U., Von Eckardstein, A. & Fogelman, A. M. High-density lipoprotein: Vascular protective effects, dysfunction, and potential as therapeutic target. *Circ. Res.* **114**, 171–182 (2014).
188. Sorrentino, S. A. *et al.* Endothelial-vasoprotective effects of high-density lipoprotein are impaired in patients with type 2 diabetes mellitus but are improved after extended-release niacin therapy. *Circulation* **121**, 110–122 (2010).
189. Besler, C. *et al.* Mechanisms underlying adverse effects of HDL on eNOS-activating pathways in patients with coronary artery disease. *J. Clin. Invest.* **121**, 2693–2708 (2011).
190. Petrie, J. R., Guzik, T. J. & Touyz, R. M. Diabetes, Hypertension, and Cardiovascular Disease: Clinical Insights and Vascular Mechanisms. *Can. J. Cardiol.* **34**, 575–584 (2018).
191. Manjunatha, S. *et al.* Functional and proteomic alterations of plasma high density lipoproteins in type 1 diabetes mellitus. *Metabolism* **65**, 1421–1431 (2016).
192. Heier, M. *et al.* Reduced HDL function in children and young adults with type 1 diabetes. *Cardiovasc. Diabetol.* **16**, 1–8 (2017).
193. Gourgari, E. *et al.* Low cholesterol efflux capacity and abnormal lipoprotein particles in youth with type 1 diabetes: A case control study. *Cardiovasc. Diabetol.* **17**, 1–10 (2018).

9. Acknowledgements

Zuerst möchte ich mich bei allen Beteiligten für ihre Geduld und Zuversicht bedanken, die meine lange Doktorarbeit eingefordert hat.

Ich bedanke mich herzlich bei Dr. Lucia Rohrer, meiner direkten Betreuerin, die mich mit ihrer grossen Fachkompetenz und zahlreichen Ratschlägen unterstützte. Ich danke ihr für die kritischen Anregungen, sowie viele spannende, meist wissenschaftliche Diskussionen.
Prof. Dr. Arnold von Eckardstein danke ich sehr für die Möglichkeit, meine Doktorarbeit am Institut für Klinische Chemie durchzuführen, für die Leitung meiner Doktorarbeit, die fachliche Betreuung und die vielen Anregungen zu meinem Projekt.
Ich danke Prof. Dr. Thierry Hennet für die Unterstützung und die Begleitung meiner Doktorarbeit als Mitglied meines Komitees.
Bei Prof. Dr. Christian Widmann bedanke ich mich für die Unterstützung und die Begleitung meiner Doktorarbeit als Mitglied meines Komitees, sowie ganz besonders für die Woche, die ich in seinem Labor und Haus verbringen durfte und den Austausch über ER-Stress in β-Zellen.
Weiter danke ich Prof. Dr. Marc Donath, meinem fünften Komiteemitglied, und Dr. Sabine Rütti für die Unterstützung, insbesondere zu Beginn meines Projektes. Auch Dr. Marianne Böni danke ich sehr herzlich für ihre unkomplizierte Hilfe bei Schwierigkeiten mit den Zellen.

Mein spezieller Dank gebührt auch allen Mitgliedern des IKC-Labors und den Kolleginnen und Kollegen aus dem 1. Stock im Wagi 14, vor allem Damir Perisa, Jérôme Robert, Pascale Ohnsorg, Reda Hasballa, Diana Odermatt, Wijtske Annema und Vidya Velagapudi. Der Austausch über fachliche und teilweise auch weit darüber hinausgehende Fragen mit ihnen hat so manches Problem leichter gemacht und gelöst und für eine gute Atmosphäre gesorgt.
Ein grosser Dank gebührt auch Silvija Radosavljevic, welche mir stets mit praktischer Hilfe tatkräftig und unkompliziert zur Seite stand. Auch Daniela, Anke, Heiko, Alaa (Danke für die Erklärungen rund um Statistik), und weiteren Mitgliedern des Hornemann-Labs danke ich herzlich für die gute Zeit, die wir im Labor und auf der Dachterrasse hatten.
Auch wenn es schon etwas zurück liegt, denke ich dankbar an den Austausch mit den ehemaligen Lab C-Leuten zurück. Es war immer eine Freude, mich mit ihnen über Diabetes und andere Themen auszutauschen.

Zum Schluss danke ich von ganzem Herzen meinen Eltern, meiner Schwester und meiner Familie. Sie haben mich während meiner gesamten Ausbildung immer wieder unterstützt und mich ermutigt, meinen Weg zu gehen.

Ich bin unendlich dankbar, dass mein Mann Markus, welcher mich praktisch durch die ganze PhD-Zeit begleitete, immer für mich da war. Er unterstützte mich geduldig und mit viel Liebe, und war dazu mit seiner persönlichen und medizinischen Expertise stets hilfsbereit.

10. Curriculum Vitae

Rahel Anja Sibler

Date of Birth:	February 20, 1984
Place of Citizenship:	Zurich ZH
Nationality:	Swiss

Education

Since 2009	**PhD Thesis**, imMed program, University of Zurich Supervision: Prof. Dr. Arnold von Eckardstein and Dr. Lucia Rohrer Institute of Clinical Chemistry, University Hospital Zurich
2013-2016	**Qualification for Teaching Biology** (Secondary Level II), FHNW University of Applied Sciences and Arts Northwestern Switzerland, School of Education
2007-2009	**Master of Science in Biology / Human Biology**, University of Zurich Master Thesis entitled: „Influence of Low Density Lipoprotein on Mouse Pancreatic Islet Cell Proliferation and Function“ Supervision: Dr. Sabine Rütti and Prof. Dr. Marc Donath Division for Endocrinology and Diabetes, University Hospital Zurich
2004-2007	**Bachelor of Science in Biology**, University of Zurich
2000-2004	**Matura** mit Schwerpunkt Biologie und Chemie, kleines Latinum, Kantonsschule Wettingen AG

Publications

Low- and high-density lipoproteins modulate function, apoptosis, and proliferation of primary human and murine pancreatic beta-cells; Rütti S, Sibler RA, Ehses JA, et al.; Endocrinology. 2009 Oct;150(10):4521-30. Epub 2009 Jul 23

Possible contributions of lipoproteins and cholesterol to the pathogenesis of diabetes mellitus type 2; von Eckardstein A, Sibler RA.; Curr Opin Lipidol. 2011 Feb;22(1):26-32

Presentations

2009 (Poster)	5th Symposium of the Zurich Center for Integrative Human Physiology (ZIHP) - *Low Density Lipoproteins Impair Human and Mouse Beta-Cell Proliferation and Function*
2009 (oral)	32nd European Lipoprotein Club Meeting, Tutzing, Germany - *Low and high-density lipoproteins modulate function, apoptosis and proliferation of primary human and murine pancreatic β-cells*
2010 (Poster)	Day of Clinical Research, University Hospital Zürich, Switzerland - *HDL Protects Pancreatic β-Cells from Apoptosis*
2010 (Poster)	6th Symposium of the Zurich Center for Integrative Human Physiology (ZIHP) - *HDL Protects Pancreatic β-Cells from Apoptosis*
2010 (oral)	78th European Atherosclerosis Society Congress, Hamburg, Germany - *Low and high-density lipoproteins modulate function, apoptosis and proliferation of primary human and murine pancreatic β-cells*
2010 (Poster)	Annual Meeting of the Swiss Endocrine Society, Bern, Switzerland - *HDL Protects Pancreatic β-Cells from Apoptosis*
2011 (Poster)	Day of Clinical Research, University Hospital Zürich, Switzerland - *HDL Protects Pancreatic β-Cells from Apoptosis*
2011 (Poster)	7th Symposium of the Zurich Center for Integrative Human Physiology (ZIHP) - *HDL Protects Pancreatic β-Cells from Apoptosis*
2011 (Poster)	Annual Meeting of the Swiss Endocrine Society, Bern, Switzerland - *HDL Protects Pancreatic β-Cells from Apoptosis*
2012 (Poster)	8th Symposium of the Zurich Center for Integrative Human Physiology (ZIHP) - *Which HDL Component Protects Pancreatic β-Cells from IL-1β-Induced Apoptosis?*
2012 (oral)	35th European Lipoprotein Club Meeting, Tutzing, Germany - *How does High-Density Lipoprotein Protect Pancreatic β-Cells from Apoptosis?*
2013 (oral)	COST Meeting, Lille, France - *How does High-Density Lipoprotein Protect Pancreatic β-Cells from Apoptosis?*
2013 (Poster)	AGLA Meeting - *How does High-Density Lipoprotein Protect Pancreatic β-Cells from Apoptosis?*